TOPICAL MEETING ON

OPTICS IN ADVERSE ENVIRONMENTS

TECHNICAL DIGEST SERIES VOLUME 8

FEBRUARY 11-12, 1987
ALBUQUERQUE, NEW MEXICO

Unclassified
SECURITY CLASSIFICATION OF THIS PAGE

Unclassified

REPORT DOCUMENTATION PAGE

1a. REPORT SECURITY CLASSIFICATION Unclassified	1b. RESTRICTIVE MARKINGS
2a. SECURITY CLASSIFICATION AUTHORITY	3. DISTRIBUTION/AVAILABILITY OF REPORT Approved for public release; Distribution unlimited
2b. DECLASSIFICATION/DOWNGRADING SCHEDULE	
4. PERFORMING ORGANIZATION REPORT NUMBER(S)	5. MONITORING ORGANIZATION REPORT NUMBER(S) AFOSR-TR- 88-0643
6a. NAME OF PERFORMING ORGANIZATION Optical Society of America 6b. OFFICE SYMBOL (If applicable)	7a. NAME OF MONITORING ORGANIZATION AFOSR/NP
6c. ADDRESS (City, State, and ZIP Code) 1816 Jefferson Place, N.W. Washington, D.C. 20036	7b ADDRESS (City, State, and ZIP Code) Bldg. 410 Bolling AFB, Washington, D.C. 20332-6448
8a. NAME OF FUNDING/SPONSORING ORGANIZATION AFOSR 8b. OFFICE SYMBOL (If applicable) NP	9. PROCUREMENT INSTRUMENT IDENTIFICATION NUMBER AFOSR-87-0094
8c. ADDRESS (City, State, and ZIP Code) Bldg. 410 Bolling AFB, Washington, D.C. 20332-6448	10. SOURCE OF FUNDING NUMBERS PROGRAM ELEMENT NO. 61102F; PROJECT NO. 2301; TASK NO. A1; WORK UNIT ACCESSION NO.
11. TITLE (Include Security Classification) Organization of the Topical Meeting on Optics in Adverse Environments	
12. PERSONAL AUTHOR(S) Jarus W. Quinn	
13a. TYPE OF REPORT Final 13b. TIME COVERED FROM 01/01/87 TO 10/31/87	14. DATE OF REPORT (Year, Month, Day) 87/10/31 15. PAGE COUNT
16. SUPPLEMENTARY NOTATION	

17. COSATI CODES			18 SUBJECT TERMS (Continue on reverse if necessary and identify by block number)
FIELD	GROUP	SUB-GROUP	
			Diagnostics, Lasers, Optics

19. ABSTRACT (Continue on reverse if necessary and identify by block number)

Semiconductor Lasers: Semiconductor diode lasers remain the subject of intensive worldwide development efforts with rapid progress being made in many areas of device design and performance. In addition to their use in optical fiber systems, other applications have been identified and lasers are being fabricated to meet many different system requirements. This meeting treated all aspects of laer design, development and characterization.

Lasers in Material Diagnostics: Laser and optical techniques are increasingly important for diagnostics of a wide variety of materials and processing technologies. Applications range from diagnostics of impurities and other defects in materials, to probes of dry-processing technologies for semiconductor device fabrication, to imaging techniques for patterning and analysis in VLSI manufacture. These techniques are being used both for analytic measurements and as tools to probe new materials and effects. This meeting brought together workers from all of these areas for the exchange of results and of new directions for research. (over)

20. DISTRIBUTION/AVAILABILITY OF ABSTRACT ☒ UNCLASSIFIED/UNLIMITED ☐ SAME AS RPT ☐ DTIC USERS	21 ABSTRACT SECURITY CLASSIFICATION Unclassified
22a. NAME OF RESPONSIBLE INDIVIDUAL Dr. Howard R. Schlossberg	22b. TELEPHONE (Include Area Code) 202/767-4906 22c. OFFICE SYMBOL NP

DD FORM 1473, 84 MAR 83 APR edition may be used until exhausted.
All other editions are obsolete.

SECURITY CLASSIFICATION OF THIS PAGE

Unclassified

TOPICAL MEETING ON

OPTICS IN ADVERSE ENVIRONMENTS

Summaries of papers presented at the
Optics in Adverse Environments Topical Meeting

February 11-12, 1987

Albuquerque, New Mexico

Sponsored by the

Lasers and Electro-Optics Society of IEEE
Optical Society of America

Optical Society of America
1816 Jefferson Place, N.W.
Washington, D.C. 20036
(202) 223-8130

Articles in this publication may be cited in other publications. In order to facilitate access to the original publication source, the following form for the citation is suggested:

> Name of Author(s), Title of Paper, Topical Meeting on Optics in Adverse Environments, Technical Digest, 1987, Volume 8, (Optical Society of America, Washington, D.C. 1987) pp. xx–xx.

ISBN Number
Conference Edition 0-936659-42-4
Postconference Edition 0-936659-62-9

Library of Congress Catalog Card Number
Conference Edition 86-063943
Postconference Edition 86-063944

IEEE Catalog Number 87CH2389-5

TABLE OF CONTENTS

March 2, 1987

SOUTHWEST OPTICS '87 CONFERENCE
REGISTRATION LIST

LASTNAME	FIRSTNAM	ORGANIZA	ADDRESS1	ADDRESS2	MAILCODE	COUNTRY	DIG
ABEY	ALBERT E.	LLNL	PO BOX 808, L-86	LIVERMORE, CA	94550	USA	0
AL-JUNAILY	GHANIM A.	BARR ASSOCIATES	2 LYBERTY WAY	WESTFORD, MA	01720	USA	0
ANTHIS	JOHN P.	SANDIA NATIONAL LABS	DIV 2531 PO BOX 5800	ALBUQUERQUE, NM	87185	USA	L
APFEL	JOE	OCLI	2789 NORTHPOINT	SANTA ROSA, CA	95407	USA	O
ARIESSOHN	PETER C.	WEYERHAEUSER COMPANY	WTC 2F22	TACOMA, WA	98477	USA	L
ASAWA	CHARLES K.	TRW ELECTRO OPTICS RES CTR	ONE SPACE PARK	REDONDO BH, CA	90278	USA	S
ASHBY	CAROL	SANDIA NATIONAL LABS	DIV 1126 PO BOX 5800	ALBUQUERQUE, NM	87185	USA	L
ATKINSON	GEORGE H.	UNIVERSITY OF ARIZONA	DEPT OF CHEMISTRY	TUCSON, AZ	85721	USA	L
AVINOR	MICHAEL	UNIVERSITY OF NEW MEXICO		ALBUQUERQUE, NM	87131	USA	S
BASS	MICHAEL	UNIV OF SOUTHERN CALIFORNIA	UNIVERSITY PARK	LOS,ANGELES, CA	90089	USA	L
BECKER	MICHAEL F.	UNIVERSITY OF TEXAS	ELECTRICAL ENGN DEPT	AUSTIN, TX	28712	USA	L
BENSON	BERNARD	BDM CORPORATION	1801 RANDOLPH SE	ALBUQUERQUE, NM	87106	USA	S
BERRY	MICHAEL	RICE UNIV DEPT OF CHEMISTRY	PO BOX 1892	HOUSTON, TX	77251	USA	L
BLACK	BOB S.		7111 MOJAVE NE	ALBUQUERQUE, NM	87120	USA	S
BOLCH	JAMES B.	UNITED TECH OPTICAL SYSTEMS	PO BOX 109660	W PALM BH, FL	33410	USA	O
BOTEZ	DAN	TRW ELECTRO OPTICS RES CTR	ONE SPACE PARK	REDONDO BH, CA	90278	USA	S
BOUTOUMAT	MARIELLE S.	UNIVERSITY OF ARIZONA	DEPT OF CHEMISTRY	TUCSON, AZ	85721	USA	L
BRANNON	PAUL J.	SANDIA NATIONAL LABS	DIVISION 1124	ALBUQUERQUE, NM	87185	USA	S
BREILAND	WILLIAM G.	SANDIA NATIONAL LABS	DIVISION 1126	ALBUQUERQUE, NM	87185	USA	L
BROOKS	BOB	TRW ELECTRO OPTICS RES CTR	ONE SPACE PARK, R1-2162	REDONDO BH, CA	90278	USA	S
BROST	GEORGE A.	F J SEILER RESEARCH LAB		USAF ACAD, CO	80840	USA	S
BROWNING	STEPHEN D.	OPTICAL COATING LAB INC	2789 NORTHPOINT PARKWAY	SANTA ROSA, CA	95407	USA	O
BRUECK	STEVE	UNIVERSITY OF NEW MEXICO	CTR FOR HIGH TECH MATERIALS	ALBUQUERQUE, NM	87131	USA	L
BUSHMAN	ROBERT D.	AMOCO RESEARCH CENTER	PO BOX 400, MS-F4	NAPERVILLE, IL	60566	USA	S
CANTRELL	CYRUS D.	UNIV OF TEXAS AT DALLAS	PO BOX 830688	RICHARDSON, TX	75083	USA	S
CANNIGLIA	CHARLES K.	MARTIN MARIETTA	PO BOX 9316, INT AIRPORT	ALBUQUERQUE, NM	87119	USA	O
CARSON	SUSAN D.	BDM CORPORATION	1801 RANDOLPH RD SE	ALBUQUERQUE, NM	87106	USA	L
CARVER	GARY E.	AT&T - EPC	PO BOX 900	PRINCETON, NJ	08540	USA	L
CHEN	C. C.	BOEING ELECTRONICS COMPANY	PO BOX 24969	SEATTLE, WA	98124	USA	S
CHENG	HOOD-HI	ROCKWELL INTERNATIONAL	PO BOX 10462, MS 406-230	DALLAS, TX	75207	USA	S
CHERNG	CHUNG-PIN	UNIVERSITY OF NEW MEXICO	CTR FOR HIGH TECH MATERIALS	ALBUQUERQUE, NM	87131	USA	S
CHUN	WENG W.	HUGHES AIRCRAFT	1600 RANDOLPH CT SE	ALBUQUERQUE, NM	87131	USA	S
CHRISTENSEN	DAVID H.	BALL AEROSPACE SYSTEMS DIV	PO BOX 1062, MS-T03	BOULDER, CO	80302	USA	S
CHRISTMAN	JO-ANNE H.	JET PROPULSION LABORATORY	4800 OAK GROVE DRIVE	PASADENA, CA	91109	USA	S
CHUNG	KI-HYUN	UNIVERSITY OF NEW MEXICO	CTR FOR HIGH TECH MATERIALS	ALBUQUERQUE, NM	87131	USA	S
CHUNG	YUN C.	LOS ALAMOS NATIONAL LAB	PO BOX 1663, CLS-5, MS/E535	LOS ALAMOS, NM	87545	USA	S
COLEMAN	JAMES J.	UNIVERSITY OF ILLINOIS	DEPT OF ELECTRICAL ENG	URBANA, IL	61801	USA	S
COLTRIN	MICHAEL E.	SANDIA NATIONAL LABS	DIVISION 1126	ALBUQUERQUE, NM	87185	USA	L
COOPER	RONALD E.	ROCKWELL INTERNATIONAL	1049 CAMINO DOS RIOS	THOUSAND OAK,CA	91360	USA	L
COOPER	DAVID E.	SRI INTERNATIONAL	333 RAVENSWOOD AVENUE	MENLO PARK, CA	94025	USA	L
CROWE	VICTOR S.	ALBUQUERQUE T-VI	2632 GRANITE NW	ALBUQUERQUE, NM	87104	USA	O
CROWE	DAVID A.	EASTMAN KODAK CO FSO	901 ELMGROVE ROAD	ROCHESTER, NY	14616	USA	O
CZYZAK	STANLEY R.	FJSRL	US AIR FORCE ACADEMY	COLORADO SG, CO	80840	USA	S
DAHLHAUSER	KARL J.	US AIR FORCE	AFWL/ARDF	KIRTLAND AFB,NM	87117	USA	S
DALTON	DONALD A.	UNITED TECH OPTICAL SYSTEMS	5301 CENTRAL, STR 1617 -	ALBUQUERQUE, NM	87108	USA	3
DE HAINAUT	LINDA M.	UNIVERSITY OF NEW MEXICO		ALBUQUERQUE, NM	87108	USA	L
DE WILTON	ANGELA C.	NORTHERN TELECOM ELEC	PO BOX 3511 STATION E	OTTAWA ONTARIO	K1Y4H7	CANADA	L
DEFREEZ	RICHARD K.	OREGON GRADUATE CENTER	19600 NW VON NEUMANN DR	BEAVERTON, OR	97006	USA	S
DENTE	GREGORY	CONSULTANT	2100 ALVARADO NE	ALBUQUERQUE, NM	87110	USA	S
DEPATIE	DAVID A.	KIRTLAND AIR FORCE BASE	AFWL	ALBUQUERQUE, NM	87117	USA	S
DIADIUK	VICKI	MIT LINCOLN LABORATORY	PO BOX 73	LEXINGTON, MA	02173	USA	S
DONOVAN	TERRY M.	NAVAL WEAPONS CENTER		CHINA LAKE, CA	93555	USA	O
DREYFUS	RUSSELL W.	IBM T J WATSON RESEARCH CTR	PO BOX 218	YKTOWN HTS, NY	10598	USA	L
DUFFY	PHILIP B.	LLNL	PO BOX 808, L-36	LIVERMORE, CA	94550	USA	O
DUPUIS	RUSSELL D.	AT&T BELL LABORATORIES	ROOM 7C327	MURRAY HILL, NJ	07974	USA	3

SOUTHWEST OPTICS '87 CONFERENCE
REGISTRATION LIST

LASTNAME	FIRSTNAM	ORGANIZA	ADDRESS1	ADDRESS2	MAILCODE	COUNTRY	DIGES
EASTMAN	DANIEL R.	PERKIN-ELMER	401 MAIN AVENUE	NORWACK, CT	00859	USA	D
EATON	LARRY R.	TRW ELECTRO OPTICS RES CTR	ONE SPACE PARK	REDONDO BH, CA	90278	USA	S
ENGLERT	THAD J.	UNIVERSITY OF WYOMING	DEPT OF ELECTRICAL ENG	LARAMIE, WY	82071	USA	D
ENGLERT	SUE E.	UNIVERSITY OF WYOMING	DEPT OF ELECTRICAL ENGNR	LARAMIE, WY	82071	USA	D
EPLER	JOHN E.	XEROX PARC	3333 COYOTE HILL ROAD	PALO ALTO, CA	94043	USA	S
FACEY	TERENCE A.	PERKIN ELMER	100 WOOSTER HEIGHTS ROAD	DANSBURY, CT	06810	USA	D
FAUCHET	PHILIPPE M.	PRINCETON UNIVERSITY	DEPT OF ELECTRICAL ENG	PRINCETON, NJ	08544	USA	L
FECK	DAVID W.		1925 19TH LOOP	KIRTLAND AFB,NM	87116	USA	L
FERGUSON	THOMAS R.	AFWL/ARBL	517 MONTCLAIRE SE	ALBUQUERQUE, NM	87108	USA	L
FIGUEIRA	JOSEPH F.	LOS ALAMOS NATIONAL LAB	MS J566	LOS ALAMOS, NM	87501	USA	S
FIGUEROA	LUIS	UNIVERSITY OF FLORIDA	ELEC ENG, 216 LARSEN	GAINESVILLE, FL	32611	USA	D
FINLAN	J. MICHAEL	GENERAL ELECTRIC	PO BOX 8555 M1334	PHILADELPHIA,PA	19101	USA	S
FLOHR	MARK C.	UNIVERSITY OF WYOMING	DEPT OF ELECTRICAL ENG	LARAMIE, WY	82071	USA	D
FONG	CHUE	UNIVERSITY OF NEW MEXICO	CTR FOR HIGH TECH MATERIALS	ALBUQUERQUE, NM	87131	USA	L
FOSTER	MIKE B.	SIEMENS TRANSMISSION SYSTEM	ONE CAMINO DE LEMKURT, NE	ALBUQUERQUE, NM	87123	USA	S
FRAAS	LEWIS, M.	BOEING TECH	PO BOX 20969 MS 92 80	SEATTLE, WA	98124	USA	S
GERARDO	JAMES B.	SANDIA NATIONAL LABS	PO BOX 5800	ALBUQUERQUE, NM	87185	USA	S
GIBB	ROGER M.	STC/STANTEL	PAIGNTON	DEVON		UK	S
GILLMAN	JOEL M.	ALBUQUERQUE T-VI	525 BUENA VISTA ST	ALBUQUERQUE, NM	87106	USA	L
GLECKLER	ANTHONY D.	UNIVERSITY OF ARIZONA	OPTICAL SCIENCES CENTER	TUCSON, AZ	85712	USA	S
GOFRINGER	DOUGLAS E.	OAK RIDGE NATIONAL LAB	PO BOX Y BLDG 9735	OAK RIDGE, TN	37831	USA	L
GOTTSCHO	RICHARD A.	AT&T BELL LABORATORIES	ROOM 1A-259	MURRAY HILL, NJ	07974	USA	L
[illegible]LEY	PAUL L.	SANDIA NATIONAL LABS	DIVISION 1143	ALBUQUERQUE, NM	87185	USA	S
GREENBERG	KENNETH E.	SANDIA NATIONAL LABS	DIVISION 1124	ALBUQUERQUE, NM	87185	USA	L
[illegible]RLSON	DAVID L.	NAVAL RESEARCH LAB	CODE 6570	WASHINGTON, DC	20375	USA	D
GUEL	GRACIELA R.	UNIVERSITY OF NEW MEXICO	TAPY HALL 101	ALBUQUERQUE, NM	87131	USA	S
GUENTHER	ARTHUR H.	AIR FORCE WEAPONS LAB		KIRTLAND AFB,NM	87117	USA	D
HADLEY	G. RONALD	SANDIA NATIONAL LABS	DIVISION 1124	ALBUQUERQUE, NM	87185	USA	S
HALE	CHARLEY P.	SPECTRON/A TITAN COMPANY	2017 YALE BLVD SE	ALBUQUERQUE, NM	87106	USA	D
HANAKER	HENRY C.	VARIAN ASSOC MSK-115	GILHAMSEN WAY	PALO ALTO, CA	94303	USA	S
HARRIS	PHILIP J.	SANDIA NATIONAL LABS	DIVISION 1124	ALBUQUERQUE, NM	87185	USA	L
HARRISON	FRANCIS B.	LOS ALAMOS NATIONAL LAB	MS E-543	LOS ALAMOS, NM	87545	USA	D
HENRY	CHARLES H.	AT&T BELL LABORATORIES	600 MOUNTAIN AVENUE	MURRAY HILL, NJ	07974	USA	S
HERMAN	IRVING	COLUMBIA UNIVERSITY		NEW YORK, NY	10027	USA	L
HETHERINGTON	WILLIAM M.	UNIVERSITY OF ARIZONA	DEPT OF CHEMISTRY	TUCSON, AZ	85721	USA	L
HIGBY	PAIGE L.	NRL/SFA	1401 MCCORMICK DR	LANDOVER, MD	20785	USA	D
HILL	DAILY S.	MCDONNEL DOUGLAS OPTO CTR	3600 EXECUTIVE BOULEVARD	ELMSFORD, NY	10523	USA	S
HILLMAN	PAUL D.	AFWL/ARBF	KIRTLAND AIR FORCE	ALBUQUERQUE, NM	87117	USA	S
HJELME	DAG R.	UNIVERSITY OF COLORADO	DEPT OF EE, CAMPUS BOX 425	BOULDER, CO	80309	USA	S
HO	PAULINE	SANDIA NATIONAL LABS	DIVISION 1126	ALBUQUERQUE, NM	87185	USA	L
HOGGE	CHARLES B.	AIR FORCE WEAPONS LAB	KIRTLAND AIR FORCE BASE	ALBUQUERQUE, NM	87111	USA	D
HONIMER	JOHN P.	SANDIA NATIONAL LABS	DIVISION 1124	ALBUQUERQUE, NM	87185	USA	S
HOLLBERG	LEO W.	NATL BUREAU OF STANDARDS	325 BROADWAY	BOULDER, CO	80303	USA	S
HUTCHINSON	JAMES A.	UNIV OF CALIFORNIA, IRVINE	DEPT OF CHEMISTRY	IRVINE, CA	92717	USA	L
IACOVAZZI	ROBERT A.	MARTIN MARIETTA AEROSPACE	PO BOX 5837 MP 150	ORLANDO, FL	32806	USA	D
INAI	HAJIME	FUJITSU LABORATORIES	10-1 MORINOSATO-WAKAMIYA	ATSUGI		JAPAN	S
INGLE	JEFFREY T.	DEPARTMENT OF DEFENSE	9800 SAVAGE ROAD	FORT MEADE, MD	20755	USA	S
JANSEN	MICHAEL	TRW ELECTRO OPTICS RES CTR	ONE SPACE PARK	REDONDO BH, CA	90278	USA	S
KAMINOW	IVAN P.	AT&T BELL LABORATORIES	BOX 400	HOLMDEL, NJ	07733	USA	S
KARR	THOMAS J.	LLNL	PO BOX 808, L-495	LIVERMORE, CA	94550	USA	D
KAWANISHI	HISENORI	SHARP CORPORATION	2613-1 ICHINOMOTO-CHO	TENRI-SHI	632	JAPAN	S
KAY	BRUCE D.	SANDIA NATIONAL LABS	1841 PO BOX 5800	ALBUQUERQUE, NM	87185	USA	L
KEILBACH	KEVIN A.	UNIVERSITY OF ARIZONA	OPTICAL SCIENCES CENTER	TUCSON, AZ	85721	USA	D
KELLER	RICHARD A.	LOS ALAMOS NATIONAL LAB	4 LA ROSA CT	LOS ALAMOS, NM	87454	USA	L
KELLY	SHAWN L.	ROME AIR DEVELOPMENT CTR	RADC/OCSE	GRIFFISS AFB,NY	13441	USA	D

SOUTHWEST OPT.. . FERENCE
REGISTRATION

LASTNAME	FIRSTNAM	ORGANIZA	ADDRESS1	ADDRESS2	MAILCODE	COUNTRY	DIGES
KEMPI	DAVID J.	ROCKWELL INTERNATIONAL CORP	2397 BERNARD PL SE,SUITE 207	ALBUQUERQUE, NM	87106	USA	L
KINDER	FLOYD A.	CONAREA	509 LAS PASAS	RIDGECREST, CA	93555	USA	O
KING	C. W.	HARSHAW/FILTROL PARTNERSHIP	6801 COCHRAN ROAD	SOLON, OH	44139	USA	O
KOCH	THOMAS L.	AT&T BELL LABORATORIES	CRAWFORDS CORNER ROAD	HOLMDEL, NJ	07733	USA	S
KRANJISIC	ROMAN J.	BDM	1801 RANDOLPH ROAD SE	ALBUQUERQUE, NM	87106	USA	O
KULLENDORFF	NILS J.	RIFA ERICCSON, DEPT U/TY	S-16321	STOCKHOLM		SWEDEN	S
KUO	CHIEN-YU	AT&T BELL LABORATORIES	555 UNION BLVD, RM 2C-205	ALLENTOWN, PA	18103	USA	S
LACOURSE	JOANNE	GET LABORATORIES	40 SYLVAN ROAD	WALTHAM, MA	02254	USA	S
LAM	MARILYN A.	MARTIN MARIETTA	PO BOX 9316	ALBUQUERQUE, NM	87119	USA	O
LEE	SONG	UNIVERSITY OF FLORIDA	ELEC ENG, 216 LARSEN	GAINESVILLE, FL	32611	USA	S
LEE	T. P.	BELLCORE		RED BANK, NJ	07701	USA	S
LEGER	JAMES R.	MIT LINCOLN LABORATORY	244 WOOD STREET	LEXINGTON, MA	02173	USA	S
LEMAIRE	HERVE L.	UNIVERSITY OF ARIZONA	DEPARTMENT OF CHEMISTRY	TUCSON, AZ	85721	USA	S
LIAU	ZONG-LONG	MIT LINCOLN LABORATORY	PO BOX 73	LEXINGTON, MA	02173	USA	S
LOWDERMILK	HOWARD	LLNL	PO BOX 808	LIVERMORE, CA	94550	USA	O
LUO	JHY-MING	UNIVERSITY OF NEW MEXICO	CTR FOR HIGH TECH MATERIALS	ALBUQUERQUE, NM	87131	USA	S
MACLEOD	ANGUS	UNIVERSITY OF ARIZONA	OPTICAL SCIENCES CENTER	TUCSON, AZ	85721	USA	S
MACOMBER	STEVEN H.	PERKIN-ELMER	100 WOOSTER HEIGHTS ROAD	DANBURY, CT	06810	USA	S
MAGEE	CARL J.	NASA LANGLEY RESEARCH CTR	MS-468	HAMPTON, VA	23665	USA	S
MANTE	JOSEPH L.	SIEMPS RTL	105 COLLEGE ROAD EAST	PRINCETON, NJ	08540	USA	S
MARCHIANDO	JAY F.	NATL BUREAU OF STANDARDS		GAITHERSBURG, MD	20899	USA	L
MARION	JOHN E.	LLNL	L-456	LIVERMORE, CA	94550	USA	S
MASLEY	ANDREW J.	TRW ELECTRO OPTICS RES CTR	ONE SPACE PARK	REDONDO BH, CA	90278	USA	S
MCCRAE	JACK E.	KIRTLAND AIR FORCE BASE	AFWL/ARBE	KIRTLAND AFB,NM	87117	USA	S
MCCREADY	DAVID E.	MARTIN MARIETTA	PO BOX 9316	ALBUQUERQUE, NM	87119	USA	O
MCGARVEY	JOHN	BOEING ELECTRONICS	PO BOX 24969 MS 73-05	SEATTLE, WA	98124	USA	S
MCINERNEY	JOHN G.	UNIVERSITY OF NEW MEXICO	CTR FOR HIGH TECH MATERIALS	ALBUQUERQUE, NM	87131	USA	S
MCNALLY	JAMES J.	USAF ACADEMY	DEAP/DFP	COLORADO SGS,CO	80840	USA	O
MCNEIL	THOMAS E.	US AIR FORCE ACADEMY	4915 DOLPHIN DR	COLORADO SPG,CO	80918	USA	L
MCNEIL	JOHN R.	UNIVERSITY OF NEW MEXICO	DEPT OF ELEC ENG	ALBUQUERQUE, NM	87131	USA	L
MELNGAILIS	IVARS	MIT LINCOLN LABORATORY	PO BOX 73	LEXINGTON, MA	02173	USA	S
MILAM	DAVID	LLNL	PO BOX 808	LIVERMORE, CA	94550	USA	S
MILEY	GEORGE H.	UNIVERSITY OF ILLINOIS	214 NEL 103 S GOODWIN	URBANA, IL	61801	USA	O
MORRISON	CHARLES S.	TRW ELECTRO OPTICS RES CTR	ONE SPACE PARK B 147 RM1293	REDONDO BH, CA	90278	USA	S
MOTT	JEFFREY	PERKIN-ELMER CORP	100 WOOSTER HEIGHTS ROAD	DANBURY, CT	06810	USA	S
MULLINS	BILL	UNIVERSITY OF NEW MEXICO	CTR FOR HIGH TECH MATERIALS	ALBUQUERQUE, NM	87131	USA	L
NELSON	ROY D.	BALL AEROSPACE	PO BOX 1062	BOULDER, CO	80306	USA	S
NEWMAN	PAUL R.	ROCKWELL INTERNATIONAL	1049 CAMINO DOS RIOS	THOUSAND OAK,CA	91360	USA	L
NEWMANN	DAVID K.	USAF ACADEMY	DEPT OF PHYSICS	COLORADO SGS,CO	80840	USA	S
NEWMAN	BRIAN E.	LOS ALAMOS NATIONAL LAB	MS J566	LOS ALAMOS, NM	87545	USA	O
NOLL	ROBERT J.	PERKIN ELMER	230 LOCKWOOD ROAD	FAIRFIELD, CT	06430	USA	S
O'BRIEN	JAMES J.	UNIVERSITY OF ARIZONA	DEPT OF CHEMISTRY	TUCSON, AZ	85721	USA	L
OCHOA	ELLEN	SANDIA NATIONAL LABS	DIVISION 8435	LIVERMORE, CA	94550	USA	L
OOMEN	ROBERT W.	CHARLES EVANS & ASSOCIATES	301 CHESAPEAKE DRIVE	REDWOOD CITY,CA	94063	USA	L
OLSHANSKY	ROBERT	GTE LABORATORIES	40 SYLVAN ROAD	WALTHAM, MA	02254	USA	S
OSINSKI	MAREK A.	UNIVERSITY OF NEW MEXICO	CTR FOR HIGH TECH MATERIALS	ALBUQUERQUE, NM	87131	USA	S
OU	SIMON S.	TRW ELECTRO OPTICS RES CTR	ONE SPACE PARK	REDONDO BH, CA	90278	USA	S
OWYOUNG	ADELBERT	SANDIA NATIONAL LABS	DIVISION 1124	ALBUQUERQUE, NM	87185	USA	S
PAISLEY	DENNIS	LOS ALAMOS NATIONAL LAB	PO BOX 1663 MS J950	LOS ALAMOS, NM	87545	USA	S
PAPANNAREDDY	RAJAPPA	SOUTHERN METHODIST UNIV	ELEC ENG DEPT	DALLAS, TX	75275	USA	S
PARK	JONG-BAE	UNIVERSITY OF NEW MEXICO	CTR FOR HIGH TECH MATERIALS	ALBUQUERQUE, NM	87131	USA	S
PARTIN	JUDY K.	EG&G IDAHO INC	PO BOX 1625	IDAHO FALLS, ID	83415	USA	O
PCHELKIN	NICHOLAS R.	AIR FORCE WEAPONS LAB	AFWL/ARAF	KIRTLAND AFB,NM	87117	USA	S
PEEBLES	HENRY C.	SANDIA NATIONAL LABS		ALBUQUERQUE, NM	87185	USA	L
PENNEY	CARL M.	GENERAL ELECTRIC CORP	3 & D CENTER	SCHENECTADY, NY	12345	USA	O

March 5, 1987

SOUTHWEST OPTICS '87 CONFERENCE
REGISTRATION LIST

LASTNAME	FIRSTNAM	ORGANIZA	ADDRESS1	ADDRESS2	MAILCODE	COUNTRY	DIGI
PHILLIPS	HARVEY M.	MANAGEMENT TECHNOLOGY INT	3586 MARSHALL	RIVERSIDE, CA	92504	USA	S
PHILLIPS	DENNIS B.	MARTIN MARIETTA AEROSPACE	PO BOX 9316	ALBUQUERQUE, NM	87119	USA	J
PIERCE	BRUCE J.	SPI	PENTAGON	WASHINGTON, DC	20301	USA	G
POULESMIA	DRAGAN V.	COLUMBIA UNIVERSITY	1220 MUDD, 500 W 120ST ST	NEW YORK, NY	10027	USA	L
PORPHREY	PATRICK J.	TRW	ONE SPACE PK, MS 01-1240	REDONDO BH, CA	90278	USA	G
PREIER	HORST M.	FRAUNHOFER GESELLSCHAFT	HEIDENHOFSTRASSE 8	FREIBURG	D-7800	FED REP GER	S
PRIMAS	LORI E.	JET PROPULSION LABORATORY	4800 OAK GROVE DRIVE	PASADENA, CA	91109	USA	G
QUERNS	JOHN F.	AFWL/ARBF	KIRTLAND AFB	KIRTLAND AFB,NM	87117	USA	S
RAI	TILAK	MARTIN MARIETTA	PO BOX 9316	ALBUQUERQUE, NM	87109	USA	L
RAJA	YASIN	UNIVERSITY OF NEW MEXICO	CTR FOR HIGH TECH MATERIALS	ALBUQUERQUE, NM	87131	USA	L
RAJIC	SLOBODAN	ROCKWELL INTERNATIONAL	PO BOX 10462	DALLAS, TX	75207	USA	S
REDIKER	ROBERT H.	MASSACHUSETTS INST OF TECH	77 MASSACHUSETTS AVENUE	CAMBRIDGE, MA	02139	USA	G
REINHARDT	DIETER	CARL ZEISS	CARL ZEISS STR/POSTFACH	OBERKOCHEN	D-7082	FED REP GER	G
REISER	CHRISTOPHER	SANDIA NATIONAL LABS	DIVISION 1124	ALBUQUERQUE, NM	87185	USA	G
REYNOLDS	DONALD C.	AVIONICS LAB WPAFB		DAYTON, OH	45433	USA	L
REZEK	EDWARD A.	TRW ELECTRO OPTICS RES CTR	ONE SPACE PARK	REDONDO BH, CA	90278	USA	S
RICE	WALTER H.	ALBUQUERQUE T-VI	525 BUENA VISTA SE	ALBUQUERQUE, NM	87106	USA	S
RICKS	DOUGLAS W.	NAVAL WEAPONS CENTER		CHINA LAKE, CA	93555	USA	G
ROSENCHAIN	ALLAN	THERMA-WAVE INC	47734 WESTINGHOUSE DRIVE	FREMONT, CA	94539	USA	L
ROYCHOUDHURI	CHANDRA	PERKIN ELMER	100 WOOSTER HEIGHTS	DANBURY, CT	06810	USA	S
SALZMAN	JOSEPH J.	BELL COMMUNICATIONS RES	331 NEWMAN SPRINGS ROAD	RED BANK, NJ	07701	USA	S
SANDERS	VIRGIL F.	LOS ALAMOS NATIONAL LAB	PO BOX 1663 MS-J566	LOS ALAMOS, NM	87545	USA	L
SARDAR	DHIRAJ K.	UNIV OF TEXAS , SAN ANTONIO		SAN ANTONIO, TX	78285	USA	G
SCHAUS	CHRISTIAN F.	UNIVERSITY OF NEW MEXICO	EECE, L2150	ALBUQUERQUE, NM	87131	USA	S
SCHLOSSBERG	HOWARD	AFOSR	BUILDING 410	BOLLING AFB, DC	20375	USA	L
SCHNELL	REED A.	MARTIN MARIETTA	9316 INTERNATIONAL AIRPORT	ALBUQUERQUE, NM	87119	USA	G
SCHROEDER	HOLGER	IBM ALMADEN RESEARCH CENTER	650 HARRY ROAD	SAN JOSE, CA	95120	USA	L
SCHULTZ	JOHN F.	AIR FORCE WEAPONS LAB	KIRTLAND AFB	ALBUQUERQUE, NM	87117	USA	S
SEO	BONG-SUN	UNIVERSITY OF NEW MEXICO	CTR FOR HIGH TECH MATERIALS	ALBUQUERQUE, NM	87131	USA	S
SERGANT	MOSHE	TRW ELECTRO OPTICS RES CTR	ONE SPACE PARK	REDONDO BH, CA	90278	USA	S
SHAGAM	RICHARD N.	SANDIA NATIONAL LABS	PO BOX 5800	ALBUQUERQUE, NM	87185	USA	G
SHIAU	TIENGHUEI	UNIVERSITY OF NEW MEXICO	409 SYCAMORE ST SE	ALBUQUERQUE, NM	87106	USA	S
SHIEH	CHAN-LONG	SIEMES RTL	105 COLLEGE ROAD EAST	PRINCETON, NJ	08540	USA	S
SINARD-NORMANDIN	MARTINE	NORTHERN TELECOM ELEC	PO BOX 3511 STATION C	OTTAWA ONTARIO	K1Y 4H7	CANADA	L
SMITH	MARK W.	UNIVERSITY OF ARIZONA	OPTICAL SCIENCES CENTER	TUCSON, AZ	85721	USA	L
SNAVELY	BENJAMIN B.	EASTMAN KODAK COMPANY	901 ELMGROVE RD, DEPT 374	ROCHESTER, NY	14650	USA	G
SOARES	SCHUBERT	UNIVERSITY OF NEW MEXICO	CTR FOR HIGH TECH MATERIALS	ALBUQUERQUE, NM	87131	USA	S
SODA	HARUHISA H.	FUJITSU LAB	10-1 MORINOSTAG-WAKAMIYA	ATSUGI	243-02	JAPAN	S
SOLTZ	BARBARA A.	MCDONNELL DOUGLAS	OPTO ELECTRONICS CENTER	ELMSFORD, NY	10977	USA	S
STAMPITZ	TIMOTHY C.	UNIVERSITY OF HAWAII	603 KILOKAI ST	KAILUA, HI	96734	USA	S
STANTON	ALAN C.	SOUTHWEST SCIENCES INC.	1570 PACHECO ST SUITE E-11	SANTA FE, NM	87501	USA	G
STEWART	ALAN F.	AIR FORCE WEAPONS LAB	AFWL/ARBB	KIRTLAND AFB,NM	87117	USA	S
STOWELL	W. KENT	USAF	AFWAL/AAMD-2	WRIGHT AFB, OH	45433	USA	G
STRAND	JIM	IBM ALMADEN RESEARCH CENTER	650 HARRY ROAD	SAN JOSE, CA	95120	USA	G
STREIFER	WILLIAM	SPECTRA DIODE LABS	3333 NORTH FIRST ST	SAN JOSE, CA	94134	USA	G
STUKE	MICHAEL	MAX-PLANCK-INSTITUTE	PO BOX 2841	GOETTINGEN	D-3400	FED REP GER	L
SURGET	JEAN	ONERA	BP 72	CHATILLON CEDEX	92322	FRANCE	G
SWEATT	WILLIAM C.	SANDIA NATIONAL LABS	PO BOX 5800, DIV 7556	ALBUQUERQUE, NM	87185	USA	G
SWIHN	RANDALL T.	UNIV OF SOUTHERN CALIFORNIA	CENTER FOR LASER STUDIES	LOS ANGELES, CA	90089	USA	L
TALLANT	DAVID R.	SANDIA NATIONAL LABS	ORG 1823 PO BOX 5800	ALBUQUERQUE, NM	87185	USA	L
TAM	ANDREW C.	IBM ALMADEN RESEARCH CENTER	DEPT K07-803, 650 HARRY RD	SAN JOSE, CA	95120	USA	L
TARVIN	JEFFREY A.	SCHLUMBERGER-DOLL RESEARCH	OLD QUARRY ROAD	RIDGEFIELD, CT	06877	USA	G
THOMAS	IAN M.	LAWRENCE LIVERMORE NAT LAB	7000 EAST AVENUE L-483	LIVERMORE, CA	94550	USA	G
THOMPSON	WILLIAM E.	AIR FORCE WEAPONS LAB	AFWL/ARB	KIRTLAND AFB,NM	87117	USA	S
THORNTON	ROBERT L.	XEROX PARC	3333 COYOTE HILL ROAD	PALO ALTO, CA	94304	USA	S

SOUTHWEST OPTICS '87 CONFERENCE
REGISTRATION LIST

LASTNAME	FIRSTNAM	ORGANIZA	ADDRESS1	ADDRESS2	MAILCODE	COUNTRY	CLASS
TIHANYI	PETER L.	MCDONNELL DOUGLAS OPTC CTR	350 EXECUTIVE BLVD	ELMSFORD, NY	10523	USA	S
TROTT	WAYNE W.	SANDIA NATIONAL LABS	DIVISION 1128	ALBUQUERQUE, NM	87185	USA	L
TURANO	ANDREW J.	RAYMOND ENGINEERING, INC.	217 SMITH STREET	MIDDLETOWN, CT	06457	USA	S
TYLER	WAYNE L.	MESA COMPANY	4508 ANDREW NE	ALBUQUERQUE, NM	87109	USA	S
UCHIYAMA	SEIJI S. U.	CHIBA UNIVERSITY	IMAGE SCI ENG, 1-33 YAYOICH	CHIBA	260	JAPAN	S
VARELA	JOSEPH R.	ALBUQUERQUE T-VI	110 COLUMBIA SE 852	ALBUQUERQUE, NM	87106	USA	S
VEERAMANIKAM	CHANDRAM P.		8221 CONNECTICUT NE	ALBUQUERQUE, NM	87110	USA	S
WACHTER	JOSEPH R.	LOS ALAMOS NATIONAL LAB	MS E540 LANL	LOS ALAMOS, NM	87545	USA	L
WAGNER	DAVID K.	MCDONNELL DOUGLAS CORP	350 EXECUTIVE BLVD	ELMSFORD, NY	10523	USA	S
WAKAO	KAZUHIKE K.	FUJITSU LAB LTD	10-1 MORINOSATO-WAKAMIYA	ATSUGI		JAPAN	S
WALL	DAVID L.	SPECTRA-PHYSICS/LASER ANALY	25 WIGGINS AVENUE	BEDFORD, MA	01730	USA	L
WALPOLE	JAMES N.	MIT LINCOLN LABORATORY	240 WOOD STREET	LEXINGTON, MA	02173	USA	S
WALTHER	FREDERICK G.	MIT LINCOLN LABORATORY	BOX 73	LEXINGTON, MA	02173	USA	S
WANG	WILLIAM W.	UNIVERSITY OF NEW MEXICO	CTR FOR HIGH TECH MATERIALS	ALBUQUERQUE, NM	87131	USA	S
WARD	S. G.	LOCKHEED RESEARCH LABS	3251 HANOVER ST	PALO ALTO, CA	94304	USA	S
WATERS	ROBERT S.	MCDONNELL DOUGLAS DEC	350 EXECUTIVE BLVD	ELMSFORD, NY	10523	USA	S
WEEKS	ROBERT A.	VANDERBILT UNIVERSITY	PO BOX 1678-B	NASHVILLE, TN	37235	USA	O
WELCH	DAVID F.	SPECTRA DIODE LABS	3333 W. FIRST STREET	SAN JOSE, CA	94536	USA	S
WELFORD	DAVID	MIT LINCOLN LABORATORY	PO BOX 73	LEXINGTON, MA	02173	USA	S
WELLMAN	JOHN A.	EASTMAN KODAK COMPANY	901 ELMGROVE ROAD	ROCHESTER, NY	14650	USA	O
WESSEL	JOHN E.	THE AEROSPACE CORPORATION	PO BOX 92957	LOS ANGELES, CA	90007	USA	L
WHARTON	JOHN J.	DARPA	1400 WILSON BLVD	ARLINGTON, VA	22209	USA	O
WILCOX	JAROSLAW Z.	TRW	ONE SPACE PARK	REDONDO BH, CA	90278	USA	S
WILHELMSEN	HAROLD	MIT LINCOLN LABORATORY	WOOD STREET	LEXINGTON, MA	01781	USA	O
WILLIAMS	FORREST L.	UNM CTR FOR HIGH TECH MATLS	DEPT OF EECE	ALBUQUERQUE, NM	87131	USA	L
WILLIAMS	JAMES C.	AIR FORCE WEAPONS LAB	KIRTLAND AIR FORCE BASE	ALBUQUERQUE, NM	87117	USA	S
WILLIAMSON	BOB	SANDIA NATIONAL LABS	PO BOX 5800	ALBUQUERQUE, NM	87185	USA	L
WILLOUGHBY	CHARLES T.	TRW SPACE AND TECHNOLOGY	ONE SPACE PARK R1/1076	REDONDO BH, CA	90278	USA	S
WILSON	LOYOLA B.		3422 SMITH SE APT C	ALBUQUERQUE, NM	87106	USA	S
WILSON	KENNERLY A.	AIR FORCE	1020 VALENCIA SE #F6	ALBUQUERQUE, NM	87108	USA	S
WILSON	SCOTT R.	UNIV OF NEW MEXICO - CHTR	DEPT OF EECE	ALBUQUERQUE, NM	87131	USA	S
WOFSY	WALTER E.	US ARMY WHITE SANDS MIS RAN	1607 MEMORY LANE	ALAMOGORDO, NM	88310	USA	S
YANG	JANE J.	TRW	ONE SPACE PARK	REDONDO BH, CA	90278	USA	S
YARGER	FRED L.	NEW MEXICO HIGHLANDS UNIV	SCH OF SCI AND TECH	LAS VEGAS, NM	87701	USA	L
YOUNGER	CHRIS L.	ALBUQUERQUE T-VI	11000 SKYLINE NE #9	ALBUQUERQUE, NM	87123	USA	S
ZAH	CHUNG-EN	BELL COMMUNICATIONS RES	MYC3X361 331 NEWMAN SPG RD	RED BANK, NJ	07701	USA	S
ZAIDI	SALEEM	UNIVERSITY OF NEW MEXICO	CTR FOR HIGH TECH MATERIALS	ALBUQUERQUE, NM	87131	USA	L
ZEDIKER	MARK S.	MCDONNELL DOUGLAS ASTRO	PO BOX 516	ST. LOUIS, MO	63166	USA	S
ZMUDZINSKI	CHARLES A.	UNIVERSITY OF ILLINOIS	DEPT OF ELECTRICAL ENG	URBANA, IL	61801	USA	S
ZYSKIND	JOHN L.	AT&T BELL LABORATORIES	PO BOX 400	HOLMDEL, NJ	07733	USA	S

Total registration: 260

L = Lasers in Materials Diagnostics
S = Semiconductor Lasers
O = Optics in Adverse Environments

WEDNESDAY, FEBRUARY 11, 1987

BALLROOM LOBBY

7:30 AM–4:00 PM REGISTRATION

BALLROOM B

8:30–9:45 AM
WA, SESSION 1
W. Howard Lowdermilk, *Lawrence Livermore National Laboratory, Presider*

8:30 AM (Invited Paper)
WA1 Environmental Impacts on the Hubble Space Telescope, Terence J. Facey, *Perkin-Elmer Corporation.* This paper reviews the more significant environment factors that influence the observatory's performance, and the precautions taken during assembly operations to minimize their effects. (p. 2)

9:00 AM (Invited Paper)
WA2 Ultralightweight Optics in a Cryogenic Environment, David A. Crowe, *Eastman Kodak Company.* This paper addresses the mount attachment and mount issues related to optical design to minimize degradation of the ultralightweight mirror at 100 K with and without a kinematic mount support and mirror attachments. Key issues demonstrated by this task are: mirror optical performance room temperature to 100 K, strain-free mirror mount attachment (glass/metal), and flexured kinematic mount design. (p. 6)

9:30 AM
WA3 Learjet Observatory Operations in The Tropics, Paul H. Hagen, *Teledyne Brown Engineering;* M. G. Dix, *NASA Ames Research Center;* R. W. Russell, G. S. Rossano, D. K. Lynch, J. A. Hackwell, F. J. Rudy, D. A. Rettig, *Aerospace Corporation;* P. Alvarez, Jr., *Northrop Services, Inc.* Tropical operation of an airborne sealed open-port infrared telescope presents problems related to salt corrosion, freezing/thawing, vacuum window degradation, and elevated mirror emissivity. (p. 7)

BALLROOM LOBBY

9:45 AM–10:30 AM COFFEE BREAK

BALLROOM B

10:30 AM–12:00 M
WB, SESSION 2
Joseph H. Apfel, *Optical Coating Laboratory, Inc., Presider*

10:30 AM (Invited Paper)
WB1 Advanced Optics Fabrication Trends, William J. Kaveney. *RADC/OCSE (p. 10)*

11:00 AM (Invited Paper)
WB2 Materials for Space Optics, Bruce Pierce, *Strategic Defense Initiative. (p. 11)*

11:30 AM
WB3 Optical Fabrication Using Ion-Beam Figuring, S. R. Wilson, A. C. Barron, J. R. McNeil, *U. New Mexico.* Ion-beam figuring is a practical, efficient technique for figuring large optical components. Practical issues and performance data for a 30-cm figuring system are discussed. (p. 12)

WEDNESDAY, FEBRUARY 11, 1987—*Continued*

11:45 AM
WB4 Holography in Adverse Environments, J. Surget, *Office National d'Etudes et de Recherches Aerospatiales, France.* Holography is used for both recording an unapproachable phenomenon and restoring the 3-D real image ultimately allowed to any classical image data treatment. (p. 16)

BALLROOM B

1:30–3:00 PM
WC, SESSION 3
Benjamin Snavely, *Eastman Kodak Company, Presider*

1:30 PM (Invited Paper)
WC1 Optics for the Free Electron Laser, Thomas J. Karr, *Lawrence Livermore National Laboratory (p. 20)*

2:00 PM
WC2 All-Metal Resonator Design for Visible/Near IR Free-Electron Laser Oscillators, Brian Newnam, *Los Alamos National Laboratory. (p. 21)*

2:15 PM (Invited Paper)
WC3 Cooled Optics for High Powered Laser Applications, Patrick J. Pomphrey, *TRW. (p. 23)*

2:45 PM
WC4 Impinged Droplet Evaporative Cooling for Optical Mirrors Subjected to High Thermal Flux Loads, John A. Wellman, John J. Meyers, *Eastman Kodak Company.* Utilization of evaporative cooling for optical mirrors subjected to high thermal flux loads has been investigated. Analytical and experimental results show advantages over convective cooling. (p. 24)

BALLROOM LOBBY

3:00–3:30 PM COFFEE BREAK

BALLROOM B

3:30–5:00 PM
WD, SESSION 4
Patrick Pomphrey, *TRW, Presider*

3:30 PM
WD1 Radiation Effects in Optical Components, E. J. Friebele, *U.S. Naval Research Laboratory.* The performance of optical components is often severely degraded by exposure to radiation, usually due to the formation of defect centers. This paper reviews the effects of radiation on thin film coatings, transmissive optics, and mirror substrate materials. (p. 26)

4:00 PM
WD2 Gamma Radiation-Induced Absorptions in Calcium Fluoride; C. W. King, C. H. Nestor, *Harshaw/Filtrol Partnership.* Changes in the transmission characteristics of calcium fluoride are investigated while varying the exposure to gamma radiation. Experimental results are presented and discussed. (p. 30)

4:15 PM
WD3 Variation of the Index of Refraction in Glasses Exposed to Ionizing Radiation, Thad J. Englert, Mark C. Flohr, *U. Wyoming.* The index of refraction of optical quality glasses has been found to increase slightly with very moderate gamma-ray exposures. (p. 33)

4:30 PM
WD4 Radiation Damage to Dielectric Mirrors, Francis B. Harrison, *Los Alamos National Laboratory.* Multilayer dielectric mirrors showed no significant degradation under 120 MW/cm² of KrF light simultaneous with 10^{13} rads/s of ionizing radiation. (p. 37)

4:45 PM
WD5 Effect of Surface Pitting on Scattered Light in Transparent Domes, Douglas W. Ricks, *U.S. Naval Weapons Center.* The transmittance, total integrated scatter and near-angle scatter from several environmentally pitted glass domes have been measured and are compared. (p. 41)

BALLROOM C

6:30 PM CONFERENCE BANQUET
Colonel Lawrence L. Gooch, *Kirtland Air Force Base, Speaker*

BALLROOM LOBBY

7:30 AM–4:00 PM REGISTRATION

BALLROOM B

8:30–10:00 AM ThA, SESSION 5
Alan F. Stewart, *U.S. Air Force Weapons Laboratory, Presider*

8:30 AM (Invited Paper)
ThA1 High Damage Threshold Optical Coatings, D. Milam, *Lawrence Livermore National Laboratory.* Damage experiments with 20-ns pulses at rates up to 100 Hz indicate that some coatings survive fluences to 20 J/cm² at both 351 and 1064 nm. (p. 40)

9:00 AM
ThA2 Fluorine Resistance of Dielectric Coatings for Excimer Laser Optics, S. Foltyn, J. Boyer, G. Lindholm, K. Padgett, *Los Alamos National Laboratory. (p. 48)*

9:15 AM
ThA3 Porous Halide Antireflective Coatings for Adverse Environments, Ian M. Thomas, *Lawrence Livermore National Laboratory.* Porous magnesium and calcium fluoride coatings have been prepared from colloidal suspensions in methanol. These have excellent optical performance and high laser damage thresholds. (p. 49)

9:30 AM
ThA4 Auger Analysis of Elemental Depth Profiles Correlated with Multipulse Laser Damage of GaAs Surfaces, Dhiraj K. Sardar, Michael F. Becker, Rodger M. Walser, *U. Texas at Austin.* We study multipulse laser (10 ns, 10 Hz and 1064 nm) damage of GaAs. Damage morphologies, dependence on accumulated energy, and Auger analysis of elemental depth profiles are presented. (p. 52)

9:45 AM
ThA5 Compressive Coatings on Optical Components for Improving Mechanical Durability and Increasing Strength, J. E. Marion, *Lawrence Livermore National Laboratory.* Based on our theoretical and experimental studies, we have developed compressive coatings for slab laser components. The coatings significantly increase mechanical durability and give moderate strengthening. (p. 56)

BALLROOM LOBBY

10:00–10:30 AM COFFEE BREAK

BALLROOM B

10:30 AM–12:00 M
ThB, SESSION 6
Brian E. Newnam, *Los Alamos National Laboratory, Presider*

10:30 AM (Invited Paper)
ThB1 Natural and Induced Space Radiation Effects on Coated Laser Optics, T. M. Donovan, *U.S. Naval Weapons Center.* The results of pulsed x-ray experiments are compared with calculations of predicted melt and thermomechanical damage and discussed in the light of pulsed laser experiments. (p. 62)

11:00 AM
ThB2 Increased Visible Absorptance of Visible Reflectors due to Ultraviolet Radiation, Stephen Browning, Robert Young, *Optical Coating Laboratory, Inc.* Laser reflectors experience reversible performance degradation when exposed to ultraviolet light. Cavity ring-down lossmeter measurements show this to depend on ambient humidity, deposition conditions, and wavelength. (p. 63)

11:15 AM
ThB3 Ultraviolet Degradation of Ring Laser Gyroscope Mirrors, Austin Kalb. (p. 67)

11:30 AM
ThB4 Damage Threshold and Environmental Durability of Oxide Coatings Deposited Using Ion-Assisted Deposition, James J. McNally, *U.S. Air Force Academy;* J. R. McNeil, *U. New Mexico.* The effects of ion bombardment during deposition of Ta_2O_5, Al_2O_3 and SiO_2 thin films are presented. Laser damage, environmental durability, abrasion resistance, and fluorine gas durability results are reported. (p. 68)

11:45 AM
ThB5 Ion-Assisted Deposition of Optical Coatings at Low Temperature and Effects of Ar Bombardment and Temperature on Heavy Metal Fluoride Glass, Forrest L. Williams, D. W. Reicher, J. R. McNeil, *U. New Mexico;* J. J. McNally, *U.S. Air Force Academy;* G. A. Al-Jumaily, *Barr Associates, Inc.* Ion-assisted deposition of optical coatings at low temperature and effects of Ar bombardment and temperature on the crystalline phase of heavy metal fluoride glass are reported. (p. 72)

WEDNESDAY, FEBRUARY 11, 1987

BALLROOM B
8:30 A.M.–9:45 A.M.

WA1–3

SESSION 1

W. Howard Lowdermilk, Lawrence Livermore National Laboratory, *Presider*

Environmental Impacts on the Hubble Space Telescope

Terence A. Facey
Perkin-Elmer Corporation
Optical Group, Space Science Division
Danbury, Connecticut.

Introduction

The Hubble Space Telescope represents the largest single advance in astronomical instrumentation since the Hale 5 metre telescope at Mt Palomar. Its extreme sensitivity and resolution, however, are susceptible to degradation from a number of environmental effects. This is particularly true for observations in the ultra-violet spectrum.

Environmental factors range from dust, humidity and aerosols in the atmosphere on the ground, through the stresses and acoustic fields of the launch phase, to the thermal-vacuum rigors of the space environment itself.

Given reasonable thermal control, the near Earth orbital environment is quite benign. Essentially contamination free, and with no light pollution, space provides an almost ideal base from which to conduct astronomical observations.

The stresses of launch, too, can be overcome by reasonable design. Once the system has been designed and verified to withstand the acceleration, vibration and acoustic loads of the launch vehicle, the launch environment poses no real threat to observatory performance.

On the ground, however, during manufacture and assembly operations, there are a number of environmental factors which can significantly impact the future performance of the observatory. The two most important of these, in terms of their potential damaging impact, are dust and humidity in the atmosphere.

Atmospheric dust.

Dust particles, settling out from the atmosphere and accumulating on the surface of the mirrors will degrade performance in a number of ways. The obscuration of the primary mirror is a direct reduction in optical throughput. The small apertures have a diffraction pattern many times the full aperture diffraction limit, so light is scattered from a bright source into neighboring faint images. The particles scatter over wide angles to illuminate the telescope baffles from bright sources adding more photons to the focal plane background.

Inevitably, in the construction of a large telescope, a lengthy period of time elapses between coating the mirrors and final completion of the telescope assembly. Of course, all operations subsequent to the coating are performed in a well controlled

clean room. However, no clean room is perfectly clean, and the long duration of the assembly process makes some accumulation of dust on the optics unavoidable. In the case of Space Telescope, the primary mirror was coated in December 1981. The Optical Telescope Assembly (OTA) was completed in October 1984. During the intervening three years the mirror surface could not possibly improve - it could only deteriorate by the accumulation of contaminants.

Besides doing all assembly work in a class 10k clean room - and much subassembly work in class 1k or class 100 areas - all items of flight hardware were surface cleaned prior to their integration into the OTA.

The large light baffles, in particular, were cleaned by repeated acoustic exposure and vacuum cleaning. Their large size and close proximity to the optics make them the dominant contamination source in subsequent environmental testing, unless special care is taken in their cleaning.

Use of clean rooms, rigorous procedural control of operations and careful cleaning of hardware were all necessary - but they were not sufficient. The need for long labor intensive assembly operations in the immediate vicinity of the primary mirror, and the need to have the mirror resting face up for long periods of time made some accumulation of dust on its surface inevitable, even though it was covered most of the time.

Measurements made a year or so after the coating showed the beginning of a particulate layer which might eventually adversely affect ultra-violet sensitivity of the observatory.

A cleaning plan was developed, which would allow us to "vacuum clean" the mirror surface at the latest possible time in the assembly cycle. Thereafter, the mirror would be kept covered right up to integration with the space shuttle at Kennedy Space Center.

The special cleaning tool involved the combination of nitrogen gas jets to dislodge the particles, and a vacuum hose to suck away the debris. For the cleaning operation, the mirror was suspended face down. The cleaning head was mounted to a special carriage, which allowed the whole mirror surface to be cleaned from underneath. The cleaning was conducted during June of 1984, just prior to completion and delivery of the OTA in October. Subsequent measurements of surface particulates showed the cleaning operation to have been highly successful.

Later in the Space Telescope assembly sequence, and after the environmental tests, particulate measurements by LMSC in May of 1986 still showed very little particle contamination.

Humidity

High levels of humidity could damage the Magnesium Fluoride coatings on the mirrors. However, this was protected against by the clean room environment, in which the Relative Humidity is controlled to be below 50% at all times.

In addition to the mirrors, though, the large telescope structures are also susceptible to moisture. The major structures, and all of the optical benches, are made of graphite-epoxy. This material, chosen for its light weight, high stiffness and low expansion coefficient, is hygroscopic.

The behavior of graphite epoxy is a little like another, more common, composite material: wood. As it absorbs moisture, the material swells, and as it dries out, it shrinks again. This effect is bad enough in the floor boards of your house, but in the alignment critical structures of an astronomical telescope, it could be a disaster!

Metering Truss

The metering truss is an all graphite structure, 5 metres long by 2.5 metres in diameter. Its function is to support the secondary mirror and keep it properly aligned on the optical axis of the telescope and 4.9 metres in front of the primary mirror vertex within +/- 0.000002 metres (2 micrometres).

On the ground, in a 50% RH environment, the graphite absorbs water equal to about 0.4% of its weight. Once in space, this water will slowly evaporate from the graphite, causing the truss to shrink a total of about 350 micrometres.

In such a large structure, it is virtually impossible to prevent the absorption of water. It would take a long time to dry it out prior to launch, and would be impossible to keep dry right up to launch - especially in the high humidity of the KSC area.

Rather than prevention, in this case we opt in favor of symptomatic relief. The telescope can be refocused from the ground, by using on board wavefront sensors to determine optical image quality, and secondary mirror position actuators to realign the system. Test data and analyses have yielded a fairly good model of water desorption from the truss as a function of time and temperature. This model can be further refined early in the mission, by measuring focus errors as a function of time in orbit. Thereafter, it will be possible to make open-loop focus adjustments periodically. More accurate measurements of focus error and appropriate corrections can be made less frequently.
,cp4
Fine Guidance Sensor Optical Bench

Similar expansion and contraction occurs in the FGS optical bench. This bench is the precision support for the more than 30 elements in the FGS optical train. The purpose of the FGS is to

measure telescope pointing errors on the order of 15 nanoradians, and to do this repeatably over long periods of time. Clearly, structural distortions of its optical bench could compromise that ability.

The design of the FGS takes advantage of symmetry wherever possible to minimize the effects of mechanical growth - whether from moisture or thermal effects. Some residual moisture sensitivity remains, however. This is ameliorated by performing the final alignment in as dry an environment as possible (RH <25%) and checking the performance in a thermal vacuum chamber after it has had time to dry out. Afterward, the graphite may re-absorb water from the atmosphere, but when launched into space it will again dry out and become realigned in the process.

Management of graphite absorption and desorption is made easier in the case of the optical bench, by the shorter time constants involved. Since the graphite epoxy section thicknesses are small, the material absorbs and desorbs more rapidly than the metering truss, which can take weeks to dry out completely.

Conclusion

Environmental impacts on the Hubble Space Telescope are dominated by ground environment factors. The most important of these are associated with the atmosphere. Air-borne particulates and atmospheric humidity both present significant challenges to the assembly of a large high quality astronomical observatory. It is possible to meet these challenges, however; often not by preventing the environmental impact, but by learning to live with it.

ULTRA LIGHTWEIGHT OPTICS IN A CRYOGENIC ENVIRONMENT

DAVID A. CROWE
GOVERNMENT SYSTEMS DIVISION
EASTMAN KODAK COMPANY
ROCHESTER, NEW YORK 14650

A high performance infrared spaceborne telescope such as the Space Infra-Red Telescope Facility (SIRTF) will require aspheric optical forms with smooth, low-scatter surface, high performance coatings, and an ultra-lightweight design approach that can perform from room temperature to cryogenic temperature. The design approach must not only be rugged, low risk, and reliable, but also capable of surviving a launch environment and enduring in space for many years. A design approach, which meets performance requirements at cryogenic temperatures employing passive mirrors (without figure control actuators, sensors, electronics, etc.), offers significant advantage in weight, performance, and reliability.

For several years, Kodak has been engaged in developing passive fused silica mirrors which meet stringent weight budgets and optical figure quality requirements from room temperature to cryogenic temperature. This capability has been successfully demonstrated with ultra-lightweight fused silica, frit bonded mirrors with and without broadband multilayer high reflectance coating up to diameters of 0.5 meters. Technical issues addressed and resolved include the design and manufacture of ultra-lightweight frit mirrors, CTE match, bond strength, CTE homogeneity, polishing to diffraction limited quality, optical stability, optical performance at cryogenic temperature and coating performance.

The next logical step in this technology evolution is to demonstrate the optical performance of these new generation ultra-lightweight mirrors kinematically mounted and subjected to cryogenic environment. This paper addresses the mount attachment and mount issues related to optical design to minimize degradation of the ultra-lightweight mirror at 100° Kelvin with and without a kinematic mount support and mirror attachments. Key issues demonstrated by this task are: (1) mirror optical performance room temperature to 100° Kelvin, (2) strain-free mirror mount attachment (glass/metal), and (3) flexured kinematic mount design.

Learjet Observatory Operations in The Tropics

Paul H. Hagen
Teledyne Brown Engineering
MS 211-12
NASA Ames Research Center
Moffett Field, Ca 94035

M. G. Dix
MS 244-10
NASA Ames Research Center
Moffett Field, Ca. 94035

R. W. Russell, G. S. Rossano,
D. K. Lynch, J. A. Hackwell,
R. J. Rudy, D. A. Retig
MS M2/266
The Aerospace Corporation
El Segundo, Ca 90245

P. Alvarez, Jr.
MS 248-2
Northrop Services Inc.
Ames Research Center
Moffett Field, Ca 94035

Tropical operation of an airborne sealed open-port infrared telescope presents problems related to salt corrosion, freezing/thawing, vacuum window degradation, and elevated mirror emissivity.

NOTES

WEDNESDAY, FEBRUARY 11, 1987

BALLROOM B
10:30 A.M.–12:00 M

WB1–4

SESSION 2

Joseph H. Apfel, Optical Coating Laboratory, Inc.,
Presider

WB1

Advanced Optics Fabrication Trends

William J. Kaveney
RADC/OCSE

W52

Materials for Space Optics
Bruce Pierce
The Pentagon

Optical Fabrication Using Ion Beam Figuring

S.R. Wilson, A.C. Barron, and J.R. McNeil
Department of Electrical Engineering
Center for High Technology Materials
University of New Mexico
Albuquerque, New Mexico 87131

1.0 Introduction and Background

The application of ion beams to the figuring of optical surfaces has been examined for a number of years by several groups of investigators. The technique is generally intended to perform the final figuring of surfaces which have several optical waves of error relative to the desired figure. Until recently, ion beam figuring has not offered promise to be an efficient, practical method for figuring optics.

Today, the ion beam figuring (IBF) process appears to be very viable, based upon advances over the past several years in two areas of technology. First, ion beam sources now have current capabilities over 1000 times higher than those sources available when the IBF process was first considered. Higher current capability translates directly into higher material removal rates. In addition, the ion sources available today are relatively small and can be easily maneuvered within a vacuum system, in sharp contrast with the physically very large ion sources which were once considered for IBF.

Second, phase measuring interferometers are available which are capable of automatically acquiring a map of the optical surface. A surface map typically consists of a numerical array describing the optical phase at several thousand points on the surface. This data format is quite adaptable to automation when contrasted to fringe acquisition, processing, and reduction.

The ion beam figuring process has a number of advantages over conventional figuring techniques, especially for processing large, lightweight optics. These advantages include the following:

1. IBF is a deterministic process. Fewer figuring iterations are required to achieve a given figure.
2. IBF can figure 100% of a surface. There are no edges effects as with conventional polishing.
3. IBF can be used to figure delicate, lightweight structures: temporary warping and related problems due to weight loading are eliminated.
4. IBF is not constrained to any particular shape of optic, whereas conventional polishing techniques are most easily applied to circular optics.
5. IBF is capable of correcting long spatial wavelength figure errors. Conventional polishing becomes very time consuming when dealing with these kinds of errors.
6. IBF, metrology, and final coating can be performed in one location, with the optic in its final mount and final orientation.

The work described here summarizes several years effort investigating the IBF process. We have examined a number of practical issues, and have preliminary results from the application of IBF to figuring 30 cm diameter optics.

2.0 Experimental Arrangement

The experimental arrangement we are presently using to figure 30 cm glass and metal optics is illustrated in Figure 1. The one-cubic-meter box coater contains the optic, one or more Kaufman ion sources for slective material reomval, and a sputtering source for the selective deposition of substrate material. The sources are mounted on a computer controlled translation apparatus. The surface is monitored by a ZYGO Mark III phase measuring interferometer with a 30 cm imaging aperture. Optical surface map information is transferred to a minicomputer where system algorithms determine the ion source operation parameters required to figure the surface. The same system arrangement concepts can be scaled to accommodate large optics.

3.0 Practical Issues

Practical issues which have been considered in applying the IBF process include the effect of ion milling on surface roughness, substrate removal rate, substrate damage due to ion milling, the redeposition of sputtered substrate material on the optic, and the properties of ion sources (profiles, stability, repeatability, controllability, etc).

To examine the effect of ion milling on surface roughness, fused silica substrates were characterized for surface roughness as a function of ion milling depth. For example, in the case of fused silica, roughness does not noticeably increase for mill depths as large as 15 microns. Surface roughness does not appear to be a problem for glassy or single-crystal materials. The surface roughness was characterized using our optical scatterometer, substantiated by stylus profilometer measurements at the Naval Weapons Center.

Substrate damage due to ion milling was assessed by ion milling fused silica substrates to a depth of 1.5 microns, then examining the surface using infrared ellipsometry (performed at the Naval Weapons Center). No damage was detected, within the measurement accuracy.

The substrate removal rate was characterized using the interferometer and carefully controlled ion doses. At an ion energy of 1500eV, the removal rate for fused silica using Ar^+ ions was found to be 13.7 mg/Amp-min. Thus for a one ampere ion current (easily achieved using multiple sources), the time to remove 1 micron of fused silica from a 1 square meter substrate would be 2.8 hours. This is much faster than the time required to perform the removal using conventional polishing techniques. If Kr^+ ions were used, this time would be reduced by approximately 30 percent.

The problem of redeposition of sputtered material back onto the optic was found to be easily eliminated through the use of properly designed shields.

The ion sources were characterized using current probes and, after milling suitable test flats, interferometry. The beams were found to be temporally and spatially stable after a short warmup period. The use of intelligent power supplies greatly enhances the stability of the ion sources.

4.0 System Algorithms

The system algorithm determines the manner in which the ion beams are directed onto an optical surface to achieve a given figure, and ultimately determines the total time required to figure the surface. In addition, the system algorithm makes it possible the estimate how closely a given desired surface figure can be achieved, given the starting figure and a menu of available ion source profiles.

The computation of the dwell time of the ion beam at each point on the optic is based on deconvolution methods similar to those used in image restoration. The low image noise levels and well characterized spatially invariant ion beam milling point spread function allow the restoration to be performed using Fourier-transform based, thresholded inverse filtering techniques. The nonnegativity constraint for ion beam dwell times is satisfied when proper threshold levels are used.

For optical surfaces with a short focal length, additional processing will be necessary. This is due to the fact that the removal profile may have some spatially variant components as the surface slope becomes large.

5.0 Results of Figuring a 30 cm Optic

We have preliminary results from figuring 30-cm optical flats of both copper and fused silica. In the case of the fused silica sample, the initial surface was approximately 1.8 waves peak-to-valley (0.41 waves RMS) from flat. Using a single, 40ma ion source, the optic was figured to 0.27 waves peak-to-valley (0.042 waves RMS) from flat in 5.5 hours of beam time. The figure of the optic both before and after ion beam figuring is illustrated in Figure 2. Due to the limited metrology capability of the prototype IBF system, further figuring was not attempted.

6.0 Summary

To date there appears to be no fundamental issue to prevent the IBF process from being a practical method to figure glass-like optical materials. Preliminary performance data from figuring a 30 cm fused silica optical flat appears promising.

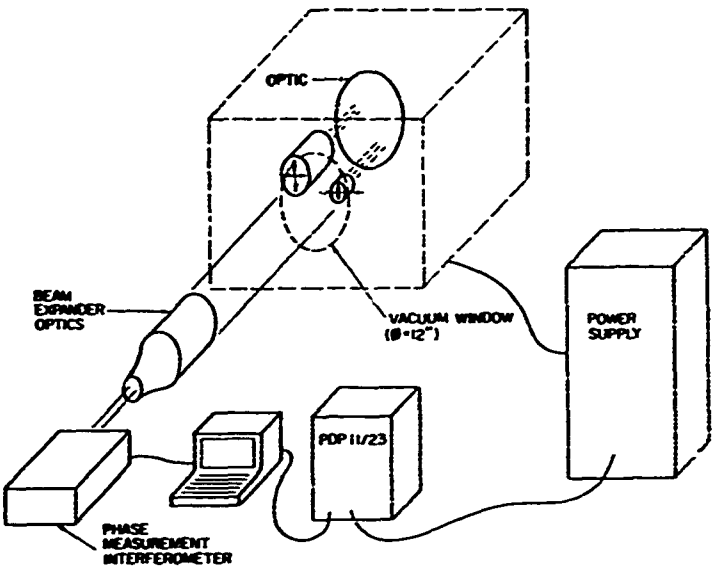

FIGURE 1. Experimental arrangement of the IBF system.

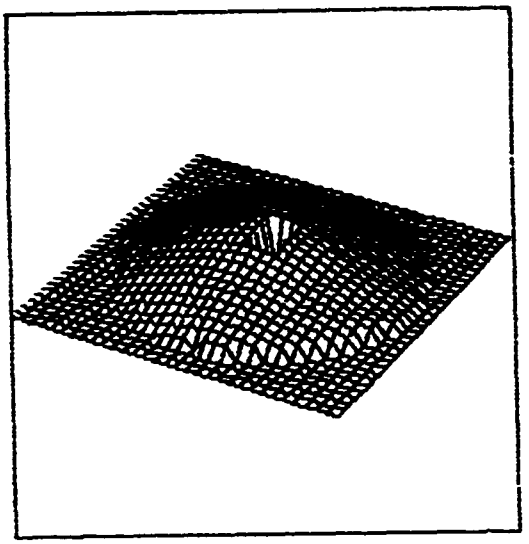

Starting surface

P-V = 1.762 waves

RMS = 0.405 waves

1 wave = 633 nm

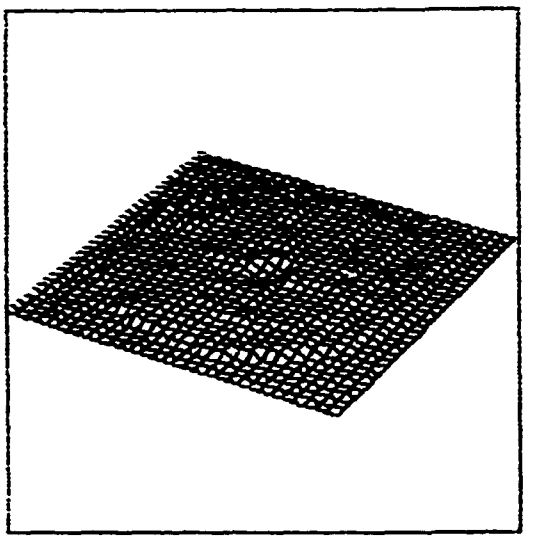

Residuals after milling

P-V = 0.267 waves

RMS = 0.042 waves

1 wave = 633 nm

FIGURE 2.

Full system demonstration to figure 30cm fused silica flat. Total beam dwell time: 5.5 hours. The apparent hole in the center of the optic is an obscuration in the interferometer beam train.

HOLOGRAPHY IN ADVERSE ENVIRONMENT

by J. Surget
Office National d'Etudes et de Recherches Aérospatiales
BP 72, 92322 Châtillon Cedex - France

The important sizes of easily available holoplates compared with the diameter of a classical microscope lens makes it possible to obtain a given value of angle u with a much greater distance of view D using holography rather than using any conventional optical system.

2 - Application to gliding spark propagation study

The holographic image transport technique was used at first for the investigation of the gliding spark propagation on a surface, intended to simulate in laboratory an atmospheric leader lightning [2,3].

The two purposes of this study are the measurements of the radius of the spark channel and its refractive index (the value of the latter being related to the local electron density).

As the radius channel varies from 100 to 300 µm depending on the test conditions, a microscope is needed to measure it. However, it is impossible to observe the arc directly through a microscope since the 120 000 V electric voltage used for the experiment requires a free distance of 400 mm for safety. Moreover, for each discharge, the channel has to be examined simultaneously over a length of some 150 mm, which is of course much greater than a microscopic field of view.

Consequently, a specially designed holographic set-up has been implemented (Fig. 3) [4,5]. An expanded laser beam (test beam T) is directed to a dielectric polished slab P on which the discharge propagates. The reflected test beam comes back to the photoplate H after double passing through the discharge channel. The laser is a pulsed yag laser, frequency doubled, delivering 0.22 J in 15 ns at 0.532 nm. The visible radiation associated with the electric discharge has a low level compared to the laser beam in plane H, so that, the channel behaves like a simple transparent medium (phase object).

A reference collimated beam R originating from the same laser is also directed to H after a symmetrical path regarding to the test path.

Figure 4 shows the apparatus as installed in the discharge laboratory. The dark pannel standing in the back is the polished black plexiglass wall serving as a dielectric. The spark glides over this pannel guided by an electrode vertically fixed on its rear face. The holographic bench does not touch the plexiglass: it is located at a distance D = 400 mm from the spark region as indicated figure 3. On account of this safety interval, the theoretical resolution limit calculated from (1) is 3.5 µm for the 102 x 127 mm photoplate area.

The laser, on the right side of the photograph is not part of the holographic device, but is placed at a safe distance (2 m) from the plexiglass pannel raised to 120 000 V.

Interferograms of the discharge channel are recorded using the double exposure holographic technique, with various delays ΔT after the spark ignition. Figure 5 shows two examples of finite fringe interferograms. The radius of the channel and the refractive index inside it are deduced from the deformation of the original straight pattern [3,5].

These interferograms (Fig. 5) reconstructed as indicated Figure 1c were photographed through an usual microscope, also used for fringe shift measurements (Fig. 3b).

3 - Conclusion

Holography has been successfully operated for the investigation of the gliding spark propagation on a surface. High voltage (120 kV) requires, for safety considerations, a minimum distance of 400 mm between the spark and the observationnal device, excluding direct observation by means of a microscope. This severe constraint has been overcome using a holoplate as an intermediate storage between the unapproachable phenomenon and instruments of observation and analysis.

The diameter of the discharge channel has been measured with an accuracy of 5 µm over a length of 150 mm. Furthermore, the value of the refractive index inside the spark has been determined.

It can be mentionned that a similar holographic device was also applied for the study of the internal structure of a turbulent seeded gas flame, and also for studying the deformation of a three dimensional opaque object placed at several meters [6].

These examples demonstrate the ability of holography as a powerfull technique for observing an unapproachable phenomenon.

Bibliography

1. Françon, M., *Holographie*, Masson et Cie, 1980.
2. Larigaldie, S., Labaune, G., and Moreau, J.P., *Lightning leader laboratory simulation by means of rectilinear surface discharges*, J. Appl. Phys., 52, n° 12, 1981.
3. Larigaldie, S, *Etude expérimentale et modélisation des mécanismes physiques de l'étincelle glissante*, Thèse de Doctorat d'Etat, Faculté d'Orsay, n° 3017, June 1985.
4. Surget, J., *Holographic device for rectilinear surface discharge visualization*, 3rd Int. Symp. on Flow Visualization, Ann Arbor (USA), TP ONERA n° 1983-104, Proceedings by Hemisphere Publishing Corporation, 1983.
5. Surget, J., *Banc d'holographie par réflexion. Application à l'étude interférométrique d'étincelles glissantes*, Proceedings 16ème Congrès Int. de Photographie Rapide et de Photonique, Strasbourg, August 27-31, 1984. SPIE Vol. 491, TP ONERA n° 1984-79.
6. Surget, J., *Holographic device for analysis of objects inaccessible by direct microscopic technique*, Proceedings 2nd Int. Symp. on Optical and Electro-Optical Applied Science and Engineering, Cannes, Nov. 25-Dec. 6, 1985, to be published by SPIE, TP ONERA n° 1985-159.

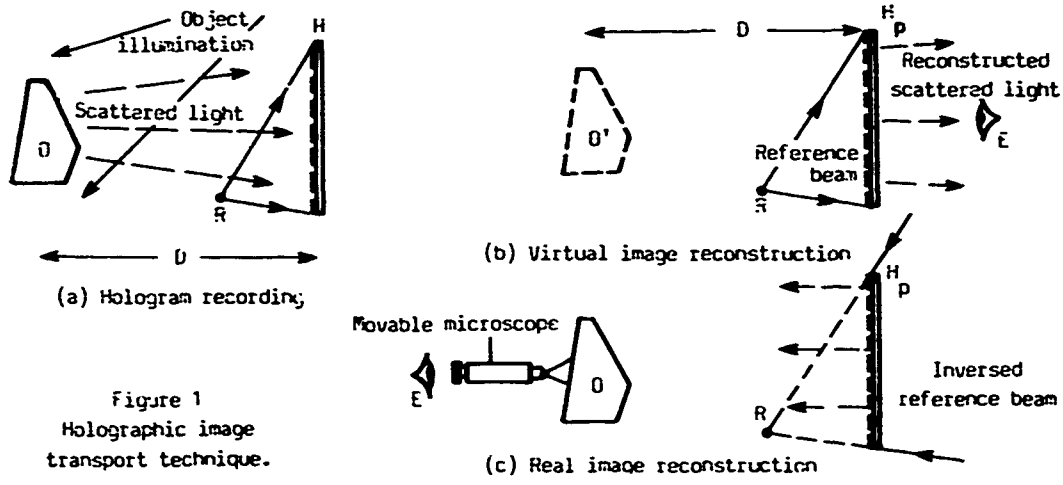

Figure 1
Holographic image transport technique.

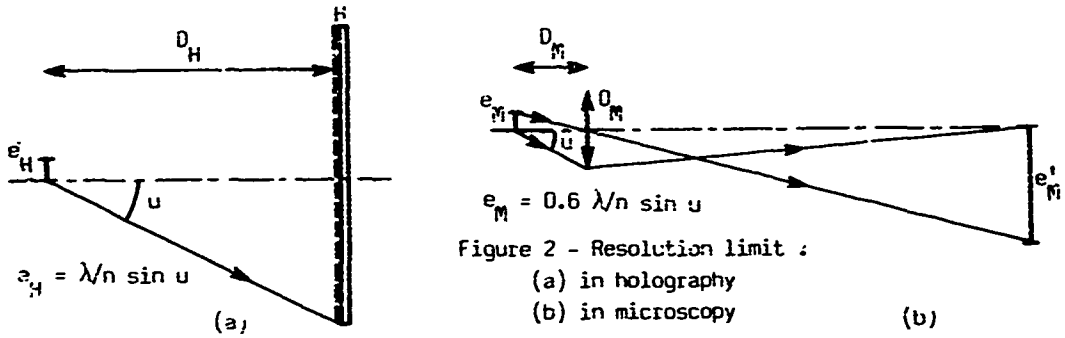

Figure 2 - Resolution limit :
(a) in holography
(b) in microscopy

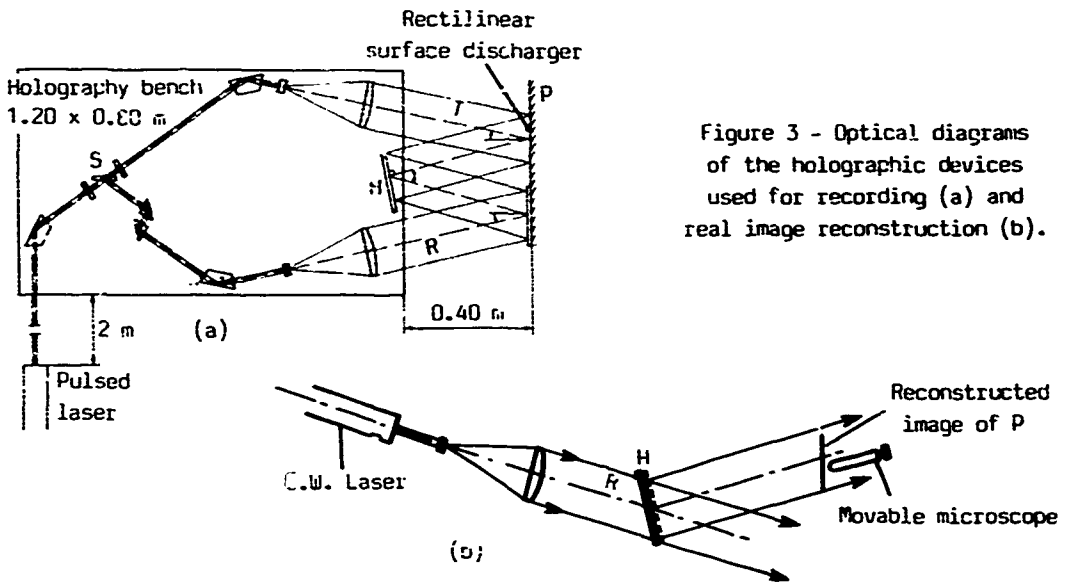

Figure 3 - Optical diagrams of the holographic devices used for recording (a) and real image reconstruction (b).

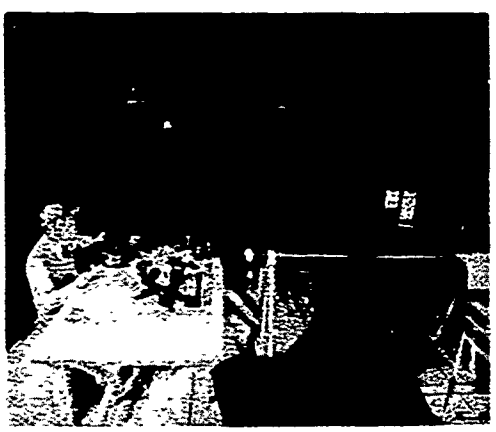

Figure 4
Experimental set-up.

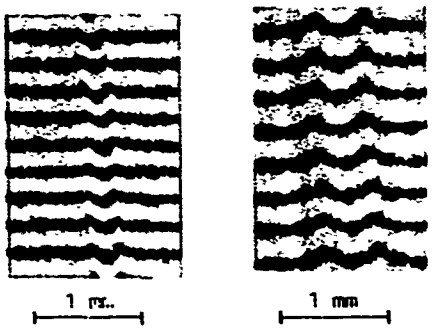

ΔT = 145 ns ΔT = 420 ns

Figure 5
Discharge channel
finite fringe interferograms

WEDNESDAY, FEBRUARY 11, 1987

BALLROOM B
1:30 P.M.–3:00 P.M.

WC1–4

SESSION 3

Benjamin Snavely, Eastman Kodak Company,
Presider

WC1

Optics for the Free Electron Laser
Thomas J. Karr
Lawrence Livermore National Laboratory

All-Metal Resonator Designs for Visible/Near-Infrared Free-Electron Laser Oscillators*

Brian E. Newnam
Chemistry and Laser Sciences Division
Los Alamos National Laboratory, MS J566
Los Alamos, New Mexico 87545

Summary

The multiple radiation environment of future high-current free-electron laser (FEL) oscillators will pose severe requirements on the resonator mirrors. In addition to withstanding the high-average power, high-repetition-rate pulses of the fundamental laser radiation, the optical properties of the mirrors must not be degraded by the attendant optical harmonics, gamma rays, neutrons, electrons, and vacuum. Furthermore, the initial mirror absorption must be low enough so that the reflected wavefront distortion is tolerable when various types of mirror cooling are employed.

Multilayer dielectric reflectors for visible- and near-infrared wavelengths are known to be susceptible to damage or degradation by several of the above radiation hazards, and experimental data to support their use in the presence of some of the other radiations is just now becoming available. To assure that future operation of high-power oscillators will not be limited by optical damage considerations, we propose the use of ring-resonators consisting of all-metal mirrors. One such resonator design, shown in Fig. 1, includes multiple-facet, end mirrors and intracavity beam-expanding mirrors each used at grazing incidence, e.g. $\emptyset_{inc} \geq 85°$. The metal of choice for wavelengths longer than 500 nm is vacuum-deposited silver although gold and copper films are possible alternatives. At such large angles with S-polarization, the metal mirrors are much less susceptible to degradation from exposure to the high-energy radiations than are dielectrics. Further, scaling to large sizes should be within the potential capabilities of the optical industry.

We have accumulated and evaluated pertinent experimental data on metal mirror reflectance, absorptance, scatter, and damage resistance, published by a number of researchers, to support the technical feasibility of all-metal FEL resonators.

---

* This work was performed under the auspices of the US Department of Energy and supported by the US Army Ballistic Missile Defense Organization.

Figure 1.

**ALL-METAL RING RESONATOR
WILL WITHSTAND HIGH-POWER LASER INTENSITY
AND HIGH-ENERGY RADIATIONS**

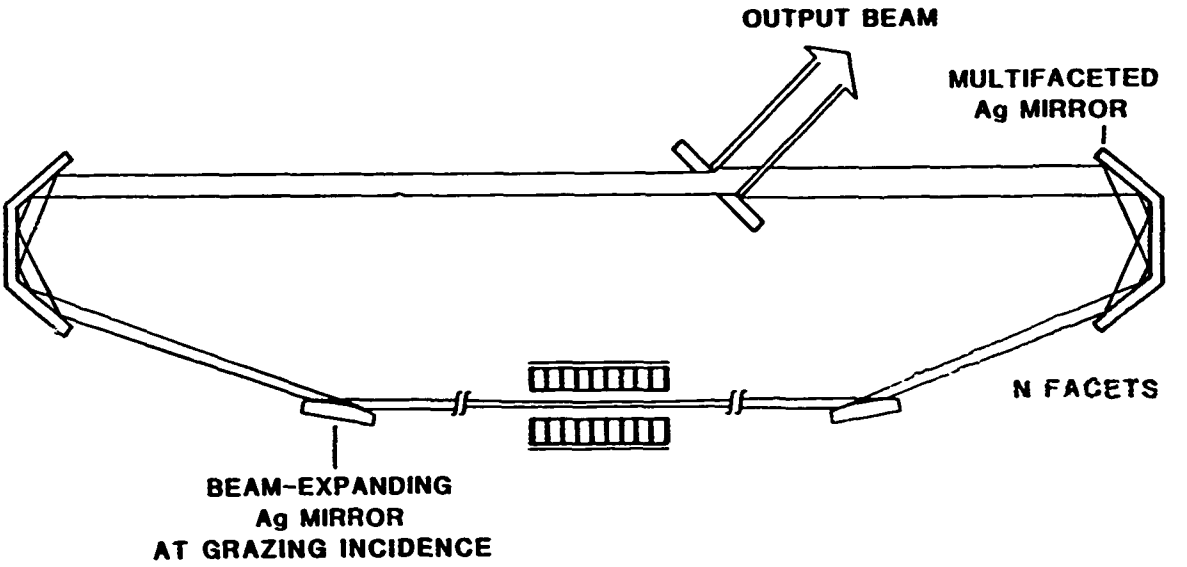

WC3

Cooled Optics for High Powered Laser Applications
Patrick J. Phomphrey

Impinged Droplet Evaporative Cooling for Optical Mirrors Subjected to High Thermal Flux Loads

John A. Wellman
Eastman Kodak Company
901 Elmgrove Road
Rochester, New York 14650

John J. Meyers
Eastman Kodak Company
901 Elmgrove Road
Rochester, New York 14650

Utilization of evaporative cooling for optical mirrors subjected to high thermal flux loads has been investigated. Analytical and experimental results show advantages over convective cooling.

WEDNESDAY, FEBRUARY 11, 1987

BALLROOM B
3:30 P.M.–5:00 P.M.

WD1–5

SESSION 4

Patrick Pomphrey, TRW, *Presider*

Radiation Effects in Optical Components

E.J. Friebele
Naval Research Laboratory
Washington, DC 20375

Components of high performance optical devices may be exposed to high energy radiation environments during their lifetime. The effect of these adverse environments depends upon a large number of parameters associated with the radiation (nature, energy, dose, dose rate, etc.) or the system (temperature, optical performance requirements, optical wavelength, optical power, path length, etc.), as well as the intrinsic susceptibility of the optical component itself to degradation. Two years ago there was a special session on Radiation Effects in Optical Materials at the Southwest Conference on Optics,[1] and the reader is referred to this volume for an in-depth description of materials effects.

Radiation Environments

The principal radiation environments to be considered in this review are defined by energies substantially greater than the band gap of the optical materials. Hence, the damage mechanisms will be primarily electronic or atomic in nature, rather than thermal, as in the case of high energy laser damage. Naturally, there will be synergistic effects in an optical element that is simultaneously exposed to nuclear and laser radiations, but the primary concern of the review is the former.

The natural radiation environment is perhaps the most benign. Terrestrial dose rates are low, ≈0.1 rads per year both at sea level or, interestingly, on the ocean floor due to ^{40}K and ^{226}Ra in both the sea water and sediment and ^{230}Th in the sediment; substantially higher dose rates can occur near high activity deposits. In space the dose rate and energy depend on the height and inclination of the orbit and can be >50 rads/day. Of course, the spectrum is highly peaked at low energy so that shielding is effective in reducing the dose rate to a point, but rates of 1 rad/day are easily anticipated on the interior of a spacecraft in a low earth polar orbit.

The system in or near which the optical device is operating can also be a source of radiation. For example, optics may be used to monitor the interior of nuclear reactors or fusion devices; the optics in high energy lasers are exposed to scattered electrons and x-rays from the pump; and the laser itself can induce color centers through multiphoton processes. The nature of the system-induced radiation environment obviously varies widely, but the more benign case of the scattered laser pump irradiation will certainly be exacerbated by the high power laser loading of the optic.

Finally, one must consider the effect of hostile radiation exposure on optical components. The nature and energy of such an environment depends on factors such as weapon type, yield, burst height, terrain, etc., and the reader is referred to the book by Glasstone and Dolan.[2] Generically, there is an initial "prompt" transient irradiation consisting of γ-rays, neutrons and beta particles from the fission and fusion reactions; the duration of this pulse is typically 10-50 nsec. [In the same time scale is the so-called thermal or

blackbody radiation of the weapon, which occurs in the 0.1-100 A (120-0.12 keV) range, corresponding to soft x-rays.] The atmosphere serves as an attenuator for the high energy radiation pulse, whereas the dose can be several orders of magnitude greater in space. Following the nuclear reaction, optical components will receive subsequent radiation due to decay of fission product isomers, γ-rays from high energy compound nuclei formed by neutron capture, and γ-rays resulting from radiative capture reactions of high energy neutrons with nitrogen nuclei. This latter component is particularly important since the γ rays have high energy. The total dose associated with these delayed γ components is limited by the overpressure and thermal radiation that the system can withstand. Finally, there are residual sources of radiation due to fallout for terrestrial systems and the enhancement of the Van Allen belts for spacecraft.

Damage Mechanisms

There are basically three damage mechanism appropriate to optical materials, whether they are crystals or glasses:

1. Knock-on damage results from the transfer of momentum and energy from an incident particle to a atom sufficient to break bonds and move the atom from its normal lattice position. As a rule of thumb, 25 eV must be transferred to the atom for this process to occur. It is easy to envision atomic displacements in materials bombarded with neutrons or ions, but electrons with energies $\approx$100 keV can transfer 25 eV energy to the lattice atom. Likewise, if incident photons such as γ rays or x rays have sufficient energy, displacements can still occur via the Compton process. ^{60}Co γ rays (1.5 MeV) can lead to copious displacements of both Si and O in SiO_2, while 100 keV x-rays cannot transfer sufficient energy to the Compton electrons to displace either.[3]

2. Damage in the form of electron rearrangement occurs when radiation-generated free electrons and holes are trapped at separate sites in the material. The formation of electron-hole pairs by ionization is the most dominate process in any irradiation, but whether or not the individual carriers are separately trapped depends on the presence of precursor trapping sites or their creation by the irradiation itself. For example, an oxygen vacancy in amorphous SiO_2 (≡Si : Si≡) can trap a hole, leading to the formation of an E' center (≡Si $^{\bullet}$), while the corresponding interstitial oxygen in the form of a peroxy linkage (≡Si-O-O-Si≡ also traps a hole to form a peroxy radical (≡Si-O-O$^{\bullet}$). Both these defect centers have been detected in irradiated SiO_2. Another example is the change of valence which occurs when multivalent ions trap holes or electrons, as in the case of Ce or Fe. It is interesting to note that irradiation of glasses with Fe impurities appears to increase the transmission in the uv as the Fe^{3+}, which absorbs in the uv, traps electrons to form Fe^{2+}, which absorbs in the ir.[4] If preexisting defects or impurities are the only available traps for the radiolytic electrons and holes, the concentration of defect centers will saturate at some fixed dose. In practice, the defect center concentration is observed to grow as some combination of linear and saturating behavior, indicating both formation and population of precursor trapping sites.

3. The radiolytic displacement of atoms has been well established in alkali halide crystals[5], but only recently attributed to oxide crystalline and amorphous materials such as SiO_2.[3] This is a multi-step process initiated by

the nearly 100% efficient formation of self-trapped excitons, which in alkali halides consists of an electron bound in a loose orbit about a hole trapped by a pair of anions. The energy for displacement is derived from the nonradiative recombination of the electron-hole pairs and typically results in propelling the anion from its lattice site. The energy required for this process is quite low, on the order of the band gap, and accounts for observed effects induced by radiations with energy insufficient to displace atoms by knock-on processes.

Optical Components

It is convenient for the purposes of this review to limit the discussion to passive optical components, and in particular to thin film reflective or antireflective coatings, bulk transmissive optics, and substrate materials. Various degradation modes are appropriate for these: decreased transmission, changes in refractive index, density and coefficient of thermal expansion, surface erosion and deformation, charge trapping and dielectric breakdown, to mention a few. In spite of these diverse phenomenologies, there is a common origin for many of the effects in the defect centers induced in the material by the radiation exposure. For example, there is evidence suggesting that both the transient compaction and transient uv optical absorption induced in amorphous SiO_2 by pulsed irradiation can be attributed to transient E' centers.[3]

The radiation sensitivity of thin films is expected to be greater than corresponding bulk materials since the purity, stoichiometry and microstructure of thin film optical coatings is usually inferior and there is a much greater surface area. However, the thickness of a coating is much less than that of a bulk optic, so a higher volumetric concentration of radiation-induced color centers can be tolerated than say in an optical fiber. Since thin film dielectric stacks are used to enhance the optical performance, decreased reflectivity/transmission, enhanced absorption, or changes in optical path resulting from refractive index variations are particularly detrimental. Coatings can be fabricated to be resistant to natural space radiation environments[6], but even the plasma of a HeNe ring laser gyroscope has been found to significantly increase the absorption of the multilayer thin films on the mirrors. The much more serious issue of enhanced γ ray environments and synergistic effects of laser and high energy radiation exposure remain unresolved at this time. A further effect of electron irradiation of thin films is dielectric charging which may cause the thickness of the film to be decreased, particularly if it initially of low density. If the charge exceeds the dielectric strength of the film, breakdown occurs resulting in catastrophic failure. A further effect of radiation is the removal of surface atoms, either by momentum transfer mechanisms such as sputtering, or by desorption induced by electron transitions. The understanding of the surface erosion phenomena by either of these mechanisms or by interaction with low energy atomic oxygen is extremely important if the films are to survive in a space environment.

The radiation resistance of bulk optical components can be increased significantly through purification and processing, the latter to remove dislocations, defects, and internal strain. This strategy is aimed at decreasing the number of sites available for trapping and stabilizing the radiolytic electrons and holes. Of course, defect creation by the incident radiation will provide a suite of traps, but processing can at least increase the resistance of an optical component to low dose exposure. Significant

tradeoffs are required in some cases, such as in refractive optics where high refractive index is achieved through incorporation of heavy metals while radiation hardening dictates removal of these high Z constituents. Because of the extensive prior studies of radiation damage in alkali halides[5] and SiO_2[3], the understanding of radiation effects in these materials is fairly advanced. However, radiation damage by multiphoton absorption during intense uv exposure and synergistic effects of laser and high energy radiation are only now being realized. Likewise, charge trapping and dielectric breakdown remains a potential problem in these materials.

At first thought it would appear that mirror substrate materials would be insensitive to radiation exposure, except for bombardment by heavy ions or neutrons. However, large optics for surveillance or high energy lasers require maintaining an extremely high optical figure and uniform thermal expansion coefficient to prevent distortion. Some materials such as Si, Mo, and Be are anticipated to fail only from melting, while glass and ceramic substrates materials such as SiO_2, Zerodur (a multiphase ceramic) or ULE (Ti-doped SiO_2) evidence changes in critical properties induced by ionizing radiation exposure. For example, radiation-induced compaction is well known in silica glass and occurs with x-ray energies as low as 2-18 keV! These increases in density will lead to surface deformation with the resultant loss of optical figure. Since all of the low CTE mirror substrate materials are insulators, they also are subject to dielectric charging and breakdown.

Motivation

As the performance requirements of optical components become less tolerant of radiation-induced degradation, conventional hardening strategies such as material selection-purification, minimization of surfaces, strains and line defects, employing higher temperature or temperature cycling, intentional doping with elements to provide competitive traps, or optical bleaching may no longer be sufficient. It then becomes imperative not only to understand the phenomenology of radiation effects in optical components, but also to understand the basic damage mechanisms and resultant defect center which are adversely affecting performance. Only by exploiting the latter will it be possible to develop materials for future optical devices. It is apparent that there is a good deal of commonality in failure mechanisms among various optical components due to their common origin in the radiation-induced defect centers. It could be reasonably expected that enhanced understanding of the defect centers and damage mechanisms in a material in one component will lead to hardening in other components.

1. "Radiation Effects in Optical Materials," P.W. Levy, Ed., SPIE Vol. 541 (1985).
2. S. Glasstone and P.J. Dolan, "The Effects of Nuclear Weapons, US Government Printing Office, 1977.
3. D.L. Griscom, ibid ref. 1, p. 38.
4. For a review, see E.J. Friebele and D.L. Griscom, "Radiation Effects in Glass," in Treatise on Materials Science and Technology Vol. 17, Glass II, M. Tomozowa and R.H. Doremus, Eds. (Academic Press, NY, 1979) p. 257.
5. R.T. Williams, ibid ref. 1, p. 25.
6. T.M. Donovan, this issue.

Gamma Radiation-Induced Absorptions In Calcium Fluoride

C. W. King
Harshaw/Filtrol Partnership
6801 Cochran Road
Solon, Ohio 44139

O. H. Nestor
Harshaw/Filtrol Partnership
6801 Cochran Road
Solon, Ohio 44139

INTRODUCTION

The characteristics of calcium fluoride under adverse conditions have received increasing attention in the last several years. Many workshops and symposia have focused on laser induced damage in calcium fluoride and other materials when used as laser windows.

The purpose of the study reported here was to investigate the transmission characteristics of calcium fluoride while varying the exposure to gamma radiation.

EXPERIMENTAL METHOD

The calcium fluoride crystals used in the experiment were 25 x 30 x 10 mm^3. The transmission measurements were made through the 30 mm path length using a Perkin Elmer Model 330 Spectrophotometer.

The radiation was 0.662 MeV gamma rays from approximately 9.0×10^6 curies of ^{137} Cesium. The radiation was incident on the crystals from both 25 x 30 mm faces. The exposure rate was approximately 1.0×10^6 Rads per hour. In this experiment 12 crystals in all were exposed; three crystals at four different exposure levels. The exposure levels were: 1.37×10^6, 2.49×10^6, 3.57×10^6 and 4.35×10^6 Rads.

All crystals were kept in the dark and at room temperature throughout the entire experiment.

EXPERIMENTAL RESULTS

Figures 1-4 show transmittance versus wavelength from 190 to 2500 nm for increasing exposure level. Measurements are shown for both before and after exposure. All absorptions appear at the shorter wavelengths and increase with increasing exposure, with the most sensitive absorption apparently centered about 380 nm.

Figure 5 shows non-typical absorptions even at the lowest exposure levels.

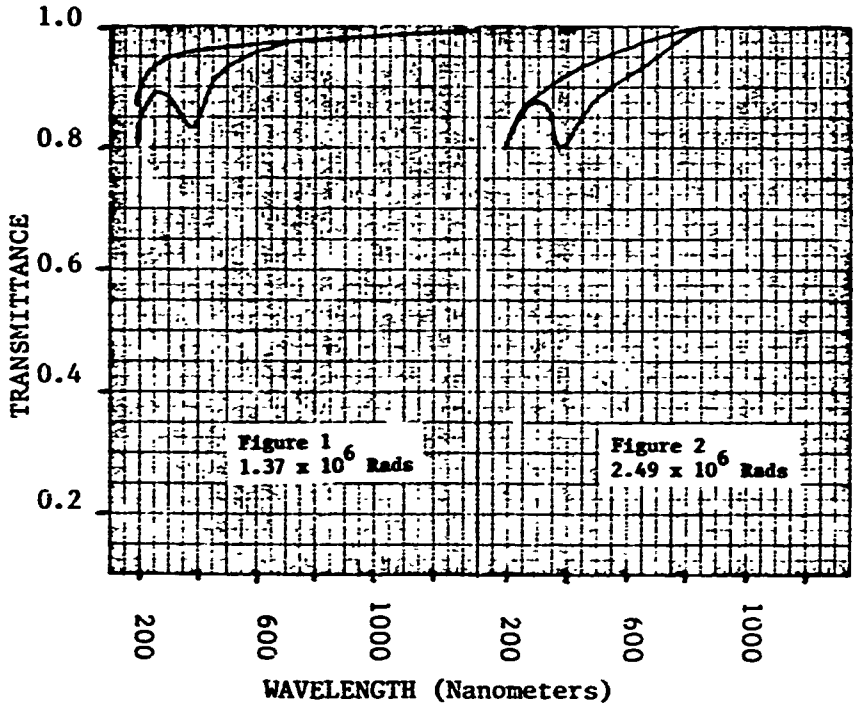

Figures 1-2: Calcium Fluoride Transmittance Pre and Post Exposure

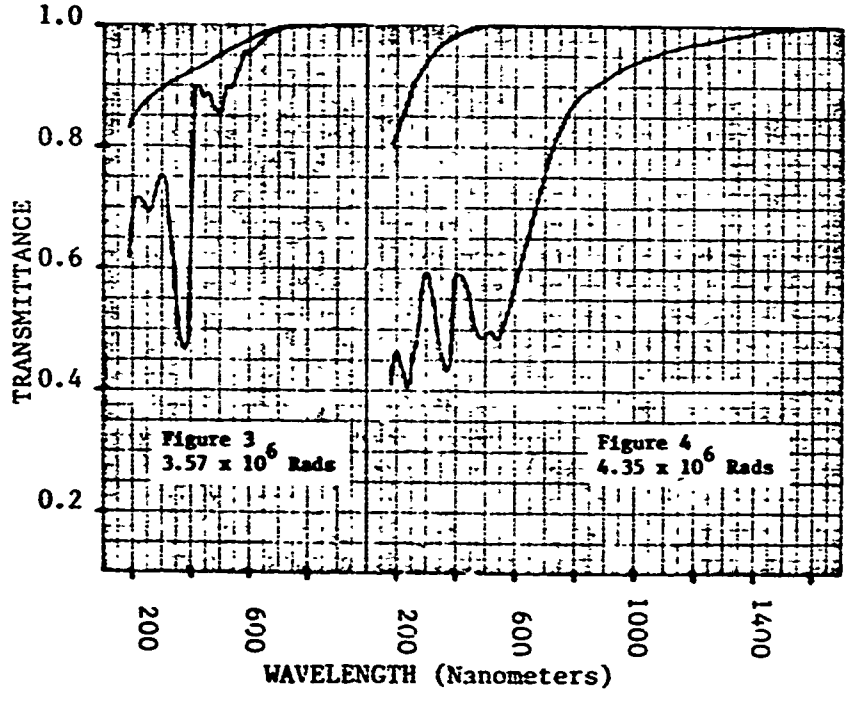

Figures 3-4: Calcium Fluoride Transmittance Pre and Post Exposure

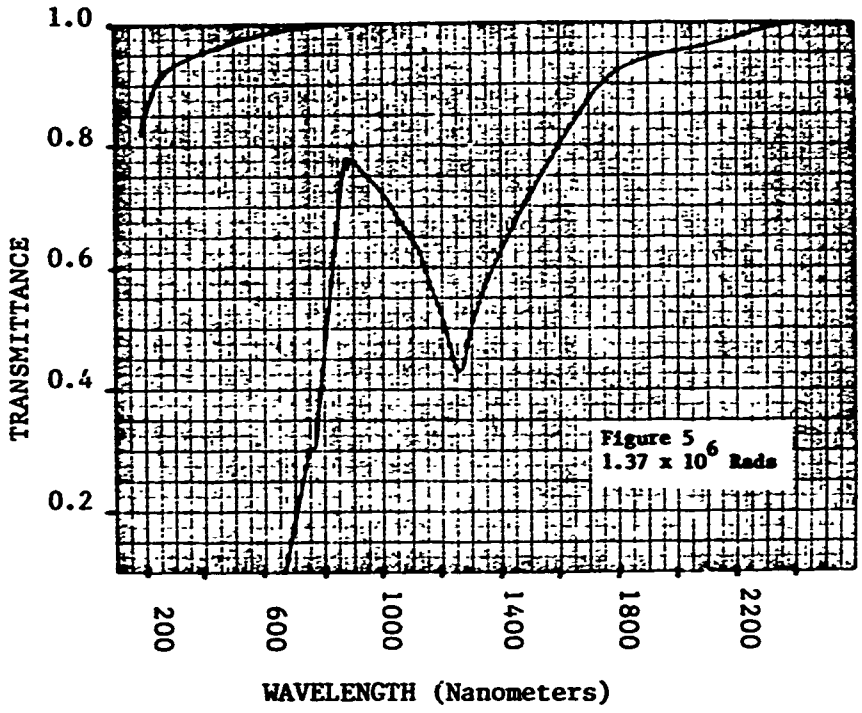

Figure 5: Calcium Fluoride Transmittance Pre and Post Exposure

CONCLUSIONS

The changes in transmission for some calcium fluoride crystals have been characterized for several exposure levels of gamma radiation.

Current work includes the investigation of fading of the absorptions at 20°C, annealing to reduce absorptions and the correlation of low levels of impurities with absorptions at certain wavelengths.

It is suggested that if, under irradiation conditions, correlations can be established between very low levels of impurities and absorptions at certain wavelengths then this could become a technique for determination of crystal purity.

VARIATION OF THE INDEX OF REFRACTION IN GLASSES EXPOSED TO IONIZING RADIATION

Thad J. Englert and Mark Flohr
University of Wyoming
Laramie, Wyoming 82071

INTRODUCTION

The attenuation of lightwaves propagating through optical fibers that have been exposed to ionizing radiation has been the subject of considerable experimental and theoretical investigation during the past few years.[1]

This attenuation has been attributed to the creation of color centers within the glass comprising the core and cladding of the fiber, these color centers generally being located at impurity sites.[2] Very little effort has been reported dealing with any study of the effects on the index of refraction of the materials of the fiber as a result of radiation exposure however.

It takes but a moment of consideration of even elementary theories to see that variations in the refraction indeces can alter the waveguide properties of a fiber,[3] and it therefore seems appropriate to make some study of the influence of ionizing radiation on the index of refraction of glasses. This report gives some preliminary results on the change in the index of refraction of glass after and during exposure to gamma radiation.

CHANGE OF INDEX OF REFRACTION OF GLASS DUE TO GAMMA-RADIATION

1. As a first attempt at determining whether gamma radiation causes any change in the index of refraction in glass, we have caused the gamma radiation from a 1-Curie cesium-137 (gamma ray energy 0.663 MeV) source to strike a high quality microscope slide and observed the change in the reflected interference pattern from the slide. The light source used to observe the interference pattern from the slide is a helium-neon laser

(wavelength 632.8 nm). The interference pattern is recorded on film for comparison with the interference pattern from the slide before irradiation. Since we are at first only interested in answering the question of whether or not any effect is expected, little attention is paid to uniformity of radiation exposure and the slides are simply centered in the diverging gamma-ray beam. Figure 1 is a representative photograph of the interference patterns from a slide before and after a gamma-ray exposure of about 4.5 rads.

The maximum change in the order of interference is about one-half a fringe corresponding to a variation in optical path of half a wavelength. A simple calculation gives a change in the index of refraction of about .02 percent.

2. To obtain a rough estimate of the rate at which the index of glass refraction changes with radiation exposure, we have placed a small, good quality prism in the gamma-ray beam and observed the change in minimum angle of deviation of a helium-neon laser beam passing through the prism during gamma irradiation. Figure 2 shows the change in index, measured to be 1.53 before irradiation, as a function of time. The prism was placed approximately 15 cm from the cesium source during irradiation. It is of interest to note that there is an apparent saturation effect as is often seen in those measurements of lightwave attenuation in irradiated fibers. Very little recovery toward the original index of refraction of the prism was observed over a time period of 30 minutes after removal of the gamma-ray beam. Higher dose rates may give results different from those noted here since the rate of radiation exposure in optical fiber glasses seems to affect the severity of optical deterioration in many reported cases.

CONCLUSIONS AND COMMENTS

Moderate doses and dose rates of 0.663 MeV gamma radiation do affect the index of refraction of glass. It is probable that higher irradiation dose and dose rates will cause even more significant variations in the index of refraction of glasses. Based on these observations, it seems advisable to make more critical measurements of the alteration of the optical qualities of fibers that have been exposed to ionizing radiation.

An additional comment regarding the detrimental effects of ionizing radiation on optical fibers is in order. Most of the past measurements have used cobalt-60 as a radiation source, the gamma-ray energies from this isotope being 1.17 MeV and 1.33 MeV. A given dose (rads) of gamma-ray exposure at these energies represents about half as many photons as the same dose using 0.663 MeV gamma rays from a source like cesium-137. It is not likely that the cross sections, for the kinds of reactions leading to deterioration of the optical qualities of fibers, are much different at these two energies. It is suggested, therefore, that the same optical effects may be observed at approximately half the radiation dose if the gamma-rays are at half the energy.

REFERENCES

1. E. J. Friebele, K. J. Long, C. G. Askins, M. E. Gingerich, M. J. Marrone and D. L. Griscom, Overview of Radiation Effects in Fiber Optics. In Critical Review of Technology: Optical Materials in Radiation Environments. (SPIE Volume 541).
2. David L. Griscom, Nuc. Inst. and Meth. in Phys. Res. B1, (1984) 481-488.
3. John Gowar, Optical Communications Systems, Prentice Hall (1984).

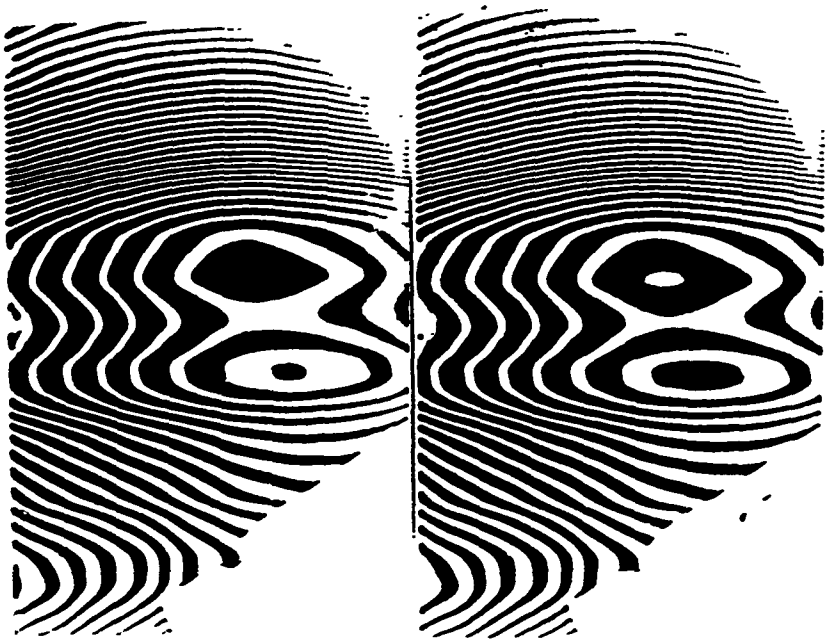

(a) (b)

Figure 1. Reflected interference patterns from a high-quality glass microscope slide before (a) and after (b) a 4.5 rad exposure to 0.663 MeV gamma rays.

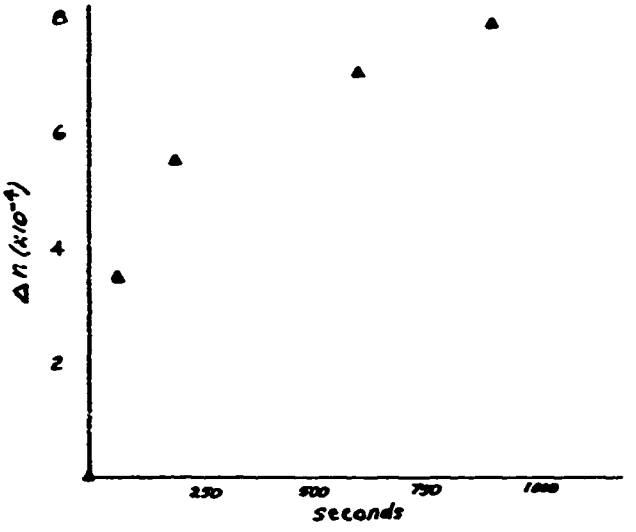

Figure 2. Change of index of refraction of a high quality prism with time of exposure at a rate of 0.4 rad/sec.

Radiation Damage to Dielectric Mirrors

Francis B. Harrison

CLS-9, MS E543

Los Alamos National Laboratory

Los Alamos, NM 87545

We have measured the change in reflectivity of multilayer dielectric (Alumina-Cryolite) high-reflectivity mirrors under simultaneous irradiation by a KrF laser (248-nm) and electrons from a (2 MeV) Febetron 705 accelerator.

Measurements were made at a number of different laser pulse energies and electron intensities. In no case but the last (highest intensity) was there any indication of a reduction in reflectivity due to the radiation pulse. We shall give the results only for the last run.

The Questek Series 2000 excimer laser put out a pulse about 20 nsec long, with a shape indicating longitudinal mode beating (fig. 1). The beam was rectangular. Vertical scans at different horizontal positions gave a smooth, approximately Gaussian profile, but the horizontal scan showed an irregular shape (fig. 2) which was not improved by spatial filtering. The quoted beam intensities correspond to the highest peak.

Radiation Damage...Mirrors

F. B. Harrison

The radiation pulse shape (fig. 3) was measured by an x-ray detector placed on the wall behind the target mirror. The low-intensity tail is due to electrons of lower energy than the main peak. The radiation dose was measured with radiochromic film, and the peak dose rate deduced from the shape of the x-ray pulse. No correction was made for the difference in x-ray yield of the lower energy electrons, or for the difference in dose rate in the film as compared to the dielectric layers.

The mirror was coated by Litton Airton. Measurements at Los Alamos have shown a KrF laser damage threshold for similar mirrors from 1 to 3 J/cm^2, and 100% damage points as high as 8 or 10 J/cm^2.

The position of the test spot on the mirror was not changed between shots.

Because of jitter in the laser and Febetron firing circuits, it was necessary to take a number of shots in order to get a coincidence between the peaks. Both the x-ray and the laser traces were very reproducible.

For the last run, the dose per shot was 360 krad, giving a peak dose rate of 1.4×10^{13} rads/sec. The laser energy on target was 105 mJ, giving a peak fluence of 1.54 J/cm^2. The flux was 120 MW/cm^2 at the first pulse (see fig. 1), 150 MW/cm^2 at the second pulse.

In five cases the first pulse was at or near the radiation peak. The

Radiation Damage...Mirrors

F. B. Harrison

pulse heights were compared to those in seven shots, in which either the Febetron was not fired, or there was no overlap. The result showed an increase under radiation of

$$(1.9 \pm 3.8)\ \%$$

Similarly, in five cases the second pulse was at or near the radiation peak. A comparison with seven no-radiation cases gave a decrease under radiation of

$$(6.3 \pm 2.6)\ \%$$

Visual examination of the mirror after the test showed no gross damage.

We plan to measure damage thresholds with and without ionizing radiation pulses, in the hope of gaining information on the damage mechanism.

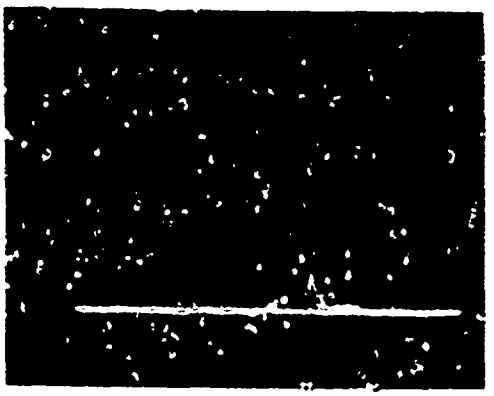

Fig. 1: Temporal profile of laser pulse.

Radiation Damage to Dielectric Mirrors

Francis B. Harrison

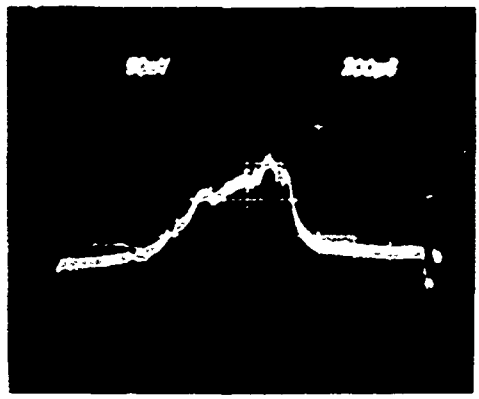

Fig. 2: Horizontal spatial profile of laser pulse.

1 div (200 μsec) = 1.25-mm

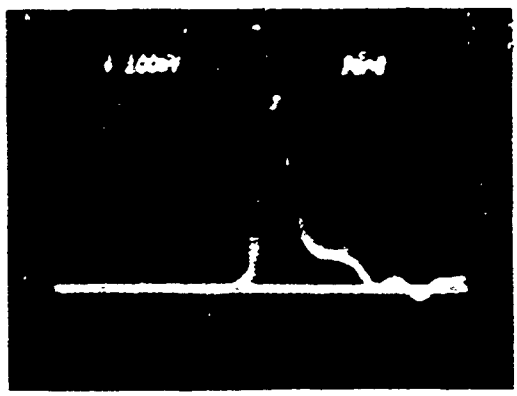

Fig. 3: X-ray pulse shape

Effect of Surface Pitting in Transparent Domes on Scattered Light

Douglas W. Ricks, Naval Weapons Center, Code 3151, China Lake, CA 93555

Introduction: A dome which covers an optical instrument is designed to protect the optical instrument from pitting caused by the impact of dust, rain or hail. When flown on the wing or nose of high speed aircraft the erosion can be severe. This adverse environment will degrade the optical performance of the instrument by decreasing transmittance and by increasing the amount of light scattered by the dome.

Four domes were investigated in this study. The domes are nearly hemispherical with an outside radius of curvature of 4.235 inches. The dome thickness is 0.25 inches. The dome material is a zinc crown glass, ZKN7. Each dome was flown on the nose of an A-4M Navy plane; the most pitted dome (No.3) for 701 flight hours. One relatively new dome was flown through hail. Each dome showed numerous tiny pits. Dome No.3 appeared to have 25,000 pits per square inch at the center when viewed under low magnification. The hail-damaged dome (No. 4) had noticeably larger pits and only a few small pits. Initially both surfaces of each dome were coated with a single layer of MgF_2 to reduce reflection losses at 760 nm.

Measurement Apparatus: The measurement of total integrated scatter was made by Phil Archibald of the Naval Weapons Center. The total integrated scatter represents the fraction of the incident light that is scattered in the forward direction 2.25° to 170° from the transmitted beam axis. All measurements of scatter were made with the beam incident along the surface normal. There were measurements made at the dome center, at 8 points in a circle 1.1 inches from center, at 15 points 2.2 inches from center and at 15 points 3.3 inches from center. After the measurements were made using a 647.1 nm laser source the measurements were repeated using a 1150 nm laser source.

Transmittance was measured at 633 nm using a HeNe laser for a source. The beam was polarized then split into a reference beam and the transmittance measurement beam. Two EG&G High Sensitivity Infrared Radiometers were used to detect the two beams. The transmitted light collected was within 2.25° of the transmitted beam axis. The energy was incident along the surface normal at the dome center. Transmittance measurements were also made along the surface normal at 1.1, 2.2 and 3.3 inches from the dome center.

The near-angle scatter was also measured at 633 nm. The measurement system consists of a HeNe laser (1 mW) which is focused through a 0.01 inch diameter aperture by an achromat lens of focal length 3 inches. The beam is collected and collimated by a 12 inch diameter mirror (focal length 71.6 inches) which is tilted in the horizontal plane. The diameter of the collimated beam is about 1 inch. The dome is placed at a distance of 4 feet from the mirror. The transmitted and scattered light is collected by another 12 inch diameter

mirror (focal length 71.6 inches) located 5 feet from the dome. A 0.001 inch diameter pinhole is placed at the tangential focal plane. The distance from the mirror to focal plane is 100 inches due to the combination of weak negative power in the dome, the long distance from dome to mirror, and positive power in the mirror. The angle of incidence is made equal on the two 12 inch mirrors to reduce coma. Lens, mirrors and apertures are several times larger than the beam to minimize diffraction.

Five inches behind the pinhole is placed an EG&G High Sensitivity Infrared Radiometer. A narrow band optical filter between the detector and pinhole blocks out 99% of the ambient light which passes through the pinhole. The pinhole and detector are located on translation stages and are moved together. In a typical measurement scan 100 data points are taken at a spacing of 0.0002 inches which corresponds to about .00015 degrees, another 100 data points spaced 0.001 inches (.00074 degrees) and 88 points at intervals of 0.01 inches.

Results: The most severe erosion is at the center of the dome and becomes much less severe away from the center. As expected, the transmittance is lower and the scatter generally highest at the center of each dome.

The total transmittance loss in the most severely eroded dome (No. 3) varied from 50% for light incident at the center to an average of 25% 3.3 inches away from the center. For 3 of the 4 domes the transmittance varied less than 5% from average at a given distance from the dome center. For the hail-damaged dome the total transmittance loss varied greatly near the dome center; transmittance loss at some damage locations was nearly 100% but only 8% in clear areas near the center. In a circle 3.3 inches from the dome center the average transmittance loss in the hail-damaged dome was only about 7% and did not vary much from point to point.

The total integrated scatter (2.25° to 170°) in the forward direction is approximately half the transmittance loss. This relationship holds for all areas of each dome. The amount of light scattered from these pitted domes does not depend on the wavelength.

The hail-damaged dome near the center had the greatest intensity of near-angle scatter. The scatter component of the transmitted beam could be seen at an angle of about 0.002°. The relative intensity at this angle is a little less than 1% of the peak intensity. Near the center of the hail-damaged dome the relative intensity of the scattered light decreases at the rate of about two orders of magnitude for every one order of magnitude increase in scatter angle. This rate of decrease continues down to the minimum measureable scatter level which in the present apparatus is 0.00001% of the peak intensity. The scatter intensity does not smoothly decrease with angle; instead it varies by about an order of magnitude every 2 or 3 thousandths of a degree. Several inches away from the center of the hail-damaged dome we find that the scatter intensity drops about 7 orders of magnitude for 3 orders of magnitude increase in scatter angle.

For the domes with smaller size pits the scatter component of the beam is too small to be distinguished from the unscattered beam for angles smaller than 0.01 degree. The relative intensity of the scatter decreases at the rate of only 3 orders of magnitude for every 2 orders of magnitude increase in angle. At the center of dome No. 3 the relative intensity of the scattered light at the scatter angle of 0.01 degrees is about 0.01% of the peak intensity.

Conclusions: The following tentative conclusions can be reached. The measurement of transmittance at a convenient wavelenth is a good indication of the total amount of scattered light when the surface pitting is large compared to the wavelength of light. The larger the size of the pits the smaller the angle at which the scattered light will be observable. The relatively low level of scattered radiation (less than 1% for large pits and .01% for the small pitted domes) indicates that in many cases the performance of the system will be primarily degraded by the loss of transmittance somewhat degraded by scatter from large background radiation sources and only slightly by a small loss of resolution or contrast due to near-angle point source scattering. Near-angle scattering is important when it is necessary to resolve a faint object in the neighborhood of a much brighter object.

THURSDAY, FEBRUARY 12, 1987

BALLROOM B
8:30 A.M.–10:00 A.M.

ThA1–5

SESSION 5

Alan F. Stewart, U.S. Air Force Weapons Laboratory, *Presider*

High Damage Threshold Optical Coatings*

D. Milam

Lawrence Livermore National Laboratory

University of California

P.O. Box 5508, L-490

Livermore, California 94550

SUMMARY

Projects at Lawrence Livermore National Laboratory require optical coatings capable of withstanding fluences of 8-10 J/cm^2 delivered in single laser pulses with durations of 1-3 ns, or in repeated irradiations, at rates exceeding 100 Hz, by pulses with durations of 10-50 ns. Future fusion lasers will require coatings with higher thresholds. To develop these coatings, we maintain a program that is evaluating sol-gel coatings deposited from solutions, single-layer films made by chemical vapor deposition (CVD) and coatings made by conventional physical vapor deposition (PVD).

Porous sol-gel AR coatings are the only optical films known to satisfy all current threshold requirements. The median, single-pulse, 1064-nm thresholds of these coatings range from 11 J/cm^2 at 1-ns to 33 J/cm^2 at 9 ns. They survive 100 Hz irradiation by 16-ns, 1064-nm pulses at fluences above 20 J/cm^2, have thresholds above 15 J/cm^2

*Work performed under the auspices of the U.S. Department of Energy by Lawrence Livermore National Laboratory under Contract No. W-7405-ENG-48.

when tested at 100 Hz with 25-ns, 350-nm pulses. We recently found that thick (500-800 nm) silica coatings made by stacking 5 to 10 thin solution-deposited layers have reduced thresholds at 351-nm, and that subjecting a thick layer to an ozone treatment usually improves its threshold.

The HR coatings and thin-film polarizers currently available in large sizes are made by standard electron-beam evaporation. These coatings usually withstand irradiation by single 1064-nm pulses (1-3 ns) at fluences of 5-10 J/cm^2. For 350-nm, 25-ns pulses, the thresholds are typically 1-3 J/cm^2. We have used sol-gel deposition to produce single layers of several high-index materials, and find that Y_2O_3 and HfO_2 show significant promise at both 350-nm and 1064-nm. Efforts to produce HR coatings by sol-gel deposition will be reviewed.

Little progress has been made in improving thresholds of thin-film polarizers. Even if sol-gel deposition results in improved thresholds for HR coatings, it may be very difficult to attain sufficient control of layer thickness to allow sol-gel fabrication of polarizers. For this reason, we have begun evaluation of optical coatings made by CVD. Single layers of TiO_2, produced by CVD using metal organic starting materials, have exhibited 1064-nm thresholds > 10 J/cm^2 (1-ns, 1064-nm). Production of these coatings will be reviewed.

ThA2

Fluorine Resistance of Dielectric Coatings for Excimer Laser Optics

S. Foltyn, J. Boyer, G. Lindholm and K. Padgett

Porous Halide Antireflective Coatings for Adverse Environments*

Ian M. Thomas

Lawrence Livermore National Laboratory

University of California

P.O. Box 5508, L-483

Livermore, California 94550

SUMMARY

Many metal fluorides are stable in adverse environments and some are used as coatings for optical components. In general, these materials have low refractive indices and are therefore of use as the low index component in multilayer AR or HR coatings or, in some cases, notably MgF_2, as the single component in simple 1/4 wave AR coatings. These coatings are normally prepared by evaporation or sputtering and as such are substantially dense and therefore of an index close to that of the bulk fluoride material. This is quite satisfactory for multi-layer application but is inefficient in 1/4 wave AR coatings on typical substrates of index about 1.5 because the index is too high.

*Work performed under the auspices of the U.S. Department of Energy by Lawrence Livermore National Laboratory under Contract No. W-7405-ENG-48.

To this end we decided to investigate the possibility of preparing MgF_2 or CaF_2 high damage threshold, porous (hence low index) AR coatings that could be used at efficient 1/4 wave AR coatings. Our previous experience with silica indicated that colloidal solutions could be used to prepare excellent porous coatings at room temperature these coatings consisting of layers of silica particles. In addition, these solutions could be applied to water sensitive substrates because anhydrous suspending solvents were used. By using high purity metal organic compounds for the preparation of the colloids high damage thresholds were also obtained. It was hoped that colloidal fluoride suspensions could be used in like manner to prepare porous fluoride coatings.

Calcium and magnesium fluorides may be prepared by several methods and from many different starting materials. A number of combinations were investigated before satisfactory preparations were discovered, these being ones in which useful colloidal solutions of the right particle size could be obtained. Two preparations were developed for MgF_2 one using magnesium acetate and the other using a magnesium alkoxide as magnesium sources:

$$Mg(OCOCH_3)_2 + 2HF \rightarrow MgF_2 + 2CH_3COOH.$$

$$Mg(OCH_3)_2 + 2HF \rightarrow MgF_2 + 2CH_3OH.$$

Only one preparation was found for CaF_2, this from calcium acetate, because the insolubility of calcium alkoxides precluded their use:

$$Ca(OCOCH_3)_2 + 2HF \rightarrow CaF_2 + 2CH_3COOH.$$

All coatings were applied using a spin coater on fused silica or calcium fluoride substrates. In all cases, excellent 1/4 wave AR coatings were obtained.

Laser damage threshold measurements were carried out at 355 nm with a single shot 0.6 ns pulse and also at 351 nm with 1000 shots at 25 Hz with a 25 ns pulse. Thresholds in the range 6-8 J/cm^2 were obtained under the former conditions and 20-25 J/cm^2 under the latter. All coatings were prepared such that the maximum transmission occurred at the measurement wavelength.

AUGER ANALYSIS OF ELEMENTAL DEPTH PROFILES CORRELATED WITH MULTI-PULSE LASER DAMAGE OF GaAs SURFACES

Dhiraj K. Sarder[1], Michael F. Becker, and Rodger M. Walser
The University of Texas at Austin
Department of Electrical and Computer Engineering and
Center for Materials Science and Engineering
Austin, TX 78712

A great deal of effort has been made in recent years to understand the mechanisms of laser induced damage in solids. Semiconductors, in particular, are of interest both becuase of fundamental questions concerning their damage processes for which they are model systems, and because of their technological importance.

We present results of a statistical study of the nature of single and multiple-pulse laser damage to single crystal GaAs surfaces for pulsed laser radiation (t_p=10 ns and λ=1064 nm). Surface morphologies resulting from chemical surface cleaning processes and laser damage itself are discussed. The nature of the dependence of damage on accumulated energy in multi-pulse experiments is determined and correlated with the behavior of other semiconductor and metal material surfaces. Finally, we present results of the Auger analysis of elemental depth profiles in laser-damaged and control regions of the GaAs surfaces.

The GaAs wafers used in these experiments were production quality wafers from the Microwave Integrated Circuit Production Group at Texas Instruments, Dallas TX. They were 0.56 mm thick, 50.8 mm in diameter , <100> orientation, doped with Cr to about 1×10^{-16} cm^{-3} to make them semi-insulating, and polished only on the front surface.

Three investigations were carried out in the course of this study: (1) Sample preparation was studied via the use of chemical cleaning and the controlled growth of surface oxides. (2) Single and multiple laser pulse damage statistics were accumulated for various surface preparation conditions. (3) By using sputter etching in conjunction with Auger electron spectroscopy, changes in elemental depth profiles produced by laser damage were studied. The experimental procedures used in these investigations are summarized below.

After cleaning in organic solvents, surface preparation was conducted in room temperature $8H_2SO_4 : 1H_2O : 1H_2O_2$ and $1H_2SO_4 : 1H_2O : 1H_2O_2$ solutions for 10 - 20 s with agitation. The etch solution was then diluted rapidly with de-ionized water, without exposing the wafer, and it was kept submerged for 5 min until the surface oxide had been stabilized in a controlled manner. Finally, the surface was dried with low pressure dry nitrogen.

In the laser damage experiments, a Q-switched Quantel Nd:YAG laser operating at a pulse repetition rate of 10 Hz, at the fundamental wavelength 1064 nm, with a pulse duration of 10 ns FWHM was used. A computer experimental control and data acquisition system directed the irradiations and collected data for every laser pulse incident on the sample. The incident laser energy was attenuated by a rotating half-wave plate and a polarizer before being focused by a 460 mm focal length lens to a near-Gaussian spot at the sample of 270 μm ($1/e^2$ radius) as determined by a scanned knife-edge technique.

Finally, elemental analysis of the surfaces was performed using a Physical Electronics Scanning Auger Electron Microscope. Depth profiles were taken for Oxygen, Carbon, Arsenic, and Gallium while sputtering a 2 mm x 2 mm area centered on a laser damage spot and again at a control area. Several locations relative to the center of the laser damage spot were examined. Sputtering rates were calibrated using a stylus profilometer.

In the experiments, it was found that the stronger etching solution etched the GaAs surface deeply and left unevenly distributed pits. Subsequent laser damage testing showed that these wafers had higher damage thresholds for N>10 than lightly etched wafers. For the more dilute etch solution, a 10 s etch was found to be sufficient to clean the surface without producing surface pitting.

For each number of laser pulses, N, several sites were irradiated at each energy over a range of energies bracketing the damage threshold (from below the lowest damaging fluence to above the highest non-damaging fluence). Damaged sites were later identified under a Nomarski microscope at 200x. From these data, the 50% probability damage threshold

fluence,F_N, was computed for each value of N.

Accumulation was evident as the damage fluence was found to decrease monotonically with increasing N. Accumulation is most conveniently plotted in an accumulation curve as log $[F_N \cdot N]$ versus log N which tends to linearize the data. Data for a lightly etched and a heavily etched GaAs wafer are shown in Fig. 1. A slope less than one shows the presence of accumulation and a slope of exactly one indicates that no accumulation is present. Previous studies of accumulation in single crystal Si, Cu and Al indicate that higher quality material surfaces tend to have slopes closer to one and that lower slopes in the region N<10 indicate the presence of defect dominated damage mechanisms. Both the presence of the lower slope for N<10 and the microscopic evidence indicate that this is also true for these GaAs samples Previous experiments on unetched GaAs wafers showed the same local defect dominated damage morphologies.

For elemental depth profiling, a site near the edge of a heavily damaged spot, N=30, was chosen. Figure 2 depicts the unnormalized depth profiles for O, C, As, and Ga at this site. Both C and O decrease rapidly with Ar^+ sputtering as expected; however, similar dependence is observed at the control site. Surprisingly, the surface layer appears to be As rich even though As is the more volatile specie. The exact form of this As rich surface layer changes at the control site but is still generally similar to the laser damaged site.

In conclusion, we found that although heavy etching, which leaves surface pits, lowers the laser damage threshold for GaAs; light etching and controlled surface oxide growth does not affect the damage behavior. In either case, GaAs shows accumulation behavior similar to un-etched GaAs and to many other materials. Damage for pulse numbers less than 10 showed defect dominated characteristic morphology and accumulation behavior. Auger elemental depth profiles of carbon and oxygen showed little change due to laser damage. The arsenic rich surface layer was only subtly changed.

[1] Permanent address: The University of Texas at San Antonio, Division of Earth and Physical Sciences, San Antonio, TX 78285.

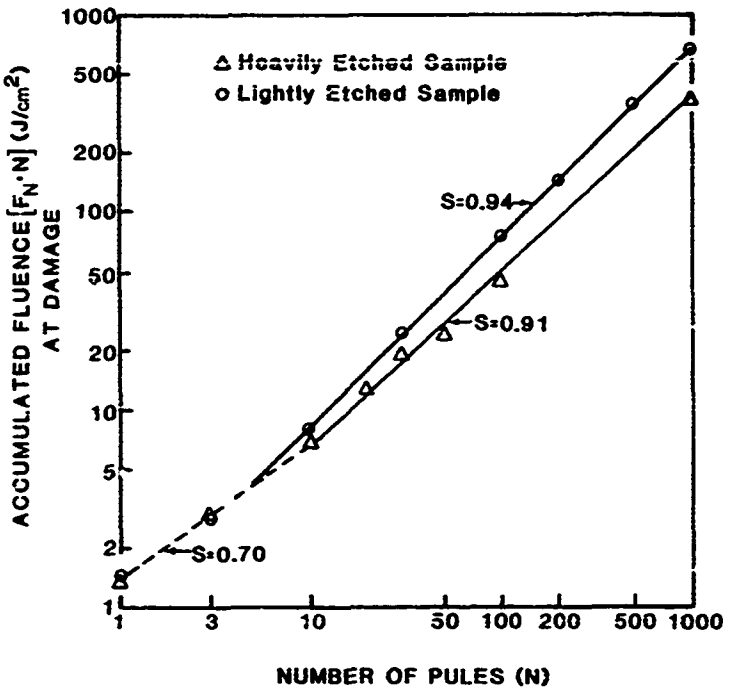

Figure 1. Accumulation curves for laser damage of two GaAs samples at 1064 nm, 10 ns pulses. Accumulated fluence [$F_N \cdot N$] is plotted versus N. Slopes are indicated on the curves.

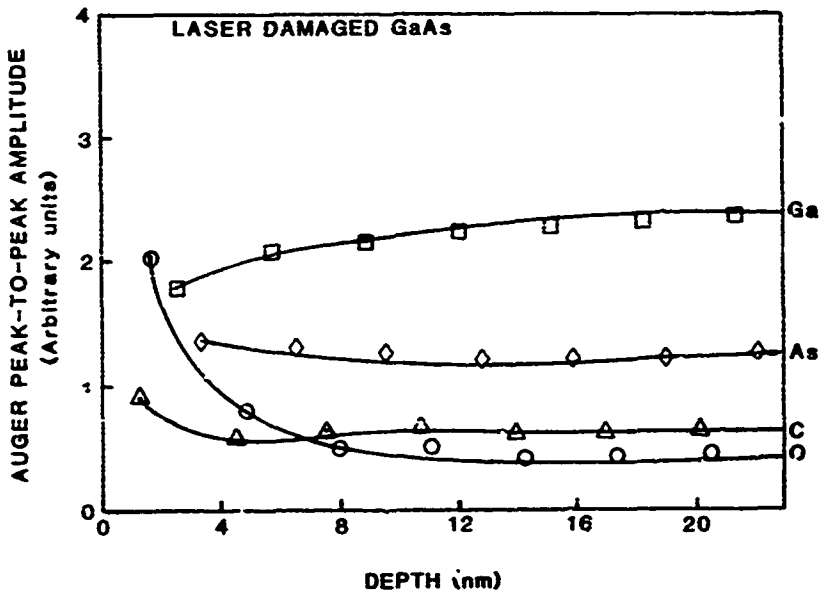

Figure 2. Un-normalized Auger depth profiles of carbon, oxygen, arsenic, and gallium at a laser damged site, N=30, at a fluence about 2 times the single pulse damage threshold.

Compressive Coatings on Optical Components for Improving Mechanical Durability and Increasing Strength

J. E. Marion
Lawrence Livermore National Laboratory, University of California
P.O. Box 5508, L-490, Livermore, California 94550

I. Introduction

Techniques for realizing high strength and good mechanical durability in optical components is the focus of the present work. Currently, we are investigating methods applicable to slab geometry solid state lasers for high average power output.[1] However, many of our analyses and methods are applicable to glass and single crystal components in other applications.

In the slab lasers, the active elements are single crystals or glass with rectangular geometries in sizes up to 1 x 10 x 20 cm for single crystals and 2 x 25 x 70 cm for glass. During laser operation, the slabs are heated throughout their bulk by absorption of flashlamp light, but only the surfaces are cooled by flowing liquid or gas. The consequent steady state thermal gradient results in surface tensile stresses that can exceed the component strength, resulting in catastrophic failure. Furthermore, during handling and operation, the slab strength degrades by the accumulation of physical damage on the slab surface. Therefore, in addition to high strength, the slabs must be mechanically durable. We investigate a variety of methods to achieve good mechanical durability and high strength within the context of optically flat, low scatter, low absorption surfaces.

II. Theoretical Considerations

A. Component Strength

(i) Optical surfaces

In this section, we theoretically assess the strength of optical surfaces both with and without compressive surface layers. We assume that all surfaces contain numerous flaws from machining damage[2] and that the largest flaw has depth, a. Standard fracture mechanics gives the strength of the component, σ_f as[2]

$$\sigma_f = YK_c/[\pi a]^{1/2} \qquad (1)$$

where K_c is the fracture toughness of the material, a materials property which characterizes its inherent resistance to crack growth, and Y is a geometrical constant near unity for the surface flaws.

(ii) Compressive layers over optical surfaces

An example of compressive coatings over optical surfaces is an ion-beam sputtered film deposited on a polished component. Two changes from a bare optical surface are evident: first, the surface flaws are now internal flaws and second, these flaws are now acted on by a tensile stress, σ_t, whose magnitude is determined by the thickness and strain of the compressive layer.

The strength of components with compressive layers on top is thus

$$\sigma_f = [YK_c/[\pi(a/2)]^{1/2}] - \sigma_t \qquad (2)$$

where Eq. 2 is similar to Eq. 1 except that the crack size a, is replaced by a/2 because the crack is now an internal flaw (as opposed to a surface flaw) and σ_t is the tensile stress acting on the cracks due to the compressive layer on top. The internalization of the crack serves to increase the strength by about forty percent ($\sqrt{2}$). The decrease due to the tensile stress term is a small factor for most films of practical interest.

(iii)Compressive layers incorporated into the surface

Examples of this configuration are components strengthened by thermal tempering, chemical ion exchange, or by ion bombardment. For small cracks that are completely contained within the compressive layer, having a stress σ_c, the component strength is enhanced as

$$\sigma_f = \sigma_c + YK_c/(\pi a)^{1/2} \qquad (3)$$

When the crack size exceeds the depth of the compressive layer, the analysis is substantially more complex because the cracks may now be partially open. Green has numerically determined the stress intensity factor for this case.[5] Based on his analysis, we have expressed the strengthening graphically (Fig. 1).

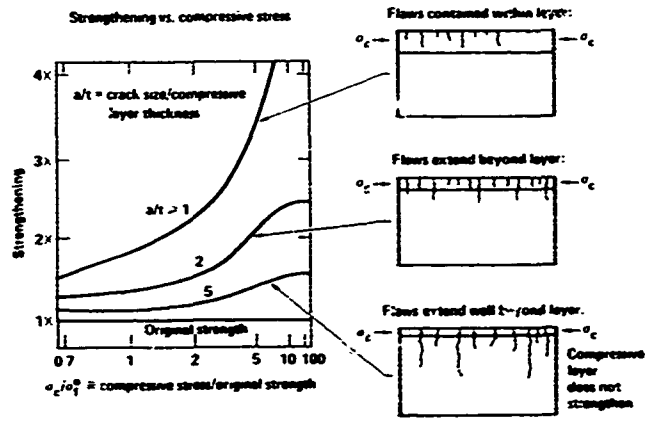

Fig. 1 Strengthening vs. compressive stress. Strengthening (> 5x) is achieved by thick layers and small cracks (t > a) together with high levels of compression. Little or no strengthening results from cracks larger than about five times the compressive layer thickness, regardless of whether the compressive stress is high or low.

B. Component Mechanical Durability

In the absence of a compressive surface layer, the strength of a component degrades in accordance with Eq. 1, from physical damage which causes a crack of depth, a. When a compressive surface layer is present the substrate's durability can be substantially improved. The component strength is not decreased if the crack does not extend beyond the compressive layer and if the extent of the compressive stress in the layer exceeds the applied stress. Under these conditions the crack remains always closed. However, if the crack extends beyond the layer, the analysis must again consider partially closed cracks. Here, we adapt portions of Green's numerical solutions[4] to illustrate the salient points (Fig. 2).

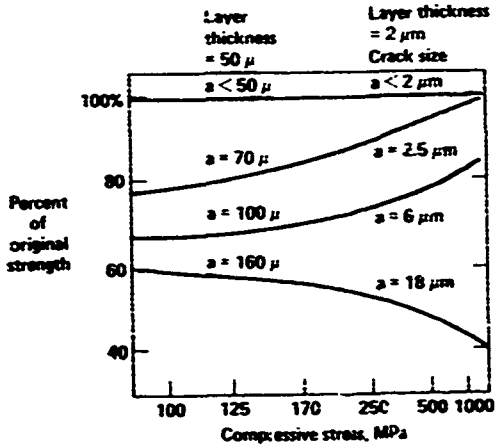

Fig. 2 The percent of the original strength that can be maintained in the presence of a compressive layer for two layer thicknesses, 2 and 5 μm, using several different crack depths. a is the crack depth due to the damage. Cracks up to about 2x the layer thickness can be resisted without excessive strength degradation. For resisting damage, the compressive layer thickness, rather than the magnitude of stress in the layer, is the most important parameter.

III. Experiments

A. Strength

In the absence of a compressive layer, the strength is related to the depth of the surface damage. Figure 3 illustrates the remarkable strengthening (~ 15 x) than can be achieved by minimizing the subsurface damage.[5]

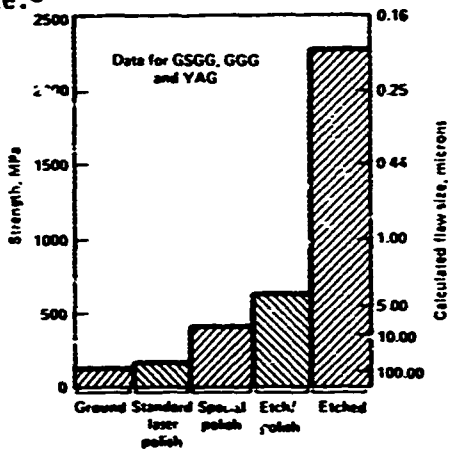

Fig. 3 Mean strength of laser garnets with various surface treatments. Special polish refers to the samples in which large amounts of material were removed during each grinding operation; 250 μm of material was removed during the 30-μm loose abrasive grind, 100 μm removed by 12-μm grit, and 75 μm removed by 3-μm grit, followed by polishing. Etching is for 20 min. in 200°C orthophosphoric acid.

We are now experimentally assessing the change in strength of components when a compressive layer is applied over the optical surface. We have not yet examined cases where the layer is incorporated into the surface. We currently employ two methods for producing compressive layers: ion beam sputtered films and epitaxial films. Ion beam sputtered silica films are deposited on glass[5] and on garnet single crystal substrates.[7] These films are fairly thin, between one and two microns, and have fairly high levels of compressive stress (~ 400 MPa). On single crystal garnets we have also grown compressive epitaxial single crystals films. $Gd_3Ga_5O_{12}$:Nd was grown on $Gd_3Ga_5O_{12}$ substrates in thicknesses between 5 and 50 μm and with stresses between 50 and 250 MPa. Table 1 illustrates the modest changes in strength which occur when compressive layers are added on top of coatings. These results are in general agreement with our expectations (Eq. 2).

B. Mechanical Durability

To assess the compressive layers resistance to abrasion and in-service flaw generation, we model these damage processes using two techniques. Careless cleaning and handling damage is modeled by abrasion of the substrates using 5 μm diamond and laser damage is modeled by a Vickers micro-hardness indentation at a 2N load. This load is sufficient to nucleate small radial cracks from the corners of the indentation, causing surface flaws in the sample similar to the damage pits.

Table 1. Strength with and without compressive layer

Substrate Material	Layer Material	Deposition Method	Layer Thickness, μm	Layer Stress, MPa	Strength without layer, MPa	Strength with layer, MPa
LHG-5	SiO_2	IBS	2	400	360	680
GGG	SiO_2	IBS	2	400	440	430
GGG	GGG:Nd	LPE	6	220	3010	2140
GGG	GGG:Nd	LPE	43	50	3010	1870

LHG-5 is a Hoya phosphate glass, GGG is $Gd_3Ga_5O_{12}$ single crystal, IBS is ion-beam sputtering, LPE is liquid phase epitaxy.

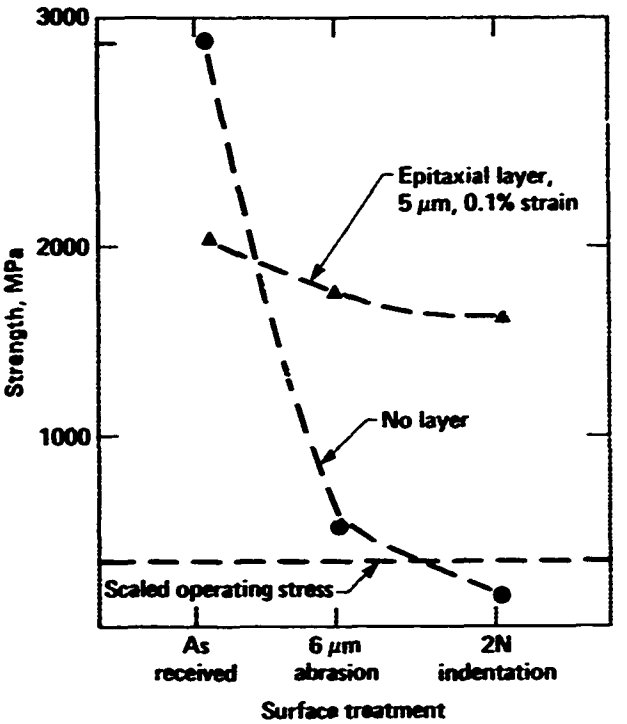

Fig. 4 Abrasion of compressive epitaxial layers on garnet substrates. The strength of the substrates without compressive layers decreases after abrasion by factors between 5 and 20. In the presence of the epitaxial layers, the strength is not significantly reduced after the moderately severe abrasion treatments.

IV. Conclusions

Compressive layers applied onto the optical surfaces do not change the strength very much; the extent of the subsurface damage has a much more profound effect (Eq. 1 and Fig. 3).

In general, the substrates with the compressive layers resist physical damage, of the moderately severe level studied, without significant deterioration in strength and can therefore be regarded as being mechanically durable (Fig. 4). The trends predicted by our mechanical durability models are in general accordance with our experimental observations. However, both more theoretical work and additional experiments are required to adequately characterize these systems.

In conclusion, the combination of a low sub-surface damage polish to give high strength, coupled with a thick compressive layer for good mechanical durability will give strong components in service applications. We have shown that optical components with low subsurface damage and thick compressive layers, are strong and mechanically durable.

The compressive layers were applied by T. Allen, Optical Coating Laboratory, Santa Rosa, CA., and D. M. Gualtieri, Allied-Signal Corp., Morristown, N.J. This work was performed under the auspices of the U.S. Department of Energy by Lawrence Livermore National Laboratory under Contract No. W-7405-ENG-48.

References

1. J. L. Emmett, W. F. Krupke and J. B. Trenholme, Sov. J. Quantum. Elect. 13, 1 (1983).
2. J. E. Marion, J. Appl. Phys. 60, 69 (1986).
3. D. J. Green, J. Amer. Ceram. Soc. 66, 807 (1983).
4. D. J. Green, J. Mat. Sci. 19, 2165 (1984).
5. J. E. Marion, Appl. Phys. Lett. 47, 694 (1985).
6. J. E. Marion, Advances in Laser Science, Proc. Amer. Inst. Physic. 146, 234 (1986).
7. J. E. Marion, D. M. Gualtieri and R. C. Morris, UCRL#95778, Lawrence Livermore National Laboratory, 1986.

THURSDAY, FEBRUARY 12, 1987

BALLROOM B
10:30 A.M.–12:00 M

ThB1–5

SESSION 6

Brian E. Newnam, Los Alamos National Laboratory,
Presider

Natural and Induced Space Radiation Effects on Coated Laser Optics

T. M. Donovan

Michelson Laboratory, Physics Division
Naval Weapons Center, China Lake, California 93555-6001

Summary

The reflectance of metal-enhanced, high-reflectance mirrors containing amorphous Si and SiO multilayers has been found to be stable in a simulated natural space environment containing the combined effects of solar ultraviolet light, energetic protons, and electrons.[1] By eliminating the metal-enhancing layer from the stack and depositing the coating design on a silicon or fused silica substrate, the resulting low atomic number (Z) structure presents a low-absorption cross section for x-rays. Thus, it becomes an interesting design for studying the thermal and thermomechanical response of multilayer coatings to pulsed x-ray deposition.

In this paper, the results of pulsed x-ray experiments will be compared with calculations of predicted melt and thermomechanical damage. The results will be discussed in light of pulsed laser experiments.

---

[1]T. M. Donovan, S. J. Holmes, and L. B. Fogdall, "Enhanced Reflectance Mirrors for Space-Borne Laser Applications," SPIE Proceedings, High Power Lasers and Applications, Vol. 270, Los Angeles, CA, 11-13 February 1981, pp. 24-29.

INCREASED VISIBLE ABSORPTANCE OF VISIBLE REFLECTORS DUE TO ULTRAVIOLET RADIATION

Stephen Browning and Robert Young
Optical Coating Laboratory, Inc.
2789 Northpoint Parkway
Santa Rosa, CA 95407-7397

High performance laser mirrors exhibit a decrease in visible reflectance over time when exposed to the ultraviolet radiation emanating from a gaseous laser plasma. This drop in reflectance can lead to cessation of laser action in the worst cases, and unpredictable system performance in any case. Ideally the mirrors would maintain a constant high reflectance for an indefinite time period. An acceptable alternative would be for the mirror reflectance to degrade slightly over a short time to a then-constant value.

Mirror reflectance is measured using a cavity ring-down lossmeter (1) (Figure 1), operating at 633 nm. A two-mirror cavity is calibrated for total round trip radiation loss. A sample is then placed in the holder and one end mirror repositioned to form a three-mirror cavity. All the increase in loss for the new configuration is attributed to the sample, and is composed of transmission, scatter, and absorption. The sample is effectively isolated in an environmentally controlled chamber (Figure 2), which is also fitted with a penlight radiation source (2). This source does not spectrally match the laser plasma output, but provides a suitable, albeit accelerated, simulation. Additional measurements include spectrophotometric transmittance in wet and dry ambient conditions, and off-angle scatter.

Precision optical flats were coated with high reflector coatings using a variety of deposition methods. These flats were then measured using the lossmeter. The samples were irradiated by the penlight for one hour, with measurements taken every five minutes. Then the penlight was turned off, with measurements continuing for an additional half hour. "Dry measurement" indicates that the samples were baked in air for four hours minimum, then kept in a nitrogen purged environment prior to and during measurement. "Wet measurements" were performed without the bake and at ambient humidity. Figures 3-7 show the wet and dry measurements of normalized loss with time for samples coated with five different deposition methods. The loss is seen to increase for all samples when uv irradiation commences, and typically begins to decrease when the penlight is turned off. Those samples which display the largest difference in wet and dry loss behavior also exhibit larger shifts in wavelength for wet versus dry spectrophotometric transmittance. Figure 8 compares dry loss behavior for the different deposition methods. The advanced processes tend to show improved behavior. Figure 9 compares wet loss behavior for three different deposition methods when irradiated with a longer wavelength source.

All samples tested show some increase in loss when exposed to ultraviolet radiation. Most of the increase occurs within 10 minutes of the beginning of the exposure. The presence of adsorbed moisture in the coatings tends to enhance the increase in loss. All samples exhibit some degree of perfor-

mance recovery when the uv irradiation ceases. Indeed, recovery can be accelerated by a low temperature bake in air. Longer wavelength radiation is less effective at increasing loss. Scatter was not affected by uv radiation.

References:

1) Anderson, D.Z. et al: "Mirror Reflectometer Based on Optical Cavity Decay Time", Applied Optics 23:1238

2) Analamp Model 81-1057-001,-04, BHK Inc., Monrovia, California 91016

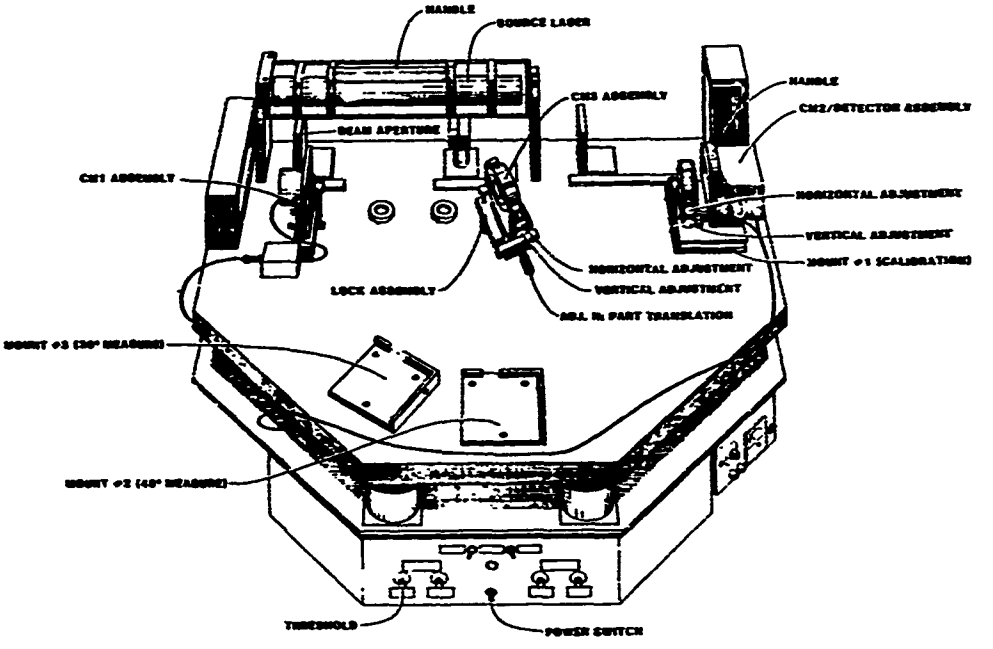

Figure 1.

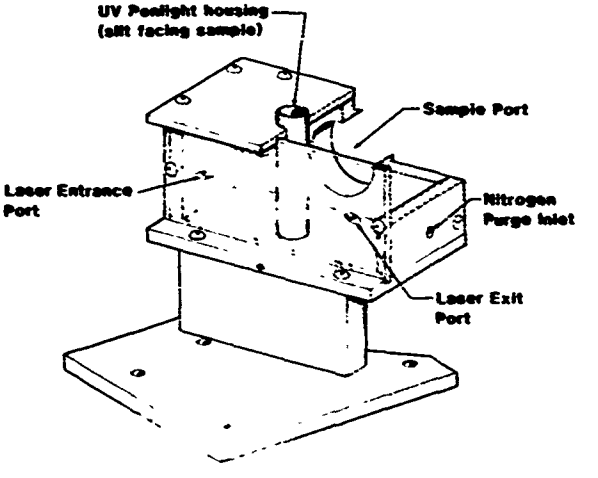

Figure 2 Environmental Chamber

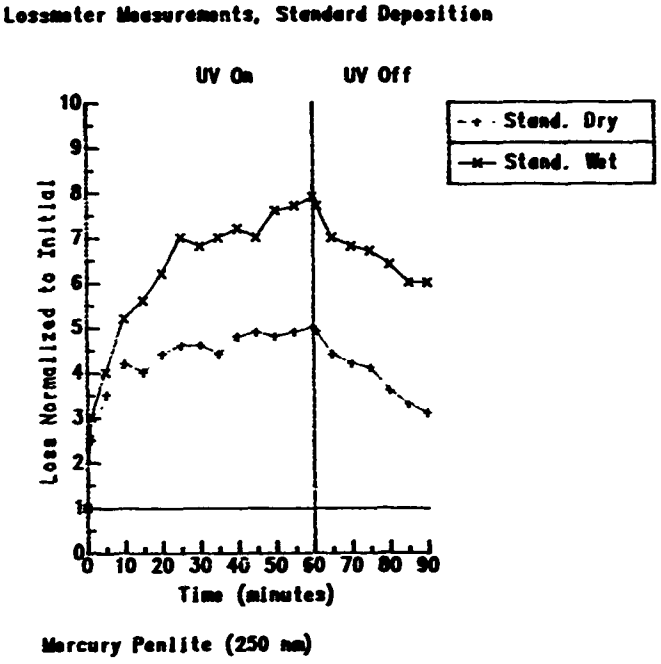

Figure 3.

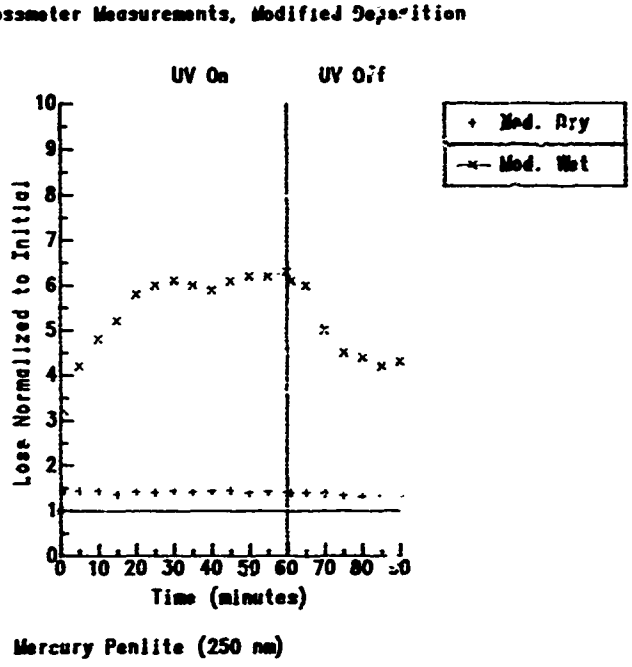

Figure 4.

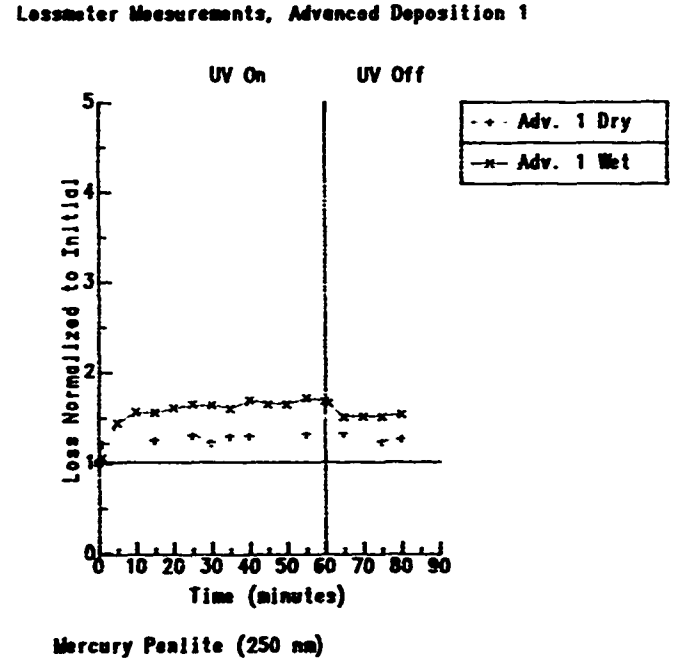

Figure 5.

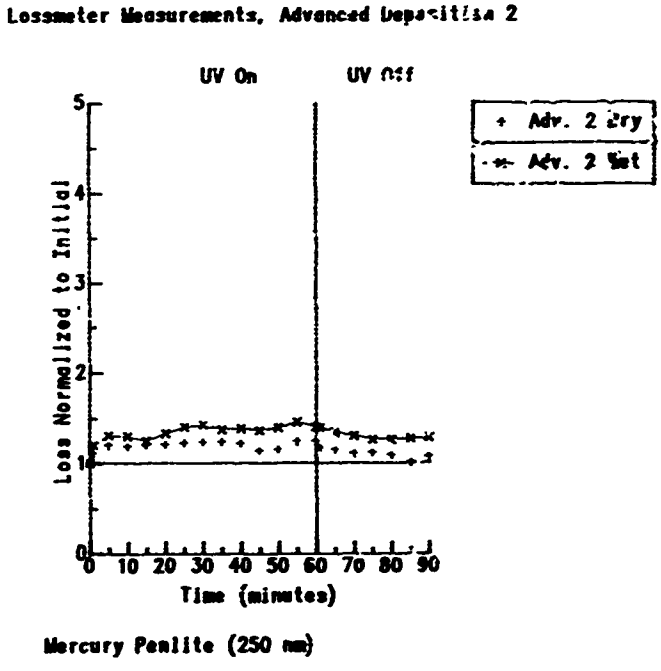

Figure 6.

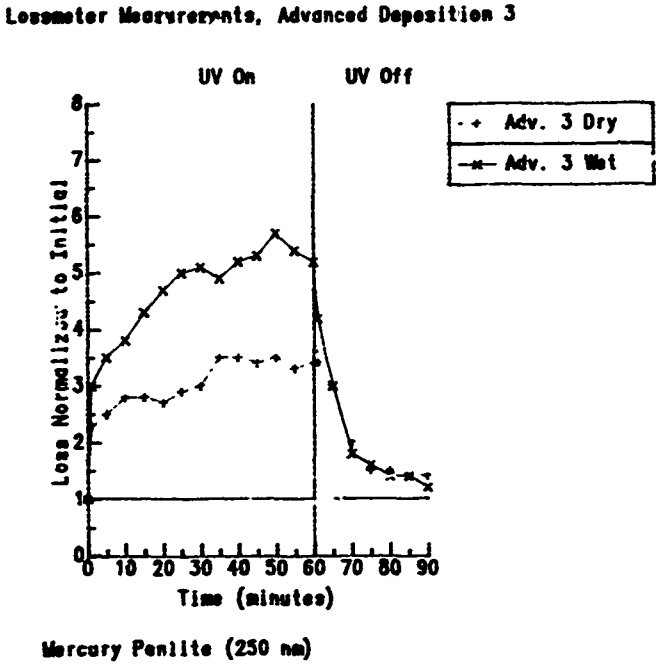

Figure 7.

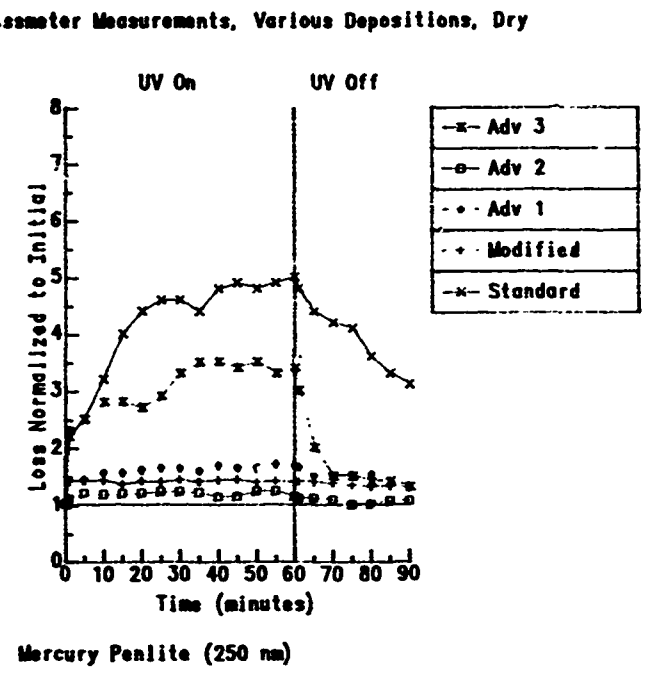

Figure 8.

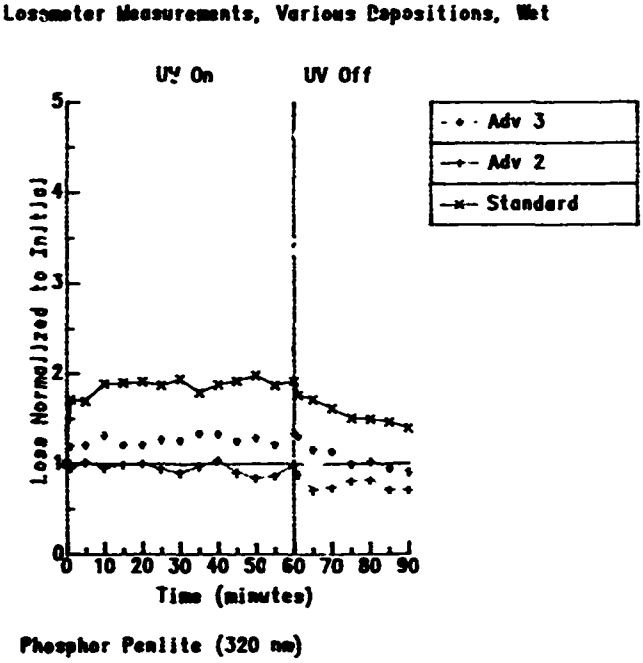

Figure 9.

ThB3

Ultraviolet Degradation of Ring Laser Gyroscope Mirrors
Austin Kalb

Damage Threshold and Environmental Durability Of Oxide Coatings Deposited Using Ion Assisted Deposition

James J. McNally
USAFA/DFP
Department of Physics
United States Air Force Academy, CO 80840
and
J. R. McNeil
Department of Electrical and Computer Engineering
University of New Mexico
Albuquerque, NM 87131

Introduction

The optical, physical and chemical properties of materials in thin film form can vary significantly from bulk properties. These differences in properties are directly related to film microstructure which is predominantly columnar, containing voids and material inhomogeneities. A number of novel deposition techniques have been developed in attempts to improve the properties of thin films. In these techniques, energetic processes are employed to increase adatom mobility and eliminate the formation of columnar microstructure. One of these techniques is ion assisted deposition (IAD).

Thin films deposited using IAD have exhibited increased packing density, improved stability, durability and stoichiometry.[1-6] Martin, et.al. have studies the effects on the properties of ZrO_2 and CeO_2 films bombarded with O_2^+ during deposition.[4,5] McNeil et.al. examined the effects of 30 and 500 eV O_2^+ bombardment on the properties of TiO_2 and SiO_2 films.[3] Al-Jumaily et.al. examined the effects of ion energy and flux on optical scatter in Cu and TiO_2 films.[6] McNally et.al. have used IAD to deposit coatings on heavy metal fluoride substrates at low temperatures.[2]

The purpose of this work was to investigate the effects of IAD parameters on the properties of Ta_2O_5, Al_2O_3 and SiO_2 thin films. The optical constants and environmental stability of single-layer coatings are reported. A number of single-layer coatings were tested for their resistance to fluorine gas attack. The results of these tests, as well as, laser-induced damage results are presented. We investigated the use of IAD to deposit protective coatings on heavy metal fluoride (HMF) glass to obtain good quality coatings at reduced substrate temperature. Single-layer coatings of MgF_2 and SiO_2 were deposited onto substrates of HfF_4-BaF_2-LaF_3-AlF_3 (HBLA) glass. Tests were performed to determine film and substrate environmental durability and scratch resistance.

Experimental Arrangement

The coatings were deposited in a 90 cm diameter, cryogenic pumped vacuum system. A 16 cm Kaufman ion source provided a monoenergetic ion beam independent of the material evaporation process. It provided a low-energy (200-1000 eV) beam of O_2 or Ar ions. The Ta_2O_5, Al_2O_3 and SiO_2 coatings were electron-beam evaporated with oxygen backfill pressure of 1.0×10^{-4} Torr.

The coatings transmittance and reflectance spectra were measured over the wavelength range 0.185 - 1.2 μm using a dual-beam spectrophotometer. The spectra were used to calculate the refractive index (n), the extinction coefficient (k) and the thickness (t) for each coating using a technique due to Manifacier, et.al.[7]

Humidity cycle tests were conducted in a controlled humidity chamber. The coatings were exposed to 97% relative humidity at 35°C for extended periods of time. The film transmittance spectra were examined before and after the humidity exposure to determine the amount of spectral shift.

Single-layer coatings were tested at Los Alamos National Laboratory for resistance to fluorine gas attack. Coated substrates were used as windows on

one end of a gas filled cannister. The gas content was 0.5% F_2 in He. Transmittance at 351 nm was monitored at various time intervals to examine the durability of coatings in fluorine gas environment.

A number of AR coatings were laser damage tested at LANL. The laser-induced damage threshold (LIDT) values were measured with 9 nsec 351 nm pulses. Pulse repetition frequency was 35 pps with mean spot diameter ($1/e^2$) of 0.46 mm at the sample surface. All damage testing was n-on-m, where m=10 sites were irradiated at each laser fluence for a maximum of n=140 pulses. Damage was defined as any visible change in the coating observed under 60X microscope examination. LIDT value was defined as the zero-probability intercept value. The coating design was SLLHL where S was the substrate, L was quarter-wave thick SiO_2 and H was quarter-wave thick Al_2O_3.

Results

The values of n (at λ = 350 nm) for Al_2O_3 coatings bombarded with 300, 500 and 1000 eV oxygen ions were determined as a function of O_2^+ current density(J). The values increased from 1.64 for coatings deposited without bombardment to maximum values of 1.70, 1.68 and 1.68 for films bombarded with 1000, 500 and 300 eV O_2^+, respectively.

The increase in the values of n with increasing O_2^+ current density indicated that bombardment during deposition modified the growth of film columnar microstructure. The results indicated that the coatings bombarded with 1000 eV O_2^+ had larger values of n than those bombarded with 500 and 300 eV O_2^+. A similar dependence of refractive index on bombarding ion energy has been reported for ion assisted CeO_2 films.[5]

The current density value (for a fixed ion energy) at which the maximum n occurs is often termed the critical value. The results illustrated that film index values decreased for (J) larger than the critical values. The decrease in index may be explained as a result of degradation in film stiochiometry, creation of closed isolated voids or oxygen incorporation into the films. The decrease was largest for bombardment with 1000 eV ions and least for 300 eV ions. Similar results for which the values of refractive index decreased for (J) larger than the critical values have been reported for ion assisted ZrO_2 films[4] and CeO_2 films.[5]

The values of n (at λ = 400 nm) for Ta_2O_5 coatings bombarded with 200, 300 and 500 eV oxygen ions were determined as a function of O_2^+ current density. The values increased from 2.16 to maximum values of 2.25, 2.28 and 2.19 for films bombarded with 500, 300 and 200 eV O_2^+, respectively. The increase in the value of n for increasing (J) is similar to Al_2O_3 results and indicated that bombardment during deposition resulted in film densification. The results indicated that the Ta_2O_5 coatings bombarded with 300 eV O_2^+ had larger values of n than those bombarded with 500 eV O_2^+. These results illustrate that the effects of ion bombardment are material dependent. The ion energy at which the largest value of n occurred for Ta_2O_5 was 300 eV, yet, for Al_2O_3 it was 1000 eV.

The results again illustrated that values of n decreased for (J) larger than the critical values. The decrease was largest for bombardment with 500 eV ions and least for 200 eV ions. This energy dependent decrease is consistent with the results for IAD Al_2O_3 coatings and results reported for ion assisted ZrO_2 film[4] and CeO_2 films.[5]

A number of Ta_2O_5 coatings were exposed to humidity testing to examine the effects of ion bombardment on film stability. The transmittance curves for the Ta_2O_5 coatings exposed to humidity testing were measured before and after exposure. The spectra for the coatings deposited without bombardment illustrated a spectral shift to longer wavelengths of 1%. No spectral shifts for IAD coatings within the measurement precision ($\pm$ 0.5 nm) of the

spectrophotometer were observed except for one case. Similar results have been reported for IAD ZrO_2.[4] The Ta_2O_5 results are summarized in Table II.

TABLE II

Spectral Shifts for Ta_2O_5 Coatings After Humidity Exposure

E (eV)	J ($\mu A\ cm^{-2}$)	Spectral Shift (%)
0	0	2.0%
300	10	0.3%
300	20	0.0%
300	40	0.0%
500	10	0.0%
500	20	0.0%

A number of coatings were studied for the effects of static exposure to fluorine gas. Three single-layer Al_2O_3 coatings were exposed to 0.5% dry F_2 in He gas mixture. The coating deposited with no ion bombardment suffered no degradation in optical transmittance after 670 hours of exposure. The optical transmittance for this coating dropped by 4% after 1003 hours. The Al_2O_3 coating bombarded during deposition with 500 eV O_2^+ at a current density of 50 $\mu A\ cm^{-2}$ suffered approximately 4.5% loss in optical transmittance after 470 hours of exposure. The coating bombarded with 500 eV O_2^+ at 25 $\mu A\ cm^{-2}$ suffered approximately 10% loss in optical transmittance after only 28 hours exposure. Four Ta_2O_5 coatings were exposed to fluorine gas tests. The four coatings all suffered a >5% loss in transmittance after only 300 hours exposure. The performance of the Ta_2O_5 coatings was very poor relative to required performance criteria.

A number of Al_2O_3/SiO_2 AR coatings were laser damage tested at LANL. The zero-probability LIDT values for Al_2O_3/SiO_2 coatings bombarded with 300 and 500 ev oxygen ions were measured versus O_2^+ current density. Tantalum (Ta) filaments were used in the ion source. With one exception, it appears that the IAD coatings did not have higher LIDT values than the coatings deposited with no ion bombardment (J=0). The coatings bombarded with 300 eV O_2^+ at a current density of 10 $\mu A\ cm^{-2}$ had an average LIDT value of 6.1 J cm^{-2} with a $\pm$7% variation for the coatings tested. This represents a 65% increase in LIDT value over the J=0 coatings.

A contamination analysis of IAD TiO_2 coatings indicated that tungsten (W) filament material was incorporated into the coatings.[8] As part of this study, a number of IAD Al_2O_3/SiO_2 AR coatings were deposited using W filaments in the ion source ("W coatings"). Another set of coatings were deposited using identical IAD conditions except Ta filaments were used in the ion source ("Ta coatings"). The purpose of this comparison was to attempt to control one defect in IAD coatings and to measure LIDT values for coatings in which different filament materials were used.

The "Ta coatings" had LIDT values consistently higher than the "W coatings". The largest difference is for the higher energy (500 eV), higher current density (40 $\mu A\ cm^{-2}$) case. The average value of the increase in LIDT for the "Ta coatings" was 40%. This exceeded the run-to-run variations in LIDT values which was $\pm$25%. The results appear to indicate an improvement in LIDT value for "Ta coatings" over "W coatings".

Heavy metal fluoride (HMF) glasses have attracted considerable interest as multispectral transmissive optical components, laser host materials and optical fibers. However, despite their promising optical characteristics, many compositions are relatively soft and hygroscopic. Fluoride glass materials have low softening temperatures, typically 200°C. This precludes application of standard thin film deposition techniques which require a substrate temperature of 250-300°C. An HBLA glass sample was coated with 0.5 μm IAD MgF_2 film, and another sample was left uncoated. A drop of water was

placed on each sample for approximately 16 hours. The samples were then examined using a Nomarski microscope. The results for the uncoated sample illustrated the known susceptibility to aqueous corrosion of an unprotected fluoride glass surface. The result for the coated sample showed that it did not suffer any noticeable degradation. An HBLA glass sample coated with 0.5 μm IAD SiO_2 was also subjected to a water drop test. Again, there was no noticeable degradation in the film exposed to the water drop; it appeared exactly as the portion not exposed. Thus, overcoating a fluoride glass with an IAD coating may offer adequate protection from moisture attack and allow the use of HMF glasses in adverse environments.

The effect of a coating on the abrasion resistance of HMF glass substrates was investigated. Samples were subjected to an eraser-rub test and examined using Nomarski microscope. A sample was divided into two section; one section was coated with 0.5 μm IAD MgF_2, and the other section was left uncoated. The sample was then subjected to an eraser-rub test. The unprotected HMF glass was soft and subject to abrasion, while the IAD coated section was hard and much less subject to abrasion. The abrasion resistance for two MgF_2 coatings on glass substrates was investigated. It is well established that MgF_2 films deposited onto unheated substrates are soft; substrate temperatures of 250°C are required to produce durable films. One sample was coated with 0.5 μm IAD MgF_2, and the other was coated with 0.5 μm MgF_2 deposited with ion bombardment. The samples were then subjected to an eraser-rub test. The unbombarded (J=0) sample was scratched, whereas the bombarded sample was much less scratched. This illustrated that the IAD coated sample was more durable than the J=0 sample. Another HMF sample was divided into two sections. One section was coated with 0.5 μm IAD SiO_2, and the other section was left uncoated. Results similar to those obtained for the IAD MgF_2 coated samples were obtained. The coated section was much less scratched than the uncoated section. Although the abrasion resistance test used was qualitative in nature, it appears that harder films may be obtained using IAD. These results indicate that overcoating a fluoride glass with an IAD coating can enhance the durability of HMF glasses.

References

1. J.J. McNally, G.A. Al-Jumaily, and J.R. McNeil, "Ion Assisted Deposition of Ta_2O_5 and Al_2O_3 Thin Films," J. Vac. Sci. Technol. A4, 437 (1986).
2. J.J. McNally, G.A. Al-Jumaily, J.R. McNeil, and B. Bendow, "Ion-Assisted Deposition of Optical and Protective Coatings for Heavy Metal Fluoride Glass," Appl. Opt. 25, 1973 (1986).
3. J.R. McNeil, A.C. Barron, S.R. Wilson, and W.C. Herrmann, Jr., "Ion-Assisted Deposition of Optical Thin Films: Low Energy vs High Energy Bombardment," Appl. Opt. 23, 552 (1984).
4. P.J. Martin, R.P. Netterfield, and W.G. Sainty, "Modification of the Optical and Structural Properties of Dielectric ZrO_2 Films by Ion-Assisted Deposition," J. Appl. Phys. 55, 235 (1984).
5. R.P. Netterfield, W.G. Sainty, P.J. Martin, and S.H. Sie, "Properties of CeO_2 Thin Films Prepared by Oxygen-Ion Assisted Deposition," Appl. Opt. 24, 2267 (1985).
6. G.A. Al-Jumaily, J.J. McNally, J.R. McNeil, and W.C. Herrmann, Jr., "Effects of Ion-Assisted Deposition on Optical Scatter and Surface Microstructure of Thin Films," J. Vac. Sci. Technol. A3, 651 (1985).
7. J.C. Manifacier, J. Gasiot, and J.P. Fillard, "A Simple Method for the Determination of the Optical Constants n, k, and the Thickness of a Weakly Absorbing Thin Film," J. Phys. E9, 1002 (1976).
8. G.A. Al-Jumaily, S.R. Wilson, A.C. Barron, J.R. McNeil, and B.L. Doyle, "Contamination Analysis of TiO_2 Thin Films Deposited Using Ion Assisted Deposition," Nucl. Instr. and Meth. B7/8, 906 (1985).

Ion Assisted Deposition of Optical Coatings at Low Temperature

Forrest L. Williams, D. W. Reicher, J. J. McNally*, G. A. Al-Jumaily† and J. R. McNeil

University of New Mexico
Department of Electrical and Computer Engineering
Albuquerque, New Mexico 87131.

*Department of Physics
USAFA/DFP
United States Air Force Academy, Colorado 80840

†Barr Associates, Inc.
2 Lyberty Way
Westford, Massachusetts 01886

The heavy metal fluoride (HMF) glasses are a new class of optically useful but environmentally unstable materials. These materials possess desirable optical properties, including a broad transmittance range from the mid-IR ($\sim$7 μm) to the near-UV ($\sim$0.3 μm), low absorption and scatter losses, low dispersion, low index of refraction and low thermal distortion.[1] However, despite their promising optical characteristics, many HMF compositions are hygroscopic and relatively soft. Thus, hermetic coatings are required that will protect HMF glasses without degrading their optical properties. The problem is compounded by the fact that HMF materials have low softening temperatures, typically $\sim$200 °C. This precludes standard thin film deposition techniques that require a substrate temperature of $\sim$300 °C. It is important to note that optical coatings conventionally deposited at low temperature usually exhibit reduced refractive index, increased optical absorption, poor environmental stability and less resistance to abrasion.

A relatively new technique for improving the optical and mechanical properties of thin films is ion assisted deposition (IAD), which involves bombardment of the growing film with ions during deposition. It has been shown that IAD can produce films with properties that approach those of bulk materials.[2,3] We have applied the IAD process to deposit optical coatings of TiO_2 at reduced substrate temperature ($T \simeq 175^\circ C$), and achieved thin films of this material that have increased refractive index and improved environmental stability.[4] In addition, we have successfully used IAD to deposit protective optical coatings of MgF_2 and SiO_2 at a lower temperature ($T \simeq 100^\circ C$) onto HMF substrates.[5] We now extend the previous work to describe the properties of Ta_2O_5, Al_2O_3 and TiO_2 thin films deposited using IAD at $\sim 100^\circ C$.

Films were deposited in a 90 cm diameter stainless steel bell jar vacuum system with a base pressure of $\sim 4 \times 10^{-8}$ Torr. The chamber was backfilled with $\sim 10^{-4}$ Torr O_2 during deposition. Substrates were heated to $\sim 100^\circ C$ with lamps actively controlled by a thermocouple monitoring system. The films were deposited at a rate of 2 Å s^{-1} using an e-beam evaporative source, and were bombarded with O_2^+ from a Kaufman ion source during deposition. A detailed description of the experimental apparatus may be found in reference 6.

The optical coatings were analyzed for their index of refraction and optical absorption.[7] For all three film materials, the values of film refractive index increase for increasing ion current density, suggesting that IAD has increased the packing density of the film material. Other methods of analysis were a test of environmental stability after exposure to humidity and an eraser rub test to study abrasion resistance. These also indicated that IAD increased the film packing density.

Another application involving ions in depositing thin films is to preclean the surface by bombarding with energetic Ar^+ prior to deposition.[8] While this is an effective way of removing contaminants from a surface, certain compositional and morphological changes in the substrate can occur which could have an effect on the properties of the film.[9,10] In the case of HMF glass, little is known about the effects of substrate precleaning with Ar^+ bombardment. We have therefore investigated the possible effects Ar^+ precleaning might have on HMF substrates by using ellipsometry to look for crystalline phase changes in the material.

Substrates of HMF glass were bombarded for five minutes with Ar^+. The Ar pressure during bombardment was $\sim 10^{-4}$ Torr, and the bombardment conditions were those typically used for precleaning ($E = 500$ eV, $J \simeq 75\ \mu A\ cm^{-2}$). After bombardment, the substrates were removed from the apparatus and analyzed using a Rudolph ellipsometer having a HeNe laser as its light source.

The low softening temperatures of heavy metal fluorides limit processes that handle these materials to temperatures below $\sim 200^\circ C$. It is not known, however, what effects, if any, might occur from using heavy metal fluorides in a process that operates at intermediate temperatures ($\sim 30^\circ C < T < \sim 200^\circ C$). In an effort to investigate the effects such processes might have on HMF materials, we have used ellipsometry to examine the possible crystalline phase changes in HMF material that has been subjected to room temperature, $\sim 100^\circ C$ and $\sim 200^\circ C$ in a $\sim 10^{-4}$ Torr Ar atmosphere. We have also simultaneously bombarded separate samples of this material with Ar^+ while they were exposed to the three different temperature conditions. Results from all three crystalline-phase studies will be presented.

[1] D. C. Tran, G. H. Sigel, Jr. and B. Bendow, IEEE/OSA J. Lightwave Technol. **LT-2**, 566 (1984).

[2] P. J. Martin, R. P. Netterfield and W. G. Sainty, J. Appl. Phys. **55**, 234 (1984).

[3] J. J. McNally, G. A. Al-Jumaily and J. R. McNeil, J. Vac. Sci. Technol. **A5**, (1986), in press.

[4] F. L. Williams, J. J. McNally, G. A. Al-Jumaily and J. R. McNeil, J. Vac. Sci. Technol. **A5**, (1986), in press.

[5] J. J. McNally, G. A. Al-Jumaily, J. R. McNeil and B. Bendow, Appl. Opt. **25**, 1973 (1986).

[6] J. R. McNeil, A. C. Barron, S. R. Wilson and W. C. Hermann, Jr., Appl. Opt. **23**, 552 (1984).

[7] H. Demiryont, J. R. Sites and K. Geib, Appl. Opt. **24**, 490 (1985).

[8] S. I. Petvai and R. H. Schnitzel, in *Surface Contamination: Genesis, Detection and Control I*, edited by K. L. Mittal (Plenum, New York, 1979), pp. 297-311.

[9] D. M. Mattox, in *Deposition Technologies for Films and Optical Coatings* . edited by R. F. Bunshah (Noyes Publications, Park Ridge, New Jersey, 1982), pp. 251-254.

[10] R. Kelly and H. M. Naguib, in *Atomic Collision Phenomena in Solids*, edited by D. W. Palmer, M. W. Thompson and P. D. Townsend (North-Holland, Amsterdam, 1970), pp. 172-191.

KEY TO AUTHORS AND PAPERS

TOPICAL MEETING ON

OPTICS IN ADVERSE ENVIRONMENTS

Postdeadline Materials

Changes to the Program

Paper WA3 entitled "Learjet Observatory Operations in the Tropics" by P. H. Hagan, et al. was withdrawn.

In its place, two papers were presented: paper WA3A entitled "Radiation Induced Absorption in Pyrex" by G. H. Miley, R. Chapman, J. Nadler, and W. Williams, University of Illinois (no written text provided); and paper WA3B entitled "Effects of Irradiation with Photons and Charged Particles on Optical Emission and TSD Currents from and in Silicate Glasses" by R. A. Weeks, et al., see page 78.

Supplementary Material

Expanded summaries are presented for two papers: paper WA2 entitled "Ultra Lightweight Optics in a Cryogenic Environment" by D.A. Crowe, see page 83; and paper WC4 entitled "Impinged Droplet Evaporative Cooling for Optical Mirrors Subjected to High Thermal Flux Loads" by J. A. Wellman, and J. J. Meyers, see page 86.

ABSTRACT submitted for the Southwest Optics'87 Conference
Feb. 9-13, 1987, Albuquerque, NM

Effects of Irradiation with Photons and Charged Particles on Optical Emission and TSD Currents from and in Silicate Glasses

R.A. Weeks & D. L. Kinser, Mech & Matls.Eng. Dept.
R.Haglund, N.Tolk, M.Shea, H.Pois, & J.Ye, Physics & Astronomy Dept.
Paul Wang, joint MME & P&A Departments
H. Mogul, Electrical Engineering Dept.

Vanderbilt University, Nashville, TN 37235

Surfaces of the silicate glasses were irradiated in ultra-high vacuum by 5 keV and 9 keV Ar^+ beams. Surface composition was monitored before and after irradiation by analyzing light emitted by excited atoms, ions and molecules sputtered from the glass surface.

Research supported in part by Naval Research Laboratory under contract N00014-86-C2546.

Effects of Irradiation with Photons and Charged Particles on Optical Emission and TSD Currents from and in Silicate Glasses

R.A. Weeks & D. L. Kinser, Mech & Matls.Eng. Dept.
R.Haglund, N.Tolk, M.Shea, H.Pois, & J.Ye, Physics & Astronomy Dept.
Paul Wang, joint MME & P&A Departments
H. Mogul, Electrical Engineering Dept.

Vanderbilt University, Nashville, TN 37235

Ion-induced desorption of Spectrosil and Spectrosil WF and charge storage of Spectrosil WF using a thermally stimulated current (TSC) technique have been measured as a function of energetic particle Ar^+ and gamma-ray irradiations. These results indicate significant differences in ion-induced desorption between the two types of Spectrosil which we tentatively attribute to material processing effects. The TSC data show that charge storage effects are surprisingly large.

Radiation Induced Charge Displacement

The displacement of charge in a dielectric by energetic radiation is a phenomena which has been known since the early observations of Lichtenberg who observed radiation induced catastrophic dielectric discharge. The displacement of charge, which produced such effects, depends upon the details of the type and energy of the radiation as well as the material and other factors such as temperature.

Figure 1 displays the results of a thermally stimulated polarization current (TSPC) measurement made on Spectrosil WF without radiation. It displays a current rise beginning at approximately 180 C. After exposure to 1.8×10^6 isotropic gamma-ray flux, in the same sample, the current rise begins at approximately 80 C. This observation indicates that the Spectrosil WF has a large number of charged defects created by this radiation flux. These are released as the sample temperature increases and recombine providing the observed current.

Ion-Induced Desorption from Spectrosil and Spectrosil WF

The impetus behind this portion of the work was the desire to find a cleaning protocol for glass samples when introduced into a ultrahigh vacuum environment. We intended to look at the radiation from particles sputtered by argon ions from the sample surface as a function of time, in order to be certain that any contaminant overlayer material was removed in a reproducible way prior to carrying our desorption studies. In addition, we wanted to find out whether the relative abundance of impurity species on the surface was correlated with the bulk compositional analysis of the glass. A typical spectrum from the excited neutrals and ions desorbed by ion bombardment from Spectrosil is shown in Figure 2, where the spectral lines of many of the desorbing species appear in addition to the normal bulk fluorescence. Many, though not all, of these spectral lines have been identified as belonging either to Si or to various impurities in the glass.

The first indication that there was a more interesting aspect of this study in surface cleaning protocols came when we irradiated Spectrosil WF -- another fused silica preparation made with a different intermediate processing step to reduce hydrogen content -- under the same conditions. These data are shown in Figure 3, in which the bulk fluorescence peak resembles in a general way the broad bulk fluorescence signal of Figure 2, but in which the individual atomic emission lines have disappeared. Since both spectra were taken for the same incident flux of 5 keV Ar^+ ions, the disappearance of the individual emission lines from desorbing atoms is an indication that the energy of the incoming ions is no longer being dissipated through excited neutral and ionic desorption channels. This is a result of immense significance, because it represents possibly the first experimental evidence that one specific mechanism of radiation damage -- namely, surface desorption -- is dramatically inhibited by an identifiable change in processing of this fused silica.

We have also measured the detailed behavior of certain of the silicon and calcium lines with a view toward establishing an "energy budget" for the incident ions and also to aid in identifying the mechanism responsible for the Si desorption. For the Si line at 2516 Å, for example, the decrease in total peak area at high total doses means that less of the incident ion energy is being metabolized by the material through that channel. In contrast, the relative intensity of the Si line at 2881 Å actually increases slightly -- suggesting that at high doses, it is likely that it is the dominant desorption event leading to loss of Si from the surface. Similar contrast may be drawn for the two Ca II lines studied.

The width of an emission line is well known to be one benchmark indicator of the velocity of the velocity distribution of atoms emitted. The Si line at 2516 Å has a width approximately four times as large as that of the Si line at 2881 Å, indicating that the desorption event represented by the former results in higher velocity Si. For the Ca lines, by comparison, the relative linewidths are nearly equal, but there is a strong dose-rate dependence which suggests that the mechanism producing the Ca II desorption is changing, probably due to radiation-induced changes in the environment of the desorbing Ca ions. In the future, it should be possible using well-known laser induced fluorescence techniques to measure the actual velocity distribution of these species.

In summary, we have demonstrated even in these early experiments that the study of optical transitions in desorbing neutrals and ions from Spectrosil and Spectrosil WF is providing significant microscopic insights on the radiation-damage process as well as on the effects. Further study using electrons and photons is expected to provide complementary information, particularly with respect to the detailed desorption mechanisms.

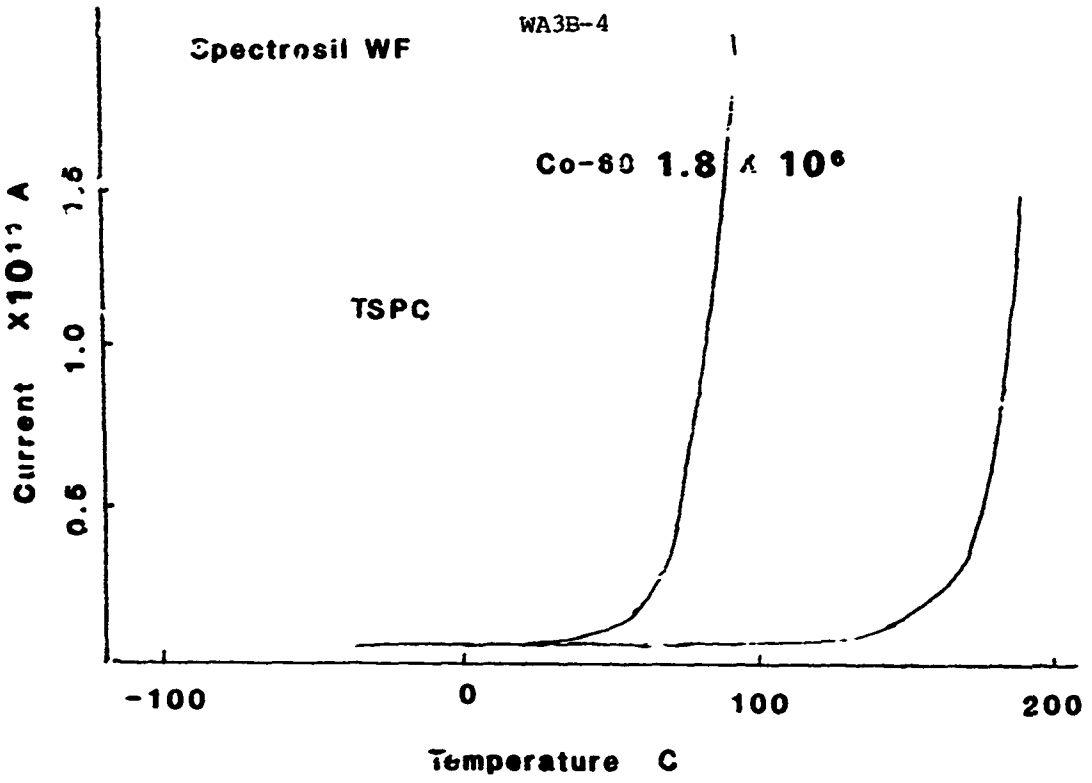

Figure 1. Thermally stimulated polarization current observed in a synthetic silica (Spectrosil WF) subjected to isotropic 60-Co radiation flux of approximately 1.8 x 10^6.

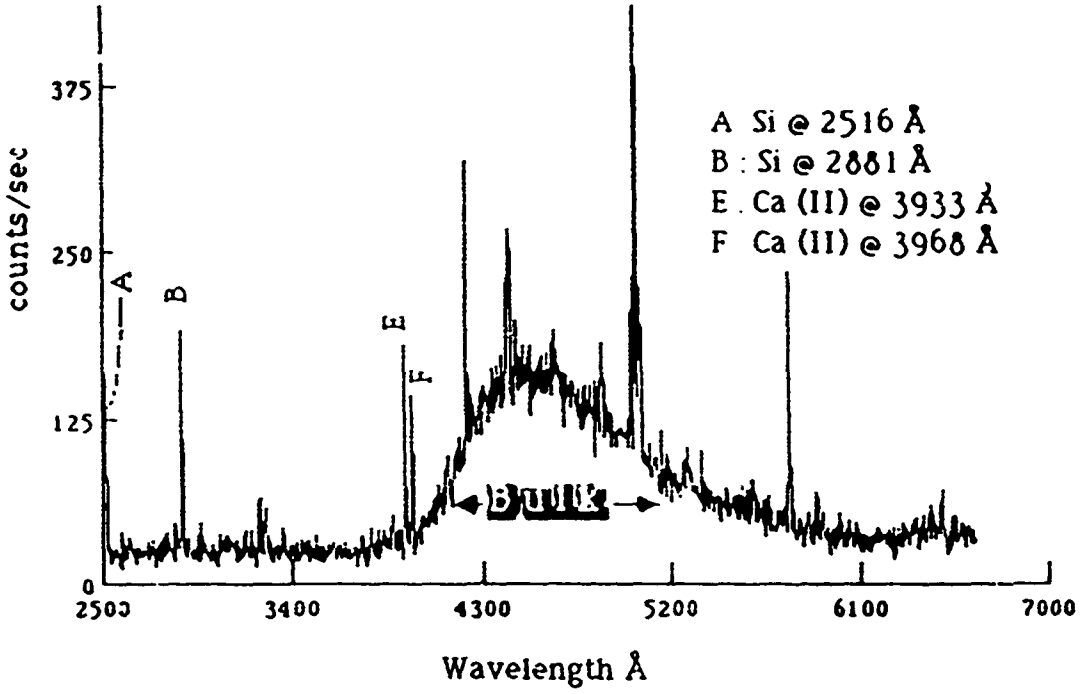

Figure 2. Typical optical spectra from excited neutrals and ions desorbed by ion bombardment of synthetic silica glass (Spectrosil).

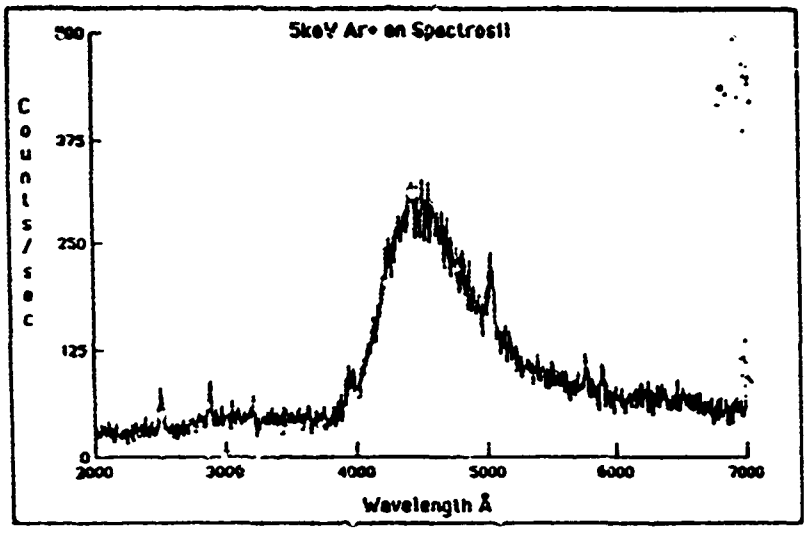

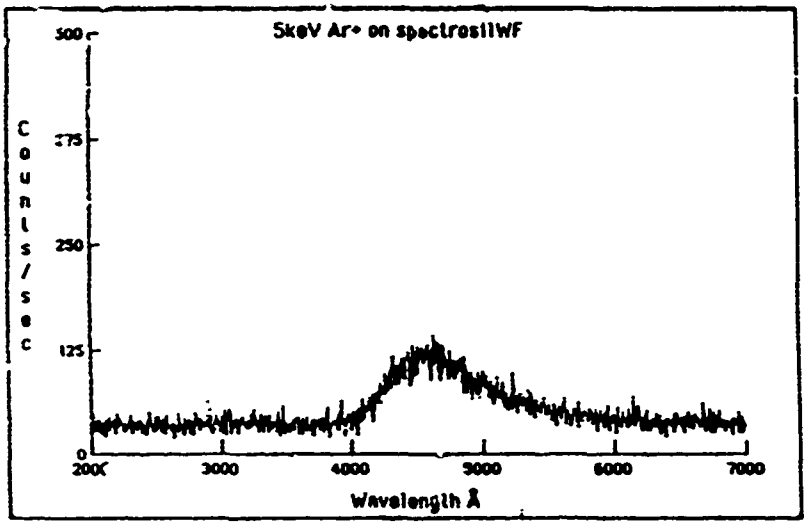

Figure 3 Optical spectra from Spectrosil and Spectrosil WF during irradiation with 5 keV Ar^+ ions.

ULTRA LIGHTWEIGHT OPTICS IN A CRYOGENIC ENVIRONMENT

David A. Crowe

Eastman Kodak Company, 901 Elmgrove Road, Rochester, N.Y. 14650

Infrared sensing systems require optics to operate at cryogenic temperatures for reduction of signal-to-noise ratios. Current systems such as Infrared Astronomical Satellite have used beryllium mirrors for these applications. Substantial system performance improvements can be obtained by using glass optics. Fused silica is the mirror material of choice at cryogenic temperatures because of its low total strain and the near zero CTE (Coefficient of Thermal Expansion) at 150 K. Kodak has verified the cryogenic performance of fused silica, frit bonded mirrors and has developed mount attachments for low temperature applications. The next step is development of the kinematic connection of the attachments to a mounting ring while minimizing focal shift and mirror decenter. The development of a mounted mirror assembly capable of operating from room to cryogenic temperatures with little change in optical figure will increase performance capability for all programs involving cold optics.

The objective of this task was to evaluate the optical performance of a mounted ultra lightweight frit bonded fused silica mirror at 100 K. Demonstration of cryogenic performance of mounted glass optics coupled with Kodak's glass technology expertise, will result in improved performance of high quality, cooled optical systems.

The kinematic mount designed and fabricated for this task is directly scaleable to larger diameter optics. A NASTRAN finite element model was constructed and used to analyze conceptual designs. Natural frequencies, surface figure degradations, despace deflections, and thermally induced stresses were analyzed and traded to arrive at the final design geometry.

Optical evaluations conducted before and after assembly verified acceptable levels of mount strain are present in the mirror. The mounted mirror assembly was installed in liquid nitrogen cryogenic shrouds in the thermal/vacuum chamber and cooled to approximately 100 K. Optical evaluations of the mirror at room and cryogenic temperatures were used to evaluate any changes of the surface. The optical evaluations were compared with cryogenic tests of the unmounted mirror to determine mount-induced effects.

A mirror assembly is shown in Figure 1. The mirror is an f/2.0, 0.5 meter diameter with 0.368 cm plates, 0.127 cm struts for a total weight of 4.3 kg. The mount weight is 2.7 kg.

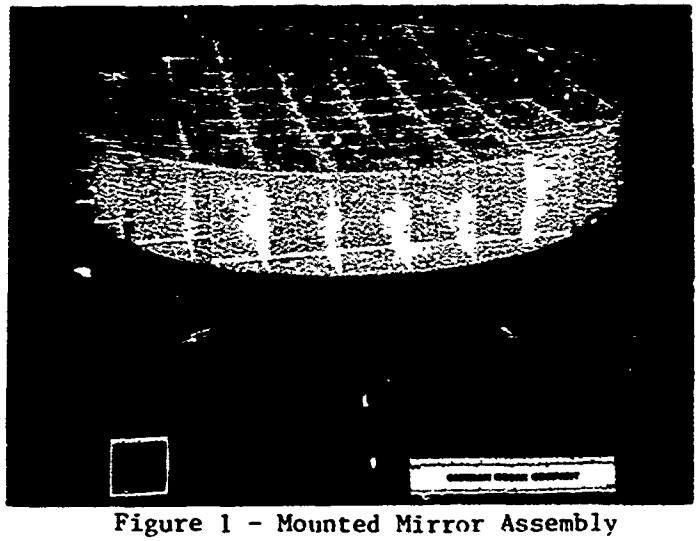

Figure 1 - Mounted Mirror Assembly

The mount concept uses six flexures arranged in three sets of bipods. This concept, rigidly supports the mirror and isolates the optic from motions of the supporting structure. The mount stiffness is a function of the cross sectional area of the flexure while the isolation is provided by the significantly lower bending stiffness of the flexure. Thus, in the design of these components it is possible to optimize the geometry to satisfy both dynamic and thermoelastic performance requirements.

One of the most important mount design requirements was to minimize optical surface deformation due to thermal expansion of the mount components. To address this goal, a trade study comparing the load transmitted to the mirror versus the flexure buckling strength and induced stresses was performed by varying the flexure length and diameter. The analysis indicate the flexure design would satisfy the requirements for thermo-elastic performance and provide design margins greater than 2.

This analysis determined the loads transmitted to the mirror at the mount/mirror interface. These loads were applied to the finite element model of the test mirror to determine the resulting deflections of the optical surface. The result were evaluated using NASTRAN to determine the magnitude of the induced figure error. The results for 10 K indicated the maximum optical surface degradation to be 0.002 λ RMS surface at 6328 A.

The finite element model of the structure was used to determine the natural frequency (>220 Hz.) of the mounted mirror and the flexure stresses. Using both the microyield of Invar and the critical buckling stress of the flexure as design criteria, the maximum tolerable g loads were established as critical buckling, axial 13.0g and tranverse 7.5g and for compressive microyield, tranverse 10.0g (mircoyield of Invar 51.7 MPa).

The mount was fabricated from Invar to take advantage of its low CTE. The attachment to the mirror used a technique developed under a previous DARPA study "CRYO PASSIVE MIRROR TECHNOLOGY STUDY", January 1984. This technique consists of frit bonding three oblate spheroid knobs to the mirror back surface, then loading them in compression with Invar clamps. The challenge for the task being reported was to couple these clamps to a stiff reaction structure while maintaining the mirror's exceilent cryogenic performance.

The mirror and shroud assembly is shown by Figure 2. The mirror and inner shroud are inserted into the larger shroud, then the lower pan is attached in place. Testing was performed through an optical window using a Twyman-Green interferometer at the center-of-curvature.

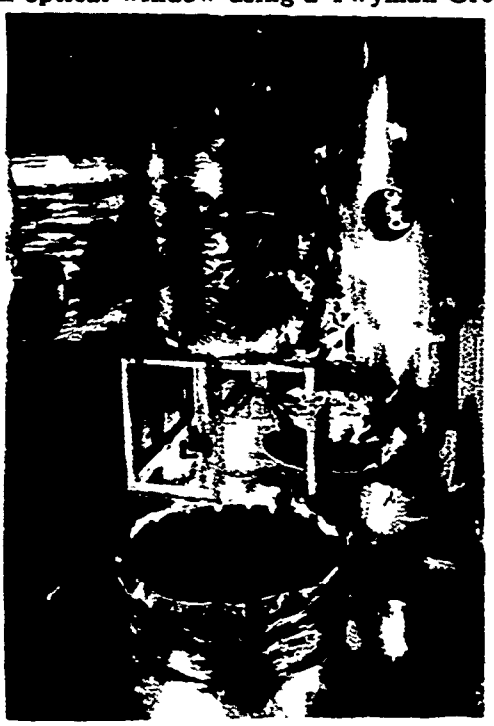

Figure 2 - Mirror and Shroud Assembly

A summary of optical test results are shown in Figure 3. The low levels of mirror surface distortion are evident. A qualitative representation of the results is shown in Figure 4. These interferograms show the wavefront under progressive tests. The largest effects (spherical error) are introduced by the vacuum chamber window.

The effects of assembly and test operation was quantifiably assessed by performing point-for-point subtractions of the surface profiles of two optical tests to produce Delta maps. In each case, the mirror and mounted assembly exhibit good stability. By subtracting the unmounted thermal change from the mounted tnermal change, the effect on surface quality contributed by the mount is determined to be 0.025 λ RMS. Since this value is close to the single orientation test repeatability of 0.02 λ RMS, the actual mount effects may be lower.

The character of the mirror with and with out mounts can be seen in Figure 3. These wavefront maps are computer averages of several interferograms. Relatively dark areas indicate highs and lighter shaded areas represent low regions. Note that the wavefront map representing the mount effect is generally random. The lack of an identifible mount strain pattern indicates that much of the measured effect may be test repeatability.

The data shows this mirror has a surface quality of 0.06 RMS when mounted and cooled to 100 K. This value, determined by adding the thermally induced error to the mounted mirror figure, verifies the capability for near diffraction limited performance by this lightweight mirror assembly.

A cryogenic mounting technique capable of performance at 10 K has been developed and test at 100 K. Excellent thermoelastic performance was obtained as evidenced by the 0.06λRMS mirror surface quality.* The mounted mirror assembly was also shown to be extremely stiff and lightweight. Test and analysis valves showed good agreement, increasing our confidence in the ability to scale the design to larger diameters.

* The mount effect contributing to this value was determined to be 0.02 λ RMS. The results of this test yields confidence that the design will demonstrate excellent performance down to 10 K.

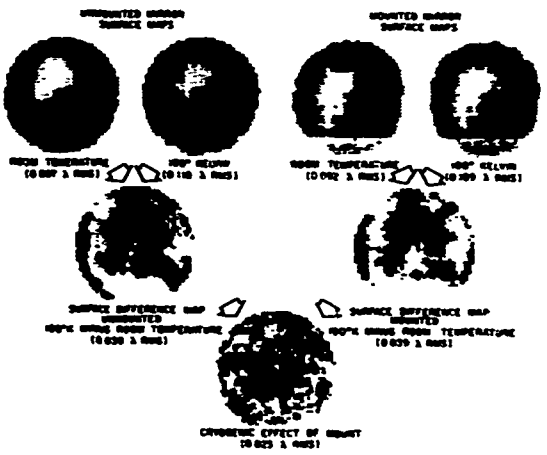

Figure 3 - Cryogenic Mount Optical Results

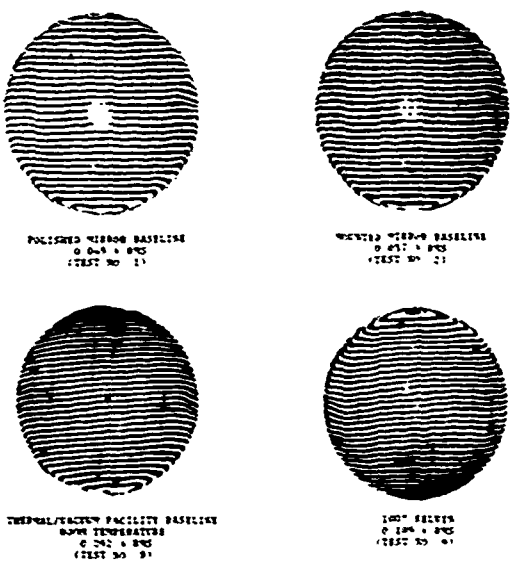

Figure 4 - Test Interferograms

Impinged Droplet Evaporative Cooling for Optical Mirrors Subjected to High Thermal Flux Loads

John A. Wellman
Eastman Kodak Company
901 Elmgrove Road
Rochester, New York 14650

John J. Meyers
Eastman Kodak Company
901 Elmgrove Road
Rochester, New York 14650

Optical mirrors used in applications where high fluxes of thermal energy are absorbed by the faceplates, such as high energy laser systems, require active cooling to prevent damage to optical coatings. Impinged droplet evaporative cooling is a new concept which can be utilized for cooling open back lightweight mirrors. The mirror will be cooled by the explosive evaporation of a fine atomized spray of water directed against the back surface of the faceplate. The temperature of the impinged water droplets will be maintained at the saturation temperature, so that all heat is removed by the latent heat of vaporization of the water. Heat transfer coefficients of 7.1×10^5 watt/m^2°C have been achieved during testing with coolant flow rates which are much less than those required for forced convective cooling.

Figure 1 is a diagram of the impinged droplet cooling concept. A matrix of spray nozzles, corresponding to the cells of the mirror structure, is mounted behind the mirror, with one nozzle directing an atomized water spray into each cell of the mirror. The steam formed by water evaporating from the back of the mirror faceplate flows out of the open cells and is either vented or can be condensed on a condenser behind the mirror. The water droplets coming out of the nozzle must move through the exiting steam as they approach the back of the mirror. If the work on the drop due to the aerodynamic drag force of the steam flowing past the droplet exceeds the kinetic energy of the drop at the nozzle, the droplet will be swept away by the exiting steam and never reach the mirror. Likewise, the drop will bounce or splatter from the surface removing very little heat, if the kinetic energy of the droplet when it hits the back surface of the faceplate exceeds the energy associated with surface tension which holds the droplet onto the surface.

Droplets which reach the surface and adhere will spread out by forces associated with surface tension into a thin film. When a drop has spread on the surface, the heat needed for vaporization is conducted into the thin film and evaporation occurs on the exposed surface until the drop has completely disappeared. Because the water droplet arrives at the saturation temperature, only the latent heat needed for vaporization must be conducted into the thin film. The rate of heat transfer into the drop is related to the contact area of the drop on the surface and inversely related to the thickness of the water film formed by the spreading droplet; the thinner the film, the higher the heat transfer coefficient. There are

two important factors affecting the thickness of a droplet spread on a surface; wetting angle and droplet diameter. Surfactants can be used to decrease the wetting angle of the droplet on the surface, causing the droplet to spread out into a thinner film. Droplet diameter will vary with the operating characteristics of the spray nozzle selected, but smaller droplets yield thinner films and, therefore, higher heat transer coefficients.

Uniformity of the spray of atomized water droplets delivered to the back of the mirror faceplate is important for controlling the temperature. If an insufficient number of drops hit the surface in a particular area, the entire flux load will not be removed and the temperature will rise. Likewise, if too many drops hit the surface in an area, a water film or puddle will form, decreasing the heat transfer coefficient in that area.

The coolant delivery efficiency is defined as the theoretical amount of coolant required to remove the flux load divided by the actual amount of coolant delivered by the nozzle. There are a number of factors governed by the characteristics of the nozzle which effect the coolant delivery efficiency of the system. These factors include the uniformity of spray coverage as related to the theoretical amount, the amount of overspray outside the heated surface to be cooled, the number of water droplets with insufficient velocity to arrive at the heated surface, and the number of water droplets having a kinetic energy in excess of the surface tension and thereby bounce from the surface without removing any heat.

Structural distortion of the mirror and the corresponding optical figure error, which would result from a pressure differential across the faceplate, can be eliminated by matching the operating evaporation pressure within the system to the ambient pressure. This will result in a change of the saturation temperature of water, resulting in the back surface of the mirror to be cooled to the new saturation temperature. This is an advantage when removing high flux loads. For example, if the threshold temperature for damage to surface coatings is 200°C and the operating pressure is 690 Pa, the saturation temperature is around 2°C, allowing the maximum temperature difference through the faceplate to be 198°C. If operating at 10^5 Pa (1 atm), where the saturation temperature is 100°C, a maximum temperature difference through the faceplate is only 100°C.

Testing was conducted to simulate a single mirror cell at atmospheric conditions, with the objective of proving validity of the concept of impinged droplet evaporative cooling. Figure 2 illustrates the test setup. The mirror simulator was a 13 cm diameter aluminum disk. Electric heaters applied to one side of the disk provided the heat source. The temperature difference across the disk, measured by thermocouples located within the disk, was used for calculating the heat flux. The cooled surface temperature was extrapolated from the temperature gradient within the aluminum disk. Water supplied to the spray nozzle was provided by pressurizing the water supply tank. The steam which was generated was vented to the room.

Testing verified that the concept of impinged droplet evaporative cooling can remove heat fluxes of 5 to 15 watts per square centimeter with high heat transfer coefficients and extremely low coolant flow rates. Limitations in the experimental apparatus prevented testing at thermal flux loads greater than 15 watts per square centimeter. Heat transfer coefficients were achieved as high as 7.1×10^5 watt/m^2°C. For demonstrated coolant delivery efficiency of about 67 percent, the needed coolant mass flux is only 6×10^{-4} grams/sec cm^2 for each 1.0 watt/cm^2 of absorbed heat flux. Figure 3 is a photograph of the aluminum disk during a test. The surface appears dry except where droplets have just impacted the surface and have not completely evaporated. The parameters which must be carefully controlled with evaporative cooling include droplet size, droplet velocity, mass flow rate, spray uniformity, surface tension and surface roughness.

An analysis was made to predict the performance limitations of evaporative cooling. Only first-order effects were taken into consideration and the results for a nozzle spacing of 5 cm and a wetting angle of 15 degrees are plotted in Figure 4. The envelope of evaporative cooling is bounded by the Leidenfrost temperature, which corresponds to a ΔT_{sat} of about 17°C and the sonic limit of the relative droplet velocity to the exiting steam. The temperature difference, ΔT_{sat}, represents the difference in temperature between the saturation temperature of the droplets and the actual temperature of the surface being cooled. The Leidenfrost temperature is the temperature where vapor will form between the droplet and the surface, reducing the conduction of heat into the drop and eliminating the surface tension forces, which hold the drop on the surface. It must be noted that there exists no spray nozzle capable of operating everywhere within the limits of spray cooling. A particular nozzle with a particular flow range and droplet distribution is only capable of operating in a region of the performance envelope. For this reason, the selection of a nozzle with the proper flow range and droplet size distribution for meeting specific system requirements is important.

The material for the mirror substrate must be selected in terms of its mechanical, thermal and optical properties. Evaporative cooling is compatible with most materials that can be used to make an open back lightweight mirror. Silicon carbide, beryllium, carbon/carbon, silver and copper are several materials which have exceptional properties for the application of evaporative cooling.

Impinged droplet evaporative cooling has several advantages over current techniques which require large volumes of liquid coolants to be pumped through small channels within the faceplate of the mirror. Evaporative cooling simplifies mirror design and construction by utilizing conventional, lightweight open back mirror designs. This concept is scalable to the largest sizes that the blanks can be manufactured and polished. The extremely low coolant flow rates required for evaporative cooling (as compared to the flow rates required for forced convective cooling) are also an advantage for scalabililty. Vibrational jitter of the mirror caused by the large volumes of liquids being pumped through the faceplate is eliminated.

NOTE: Contributors: C. N. Delametter and F. J. Sturgis

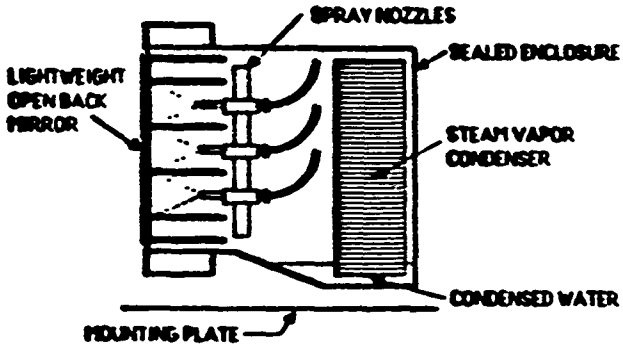

FIGURE 1 - IMPINGED DROPLET EVAPORATIVE COOLING CONCEPT

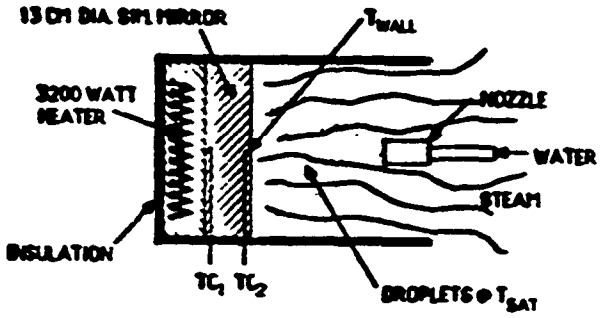

FIGURE 2 - EXPERIMENTAL TEST SETUP

FIGURE 3 - WATER DROPLETS EVAPORATING AND COOLING ALUMINUM DISK DURING TEST

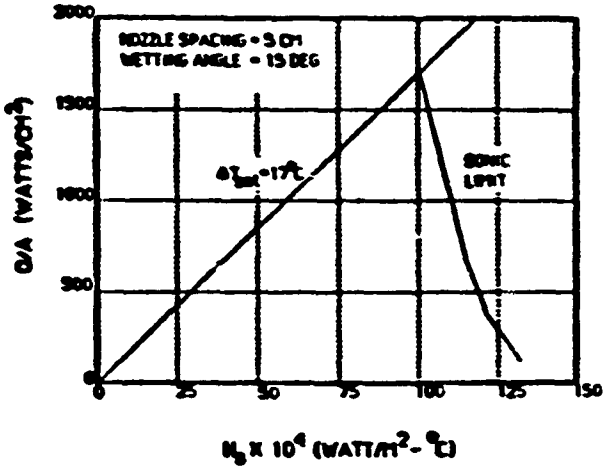

FIGURE 4 - SPRAY COOLING PERFORMANCE LIMITS BASED UPON ANALYSIS